

1-1-1988

Metal-polymer interfaces :: molecular level synthesis and characterization of a platinum-polystyrene interface and polymer monolayers prepared by the spontaneous adsorption of sulfur-functionalized polystyrene on gold surfaces/

Jan M. Stouffer

University of Massachusetts Amherst

Follow this and additional works at: https://scholarworks.umass.edu/dissertations_1

Recommended Citation

Stouffer, Jan M., "Metal-polymer interfaces :: molecular level synthesis and characterization of a platinum-polystyrene interface and polymer monolayers prepared by the spontaneous adsorption of sulfur-functionalized polystyrene on gold surfaces/" (1988). *Doctoral Dissertations 1896 - February 2014*. 743.

https://scholarworks.umass.edu/dissertations_1/743

This Open Access Dissertation is brought to you for free and open access by ScholarWorks@UMass Amherst. It has been accepted for inclusion in Doctoral Dissertations 1896 - February 2014 by an authorized administrator of ScholarWorks@UMass Amherst. For more information, please contact scholarworks@library.umass.edu.

UMASS/AMHERST



312066007697628



| DATE DUE | | | |
|-------------|--|--|--|
| MAY 11 1989 | | | |
| JAN 15 1991 | | | |
| JUN 15 1991 | | | |
| | | | |
| | | | |
| | | | |
| | | | |
| | | | |
| | | | |
| | | | |
| | | | |

UNIVERSITY LIBRARY

UNIVERSITY OF MASSACHUSETTS
AT
AMHERST

PHYS SCI

LD

3234

M267

1988

S8895

METAL-POLYMER INTERFACES:
MOLECULAR LEVEL SYNTHESIS AND CHARACTERIZATION
OF A PLATINUM - POLYSTYRENE INTERFACE
AND
POLYMER MONOLAYERS PREPARED BY THE
SPONTANEOUS ADSORPTION OF SULFUR - FUNCTIONALIZED
POLYSTYRENE ON GOLD SURFACES

A Dissertation Presented

By

Jan M. Stouffer

Submitted to the Graduate School of the
University of Massachusetts in partial fulfillment
of the requirements for the degree of

DOCTOR OF PHILOSOPHY

February 1988

Polymer Science and Engineering

© Copyright by Jan M. Stouffer 1988

All Rights Reserved

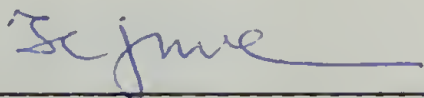
METAL-POLYMER INTERFACES:
MOLECULAR LEVEL SYNTHESIS AND CHARACTERIZATION
OF A PLATINUM - POLYSTYRENE INTERFACE
AND
POLYMER MONOLAYERS PREPARED BY THE
SPONTANEOUS ADSORPTION OF SULFUR - FUNCTIONALIZED
POLYSTYRENE ON GOLD SURFACES

A Dissertation Presented

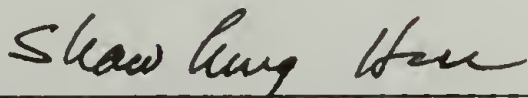
By

Jan M. Stouffer

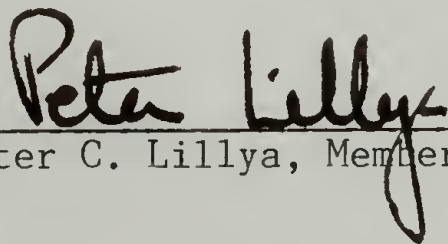
Approved to style and content by:



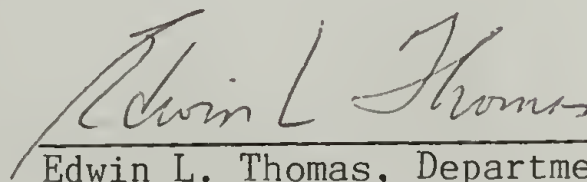
Thomas J. McCarthy, Chairperson of Committee



Shaw Ling Hsu, Member



Peter C. Lillya, Member



Edwin L. Thomas, Department Head
Polymer Science and Engineering

Dedicated to my parents, Jim and Wanda Stouffer.
Thank you for loving me and believing in me all through the years.

ACKNOWLEDGMENTS

I would like to thank Professor Tom McCarthy for his support and guidance as my research advisor. I appreciated his frank and honest appraisals of my work over the years. I would also like to thank Professor Shaw Ling Hsu and Professor C. Peter Lillya for their contributions as members of my thesis committee. I am grateful to the Army Research Office and the University Research Initiative (AFOSR/DARPA) for financial support.

Memories of Amherst will always be filled with the friends who became a part of my life during graduate school. The people of the McCarthy group -- Chris, Jay, Penney, Cady, Rick, Joan, Brant and Elisa -- were more like a family than a group of students. Between the criticism, the nagging and the teasing we all really cared for one another, and for that I thank you. I would also like to thank the guys in the glass shop -- Gordon, Larry and Tim -- for their friendship as well as their craftsmanship.

I am especially indebted to Professor S.Y. Tyree, Jr. who was my advisor and mentor at the College of William and Mary. He encouraged me to pursue research and patiently instructed me during my early days in lab. Mostly though I would like to thank Ty for having faith in my ability when others did not.

Finally, I would like to thank Robert for his patience, love and support these past six years. His vision of our future helped me keep life in perspective during those long days and nights in lab.

ABSTRACT

Metal-Polymer Interfaces: Molecular Level Synthesis and
Characterization of a Platinum-Polystyrene Interface and Polymer
Monolayers Prepared by the Spontaneous Adsorption of Sulfur-
Functionalized Polystyrene on Gold Surfaces

February 1988

Jan M. Stouffer, B.S., The College of William and Mary

Ph.D., University of Massachusetts

Directed by: Professor Thomas J. McCarthy

Metal-polymer interfaces were investigated by the synthesis and characterization of two model systems. The first system consisted of a coordinating ligand attached to a clean platinum black surface, which when activated initiated polymerization of monomer. A series of coordinating ligands were investigated and 4-picoline was chosen because it adsorbed irreversibly and perpendicularly, and its pseudo-benzylic hydrogens were acidic and could be removed to form an anionic polymerization initiator. The amount of 4-picoline adsorbed to platinum black was determined by three independent methods: UV-vis spectroscopy, gravimetric and elemental analyses.

The platinum-picoline-polystyrene interface was characterized by FTIR spectroscopy and elemental analyses. A control experiment was run in which polystyrene was polymerized anionically in the presence of

clean platinum. FTIR identified the polystyrene in the polymer-grafted-platinum sample, while none was observed in the control.

The second system investigated consisted of polymer monolayers prepared by the spontaneous adsorption of thiol-terminated polystyrene and polystyrene/poly(propylene sulfide) block copolymers from solution onto glass-supported evaporated gold films. Experiments were performed to determine what control of polymer film thickness could be exercised by changes in molecular weight, concentration, solvent composition and extent of sulfur-functionalization. The monolayers were characterized by various techniques: External reflectance FTIR spectroscopy was used to identify the polymer adsorbed to the gold surface. X-ray photoelectron spectroscopy provided information about the elemental composition of the outer surface. Liquid scintillation counting was used to determine the mass of the polymer adsorbed to the gold surface. Sulfur-containing polymers were prepared by living anionic polymerization techniques. Radiolabelled polymers were prepared using ^3H -styrene.

Polystyrene containing a terminal thiol group ($M_n = 1,000\text{--}200,000$) adsorbed to gold under conditions that polystyrene did not. At higher molecular weight ($M_n = 500,000$) adsorption did not occur. Polystyrene/poly(propylene sulfide) block copolymers adsorbed to gold and the thickness of the adsorbed layer could be controlled by the length of the poly(propylene sulfide) block. This work demonstrates the importance of using organic chemistry to make specifically designed functional polymers that can be used to investigate interfacial phenomena.

TABLE OF CONTENTS

| | <u>Page</u> |
|---|-------------|
| ACKNOWLEDGMENTS | v |
| ABSTRACT | vi |
| LIST OF TABLES | xii |
| LIST OF FIGURES | xiv |
| LIST OF SCHEMES | xvii |
| Chapter | |
| I. INTRODUCTION | 1 |
| Metal-Polymer Interfaces | 1 |
| Thesis Objectives..... | 2 |
| Theories of Polymer Adsorption | 3 |
| Isolated Polymer Chains | 3 |
| The Theory of Hoeve | 4 |
| The Theory of Silberberg | 4 |
| The Theory of Scheutjens and Fleer | 5 |
| The Scaling Theory of de Gennes | 5 |
| Polymer Adsorption | 6 |
| Graft Polymerization | 12 |
| Surface Analytical Techniques | 14 |
| Fourier Transform Infrared Spectroscopy..... | 14 |
| Radioisotopic Labelling | 18 |
| X-Ray Photoelectron Spectroscopy | 21 |
| References | 25 |
| II. EXPERIMENTAL | 28 |
| Synthetic Methods | 28 |
| Material Handling and Purification Techniques | 28 |
| Purification of Solvents | 37 |
| Purification of Reagents | 38 |

TABLE OF CONTENTS (continued)

| | <u>Page</u> |
|--|-------------|
| Methods and Instrumentation | 40 |
| Elemental Analysis | 40 |
| Gas Chromatography and Kinetic Analysis | 40 |
| Gel Permeation Chromotography | 41 |
| Gravimetric Analysis | 42 |
| Proton Nuclear Magnetic Resonance | 42 |
| Ultraviolet-Visible Light Spectrophotometry .. | 42 |
| Platinum-Catalyzed Hydrogenation of Olefins | 42 |
| Hydrogenation of Cyclohexene to Cyclohexane over a Platinum Supported Catalyst | 43 |
| Platinum on Alumina-Catalyzed Olefin Hydro- genation Poisoned with Tris(2-cyanoethyl)- phosphine and Tri-p-tolylphosphine | 43 |
| Platinum on Alumina-Catalyzed Olefin Hydro- genation Poisoned with Various Concentrations of Tris(2-cyanoethyl)phosphine | 44 |
| Platinum on Alumina-Catalyzed Olefin Hydro- genation Poisoned with Pyridine, 4-Picoline, Benzenethiol and Bis(1,2 di-p-tolylphosphino)- ethane | 44 |
| Platinum on Alumina-Catalyzed Olefin Hydro- genation Poisoned with Pyridine, Benzen- thiol, Triethylphosphine and Dimethyl- bypyridine | 45 |
| Platinum on Alumina-Catalyzed Olefin Hydro- genation Poisoned with Ethanethiol, Benzenethiol, Triethylphosphine, Triphenylphosphine, Pyridine and 4-Picoline | 45 |
| Hydrogenation Cyclohexene to Cyclohexane Using Various Concentrations of a Platinum Black Catalyst | 46 |
| Platinum-Catalyzed Hydrogenation of Cyclo- hexene Using Various Concentrations of Olefin | 46 |
| Platinum-Catalyzed Olefin Hydrogenation Poisoned with 4-Picoline | 46 |
| Adsorption of 4-Picoline on Platinum | 47 |

TABLE OF CONTENTS (continued)

| | <u>Page</u> |
|---|-------------|
| Dilute Solutions of 4-Picoline in Pentane for Beer's Law Justification | 47 |
| UV-vis Analysis of 4-Picoline Adsorbed to Platinum Black | 47 |
| Attempted Removal of 4-Picoline from Platinum with Solvent | 48 |
| Gravimetric Analysis of 4-Picoline Adsorbed to Platinum Black | 48 |
| Synthesis of a Platinum-Polystyrene Interface | 49 |
| Picolyl Anion-Initiated Polymerization of Styrene | 49 |
| Platinum-Polystyrene Interface Synthesis | 50 |
| Sulfur-Containing Polymers for Adsorption Studies | 51 |
| ^3H -Styrene Synthesis | 51 |
| Synthesis of Thiol-Terminated Polystyrene | 51 |
| Synthesis of Polystyrene/Poly(propylene sulfide) Block Copolymers | 52 |
| Synthesis of Poly(propylene sulfide) | 52 |
| Synthesis of Radiolabelled Polymers | 52 |
| Dilute Solutions of Radiolabelled Polymers for Beer's Law Justification | 53 |
| Adsorption of Polymers on Gold | 54 |
| References | 56 |
| III. RESULTS AND DISCUSSION | 57 |
| Platinum-Polystyrene Interface | 57 |
| Platinum-Catalyzed Olefin Hydrogenation | 57 |
| Survey of Coordinating Ligands | 57 |
| Effect of 4-Picoline on the Rate of Olefin Hydrogenation | 60 |
| Adsorption of 4-Picoline on Platinum | 64 |
| UV-vis Analysis | 64 |
| Gravimetric Analysis | 67 |
| Elemental Analysis | 69 |

TABLE OF CONTENTS (continued)

| | <u>Page</u> |
|--|-------------|
| Synthesis of a Platinum-Polystyrene Interface | 73 |
| Picolyl Anion-Initiated Polymerization of Styrene | 73 |
| Platinum-Polystyrene Interface Synthesis and Characterization | 77 |
| Adsorption of Sulfur-Functionalized Polymers on Gold | 88 |
| Synthesis of Polymers | 88 |
| Thiol-Terminated Polystyrene | 88 |
| Polystyrene/Poly(propylene sulfide) Block Copolymers | 93 |
| Tritiated Styrene | 95 |
| Radiolabelled Polymers | 97 |
| Beer's Law Justification for Radiolabelled Polymers | 100 |
| Adsorption of Polymers on Gold | 102 |
| Factors Influencing the Adsorption of Polymers | 103 |
| Adsorption Kinetics | 103 |
| Molecular Weight Dependence | 103 |
| Concentration Dependence | 118 |
| Effect of Solvent | 118 |
| Effect of Poly(propylene sulfide) Block Size .. | 122 |
| Summary | 124 |
| References | 125 |
| IV. CONCLUSIONS AND SUGGESTIONS | 127 |
| References | 130 |
| APPENDIX : Data Tables | 131 |
| BIBLIOGRAPHY | 139 |

LIST OF TABLES

| | | <u>Page</u> |
|--------------|---|-------------|
| Chapter III. | | |
| Table 3.1 | Effect of Poisons on Platinum Catalyzed Hydrogenations | 59 |
| Table 3.2 | Effect of Agitation on the Rate of Hydrogenation | 61 |
| Table 3.3 | UV-vis Absorbance at 254 nm for 4-Picoline Solutions Before and After Exposure to Platinum Black | 67 |
| Table 3.4 | Gravimetric Analysis of 4-Picoline Adsorbed to Platinum Black | 69 |
| Table 3.5 | Determination of the Amount of 4-Picoline Adsorbed to Platinum Black | 70 |
| Table 3.6 | GPC characterization of Polystyrene Initiated by Picolyllithium and <u>n</u> -Butyllithium | 76 |
| Table 3.7 | Elemental Analysis of Polystyrene-Grafted Platinum | 86 |
| Table 3.8 | Calculated Molecular Weight of Polystyrene-Grafted Platinum | 87 |
| Table 3.9 | GPC Characterization of Polystyrene Before and After Endcapping with Propylene Sulfide | 92 |
| Table 3.10 | Elemental Analysis of Thiol-Terminated Polystyrene ... | 92 |
| Table 3.11 | Characteristics of PSSH Polymers | 93 |
| Table 3.12 | Elemental Analysis for C, H and S in Various Polymers Containing Styrene and Propylene Sulfide | 95 |
| Table 3.13 | Characteristics of PS/PPS Block Copolymers | 100 |
| Table 3.14 | Analytical Expressions for Beer's Law Relationships .. | 102 |
| Table 3.15 | Comparison of S/C Ratios from XPS taken at 15° and 75° | 114 |

LIST OF TABLES (continued)

| | <u>Page</u> |
|--|-------------|
| Appendix | |
| Table A.1 Radioactivity (CPM) of Solutions of PSSH Polymers for Beer's Law Plots | 131 |
| Table A.2 Radioactivity (CPM) of Solutions of PS/PPS Polymers for Beer's Law Plots | 132 |
| Table A.3 Radioassay Data for the Adsorption of Polymers onto Gold. Effect of Molecular Weight (2 mg/mL, THF, 24 h) | 133 |
| Table A.4 C/Au Ratios from XPS Data. Effect of Molecular Weight on Adsorbance (2 mg/mL, THF, 24 h) | 134 |
| Table A.5 Radioassay Data for the Adsorption of Polymers onto Gold. Effect of Concentration (200,000 MW, THF, 24 h) | 135 |
| Table A.6 Radioassay Data for the Adsorption of Polymers onto Gold. Effect of Solvent Mixtures THF/Cyclohexane (2 mg/mL, 24 h, 200,000 MW, 45°C) | 136 |
| Table A.7 Radioassay Data for the Adsorption of Polymers onto Gold. Effect of Poly(Propylene Sulfide) Block Size (2 mg/ml, THF, 24 h, 60,000 MW) | 138 |

LIST OF FIGURES

| | <u>Page</u> |
|--|-------------|
| Chapter I. | |
| Figure 1.1 Grazing incidence reflection infrared technique | 16 |
| Figure 1.2 Angle-resolved XPS | 22 |
| Chapter II. | |
| Figure 2.1 Vacuum manifold | 30 |
| Figure 2.2 Storage flask | 31 |
| Figure 2.3 Schlenk tube for polymerizations | 32 |
| Figure 2.4 Schlenk tube for polymer adsorption | 34 |
| Figure 2.5 Continuous distillation apparatus | 35 |
| Figure 2.6 Trap-to-trap distillation apparatus | 36 |
| Chapter III. | |
| Figure 3.1 Disappearance of cyclohexene over time in a platinum catalyzed hydrogenation | 62 |
| Figure 3.2 Effect of cyclohexene concentration on the rate of hydrogenation | 63 |
| Figure 3.3 Effect of 4-picoline on the rate of olefin hydrogenation | 65 |
| Figure 3.4 Beer's Law plot of dilute solutions of 4-picoline | 66 |
| Figure 3.5 UV-vis spectra of 4-picoline solutions before and after exposure to platinum black | 68 |
| Figure 3.6 UV-vis spectra of pentane (B) and a pentane solution of 4-picoline (A) after exposure to platinum black . | 71 |
| Figure 3.7 UV-vis spectra of pentane washings of platinum black AW: platinum exposed to 4-picoline, BW: control platinum | 72 |

LIST OF FIGURES (continued)

| | <u>Page</u> |
|--|-------------|
| Figure 3.8 Effect of 4-picoline-poisoned-platinum catalyst on the rate of olefin hydrogenation | 74 |
| Figure 3.9 Effect of 4-picoline-poisoned-platinum catalyst sealed inside teflon filters on the rate of olefin hydrogenation | 75 |
| Figure 3.10 ^1H -NMR spectrum of picolyl anion-initiated polystyrene | 78 |
| Figure 3.11 ^1H -NMR spectrum of polystyrene | 79 |
| Figure 3.12 ^1H -NMR spectrum of poly(4-vinylpyridine) | 80 |
| Figure 3.13 Infrared spectrum of poly(4-vinylpyridine) | 81 |
| Figure 3.14 Infrared spectrum polystyrene | 82 |
| Figure 3.15 Infrared spectrum of picolyl anion-initiated polystyrene | 83 |
| Figure 3.16 Infrared spectrum of polystyrene-grafted platinum | 84 |
| Figure 3.17 Infrared spectrum of control platinum | 85 |
| Figure 3.18 Infrared spectrum of thiol-terminated polystyrene | 91 |
| Figure 3.19 ^1H -NMR spectrum of the final reaction mixture from the tritiated styrene synthesis | 98 |
| Figure 3.20 Expanded ^1H -NMR spectrum from the tritiated styrene synthesis | 99 |
| Figure 3.21 Beer's Law plot of mass versus radioactivity for PSSH 7-143H | 101 |
| Figure 3.22 Kinetics of polymer adsorption from dilute solution .. | 104 |
| Figure 3.23 Comparison of the XR IR spectrum of a gold surface exposed to a PSSH polymer solution (A) to that of a PS polymer solution (B) | 106 |
| Figure 3.24 XR IR spectrum of PSSH 7-123A adsorbed to gold | 107 |

LIST OF FIGURES (continued)

| | | <u>Page</u> |
|-------------|---|-------------|
| Figure 3.25 | XR IR spectrum of PSSH 7-123B adsorbed to gold | 108 |
| Figure 3.26 | XR IR spectrum of PSSH 7-83B adsorbed to gold | 109 |
| Figure 3.27 | XR IR spectrum of PSSH 7-89A adsorbed to gold | 110 |
| Figure 3.28 | XR IR spectrum of PSSH 7-89B adsorbed to gold | 111 |
| Figure 3.29 | Effect of molecular weight on the adsorbance of PSSH polymers onto gold, determined by LSC | 112 |
| Figure 3.30 | Effect of molecular weight on the adsorbance of PSSH polymers onto gold, determined by XPS | 115 |
| Figure 3.31 | XPS spectrum of adsorbed PSSH polymer showing shake up peak in C _{1s} region | 116 |
| Figure 3.32 | XR IR spectrum of a gold substrate exposed to a solution of PSSH 7-85A | 117 |
| Figure 3.33 | Adsorption isotherm for PSSH 7-145H determined by LSC. | 119 |
| Figure 3.34 | Effect of solvent mixtures on the adsorbance of PSSH polymers onto gold, determined by LSC | 120 |
| Figure 3.35 | Effect of poly(propylene sulfide) block size on the adsorption of PS/PPS copolymer, determined by LSC .. | 123 |

LIST OF SCHEMES

| | <u>Page</u> |
|--|-------------|
| Chapter III. | |
| Scheme 3.1 General synthetic strategy for the stepwise synthesis of a platinum-polystyrene interface ... | 58 |
| Scheme 3.2 Polymerization of propylene sulfide initiated by ethyllithium | 90 |
| Scheme 3.3 Synthesis of polystyrene/poly(propylene sulfide) block copolymers | 94 |
| Scheme 3.4 Synthesis of tritiated styrene | 96 |

Chapter I

INTRODUCTION

Metal-Polymer Interfaces

Interfacial interactions between metals and polymers are central to a range of applications: colloid stabilization¹, corrosion inhibition², composites³, electronics⁴, electropolymerization⁵, lubrication⁶, polymer-modified electrodes⁷ and prosthetic devices.⁸ The success or failure of these materials often depends on phenomena that occur at the interface. The study of interfacial interactions is a difficult problem which is best addressed using an interdisciplinary approach involving physics, organic chemistry, physical chemistry, morphology and mechanics. The investigation of a surface requires techniques that can provide information on a molecular or atomic level. Early work in this area was performed by physicists using ultra-high vacuum analytical techniques to study surfaces of single crystals and molecules adsorbed to such surfaces. These studies helped to answer questions in the area of catalysis, but could not be used for systems involving liquids or interactions that occur at atmospheric pressure. Recent developments in techniques such as infrared spectroscopy, which unlike many surface techniques does not damage the organic material being analyzed, permit one to look at very thin films (on the order of angstroms) on the surface of metals. With this surface analytical technique and others we have the tools to investigate surface phenomena in practical environments.

To explain interfacial phenomena in existing materials it is necessary to have an understanding of the structure-property relationships in model systems, and with this knowledge it is then possible to produce new and improved materials. We are interested in "polymer-wall" interactions with the objectives of understanding how polymer molecular structure, polymer solution structure, adsorption conditions and specific interactions affect the adsorption kinetics, the polymer structure and the mechanical and environmental integrity of the interface.

Thesis Objectives

The primary goal of this research was to investigate metal-polymer interfaces. The first objective was to synthesize and characterize a well defined platinum-polystyrene interface on a molecular level. The second objective was to study polymer monolayers prepared by the spontaneous adsorption of sulfur-functionalized polystyrenes on gold surfaces and to understand the effects of molecular weight, concentration, solvent power and specific interactions on adsorbance.

In this research two methods were used to prepare thin films of polymers on metals: polymer molecules were attached to a metal surface by graft polymerization and spontaneously adsorbed from solution. The following sections of this introduction present a summary of theories on polymer adsorption and a brief review of experimental work done on adsorption and grafting of polymers onto surfaces. The chapter will conclude with a discussion of the surface analytical techniques used in this dissertation.

Theories of Polymer Adsorption

Isolated Polymer Chains. The adsorption of polymers at interfaces is very different from that of small molecules. The major feature in polymer adsorption is the number of conformations in which the polymer can exist. These conformations determine the thickness of the polymer layer adsorbed to the surface. It is well known that a free flexible polymer chain in solution behaves as a random coil, upon adsorption to a surface there is a change in its conformation. The part of the polymer in direct contact with the surface is referred to as a "train" and the remaining portions of the chain extending into the solution as "loops" and "tails".

The original theoretical investigation of the change in conformation that occurs when a Gaussian coil is brought in contact with a wall was reported by Frisch, Simha and Eirich⁹ in 1953. They calculated the change in thermodynamic properties of the adsorbed layer and proposed an adsorption isotherm (FES isotherm). The important conclusion was that the thickness of the adsorbed layer at the theta point is proportional to the square root of the molecular weight of the polymer. In the 1960's extensive theoretical investigations of polymer adsorption were undertaken to improve and expand their theory. These studies used lattice model approaches¹⁰, statistical mechanical approaches¹¹, and computer simulations using Monte Carlo methods¹² to determine the conformations of isolated polymer chains adsorbed at an interface.

The important conclusions from the above theoretical investigations of an isolated adsorbed polymer chain are: (1) At low adsorption energy, long loops and tails are favored and give rise to a conformation that extends away from the surface into the solution, whereas at high adsorption energy, small loops or tails predominate, leading to a "flattened" conformation. (2) As the adsorption energy increases the number of train segments increases. (3) The distribution of loop segments is a simple exponential function of the distance from the surface while that of tail segments is the difference of two exponential functions and has a maximum at an intermediate distance.

The Theory of Hoeve. The theory of Hoeve^{13,14} considers the interaction between adsorbed polymers and assumes that the polymer chain is so long that end effects, i.e. tail formation, may be neglected. The fraction of adsorbed segments, the average loop size and the average train size are calculated from the partition function for an isolated polymer chain consisting of trains and loops. He concluded that the root-mean-square thickness of segments is approximately proportional to $n^{1/2}$ where n is the number of segments. Hoeve^{15,16} extended his theory to consider not only interactions between the train segments but also interactions among the loops. This excluded volume effect predicts that as the solvent gets better, the average loop size becomes larger and the adsorbance decreases.

The Theory of Silberberg. Silberberg¹⁷ used a quasi-crystalline lattice model for the adsorption of flexible polymers to derive the total number of configurations of the chains, then used this to obtain

an expression for the partition function. The partition function is based on that of an isolated polymer in solution, then it takes into account the energy required to replace a solvent molecule on the surface by a polymer segment and the number of arrangements possible for the polymer in solution. This theory predicts that at the theta point ($X = 0.5$) the average loop length, which is proportional to film thickness, is approximately proportional to the square root of molecular weight over a wide range, but approaches a constant for large molecular weights. Under athermal conditions ($X = 0$) the dependence on molecular weight of the average loop length is weak.

The Theory of Scheutjens and Fleer. Scheutjens and Fleer^{18,19} take a lattice model approach assuming that the system is a mixture of polymer chains, each consisting of segments, and solvent molecules, and a region adjacent to the adsorbing surface which is divided into layers parallel to the surface each containing lattice sites. They found that for $X = 0.5$, the root-mean-square thickness of the adsorbed layer is proportional to the square root of the number of polymer segments (r) when $r \geq 20$, while for $X = 0$ this quantity is not completely linear against $r^{1/2}$ and its magnitude is somewhat smaller than that for $X = 0.5$. The most important conclusion from this theory is that tail segments dominate the thickness of the adsorbed layer.

The Scaling Theory of de Gennes. de Gennes^{20,21} used scaling theory to investigate the adsorption of a flexible polymer on a flat surface from good solvents. He considered three different regimes, i.e. dilute, semidilute and plateau regions. In the dilute region he

considered a single chain of n segments confined in an adsorbed polymer layer. He found that the thickness of the adsorbed layer is independent of the number of segments in the polymer chain and that the thickness increases as the effective adsorption energy of the polymer decreases. In the semidilute region, the repulsion between adsorbed chains is dominated by the osmotic pressure in the adsorbed layer. The thickness scales with $n^{3/5}$. In the plateau region many polymer chains are adsorbed and give rise to an adsorbed layer in which the osmotic pressure again dominates. The thickness is proportional to n , but the chain is far from being in a stretched fully conformation.

Polymer Adsorption

In the past, ellipsometry has been the most commonly used technique to characterize adsorbed polymer layers. Ellipsometry is used in situ to determine the thickness of the adsorbed layer. This experimentally determined value is used to derive the root-mean-square thickness (t_{rms}) which can be compared to the value predicted by theory for the root-mean-square thickness of loops or tails.

Gebhard and Killman²² used ellipsometry to study the adsorption of polystyrene onto various metal surfaces from theta solvents. The molecular weight (M_n) of the polymer samples studied ranged from 76×10^3 to 340×10^3 . The authors observed an increase in adsorbance with rising M_n , and found that t_{rms} was proportional to $M_n^{0.5}$.

Kawaguchi and Takahashi²³ also used ellipsometry to measure the thickness of polystyrene adsorbed on a chrome plate from cyclohexane at

35°C. Their study covered a wider range of molecular weights, with M_n from 10×10^3 to 13.4×10^6 . They found that the adsorptions rose sharply with increasing bulk polymer concentration and reached a wide plateau region. The thickness (t_{rms}) exhibited the same relationship to bulk polymer concentration. They concluded that at very low bulk polymer concentration the adsorbance and t_{rms} indicated that the polymer assumed a flattened conformation consisting of small loops or tails and a large number of train segments. An increase in bulk polymer concentration caused desorption of train segments which made adsorption sites available for other polystyrene molecules, leading to a thicker adsorbed layer. They found that t_{rms} was proportional to $M_n^{0.5}$ in the plateau region. They compared their experimental results to the theories of Hoeve¹⁴, Silberberg¹⁷, and Scheutjens and Fler.¹⁸ Their experimental adsorption isotherms and t_{rms} values were in poor agreement with the theory of Hoeve which neglected the contribution of end effects resulting from tail formation. The molecular weight dependence on adsorbance that they observed was in good agreement with Silberberg's theory, but the theoretical loop size was too small to be consistent with their large measured value of t_{rms} . They used the experimental value of t_{rms} and the molecular weight of the polymer to determine that 15 to 20% of the total segments in the adsorbed layer were tails. This compares well to the theory of Scheutjens and Fler that predicted about 15% of the segments in the adsorbed layer would be present as tails. Kawaguchi and Takahashi concluded that the extension of adsorbed polystyrene normal to the surface was determined by the tail portions of

the loop-train-tail conformation, whereas the adsorbance was mainly governed by the loop-train portions of the adsorbed polymer chain.

It is well known that the dimensions of a polymer chain increase with increasing solvent power. This expanded conformation affects the adsorbance and the thickness of the polymer layer adsorbed to a surface. Kawaguchi and Takahashi²⁴ studied the effect of solvent power on the adsorption of polystyrene onto a metal surface. They observed the effect of temperature on the adsorption of polystyrene onto chrome and found that the thickness of the adsorbed layer increased and the adsorbance decreased with rising temperature. In another report²⁵, they measured the adsorption of polystyrene from carbon tetrachloride and toluene solutions onto a chrome plate at 35°C. The adsorbance was lower than that in the theta solvent (cyclohexane, 35°C) and the thickness of the adsorbed layer was larger than that in the theta solvent.

Transmission infrared spectroscopy has been used in polymer adsorption studies to determine the fraction of polymer segments adsorbed (p) and the fraction of surface sites occupied (θ). Fontana and Thomas²⁶ were the first to use this technique to measure p , θ , and the adsorbed amount of polymer per surface site (Γ). By observing IR shifts of the carbonyl bands in the polymer and the surface silanol group, they were able to determine p , θ and Γ for poly(lauryl methacrylate), with M_n ranging for 33×10^3 to 1190×10^3 , adsorbed from *n*-dodecane and *cis*-decalin onto silica particles. They found that θ increased whereas p remained nearly constant with rising Γ . Presently, this method is limited to high surface area solids and requires that

the surface area and number of surface sites (e.g. the silanol groups in nonporous silica) per unit area are accurately known in advance.

Kawaguchi and Takahashi²⁷ determined p , θ , and Γ for polystyrene adsorbed on silica from cyclohexane and carbon tetrachloride solutions at 35°C as a function of molecular weight and compared the experimental results with the theory of Scheutjens and Fleer¹⁸ and that of Silberberg.¹⁷ The amount of polymer adsorbed per surface site (Γ) was lower in carbon tetrachloride than that in cyclohexane as predicted by both theories. For each solvent system the fraction of adsorbed segments (p) diminished with increasing molecular weight while the fraction of occupied surface sites (θ) exhibited the reverse trend. These experimental results fitted well to both of the theories mentioned above. Consequently, the authors concluded that in order to obtain the predominant conformation of the adsorbed polymers, i.e. whether it was loop-train or loop-train-tail, additional data was needed on the thickness of the adsorbed layer.

This technique was also used by Kawaguchi and Takahashi²⁸ to investigate the adsorption of random styrene-butadiene copolymers on a silica surface. They observed that the total adsorbance of the copolymer onto the silica from cyclohexane at 35°C depended on chemical composition. The adsorbance increased with increasing styrene mole fraction and did not exceed the adsorbance of styrene homopolymer, but did exceed the adsorbance of the butadiene homopolymer. They attributed this result to two effects. First, the interaction between a styrene unit and a silica surface has been shown to be stronger than that of a

butadiene unit. More importantly was the effect of solubility, with an increase in styrene content the solubility of the copolymer in cyclohexane decrease, consequently the adsorbance increased since cyclohexane is a theta solvent for polystyrene and a good solvent for polybutadiene.

Another approach taken in the investigation of the conformation of adsorbed polymer molecules is based upon knowledge of the intermolecular forces between polymers and solid substrates and on how such forces are affected by environmental conditions such as temperature and solvent. Israelachvili²⁹ designed an instrument which directly measures the force as a function of distance between two polymer layers adsorbed on smooth substrate surfaces. This instrumental technique provides information on both the conformations of adsorbed polymer molecules and on the forces in the surface layer.

Klein et al.^{30,31} has used this technique to determine the force versus separation profiles between saturated adsorbed layers of polystyrene on mica immersed in cyclohexane at 34°C. The two surfaces began to exhibit mutual attraction at a distance of two to three times the radius of gyration of polystyrene in bulk cyclohexane solution. The attraction increased in magnitude as the separation decreased until it was approximately equal to the radius of gyration. At that separation there was an attractive minimum. At smaller separations the force between the surfaces became strongly repulsive. The authors^{32,33} derived analytical expressions based on a mean-field model and solved them numerically to yield (a) segmental density profiles for the

adsorbed polymer and (b) interaction-energy vs. plate-separation profiles.

This experimental technique has also been used by Klein et al.^{34,35,36} to study poly(ethylene oxide) adsorbed on mica from good solvents. From their measurements they derived a characteristic effective layer thickness (δ_{eff}) which represents the range of extension from the surface that can be detected by a similar polymer-covered surface. For poly(ethylene oxide) in good solvents, 0.1 M aqueous KNO_3 or toluene, they found that the effective extension of the adsorbed layers varied as $\delta_{\text{eff}} \propto N^b$, where N was the degree of polymerization and $b = 0.43 \pm 0.02$ for both systems studied. This result differed from de Gennes' scaling theory which predicted that the thickness of an adsorbed polymer layer in a good solvent would scale with $N^{3/5}$. If the onset of repulsive interactions between two polymer layers in a good solvent occurred as soon as the "tails" of each layer began to overlap, one would expect $\delta_{\text{eff}} \sim \delta_{\text{tail}}$. Klein did not observe this in his study, because repulsion was not detected until there was an appreciable overlap of the two layers.

Hadziioannou et al.³⁷ measured the forces between surfaces of block copolymers adsorbed on mica. Block copolymers of poly(vinyl-2-pyridine) and polystyrene were adsorbed onto mica from toluene and cyclohexane. The poly(vinyl-2-pyridine) block bound strongly to the mica in a flattened configuration while the polystyrene block extended from the surface. The polystyrene was in a more stretched conformation in toluene than in cyclohexane. The range of forces observed depended on

the molecular weights of blocks.

Graft Polymerization

From research on polymer modified electrodes various methods have been developed to covalently graft polymers to surfaces. Murray⁷ developed a general strategy based on the use of silanizing reagents. Metal oxide electrodes were treated with acidic solutions which produced hydroxyl groups on the surface. The hydroxyl groups were reacted with chloro- or alkoxysilanes. If trifunctional silanes were used and water was present polymerization proceeded and built up a coating on the electrode. Another method was to initiate polymerization directly at the electrode. Murray³⁸ polymerized tris(4-vinyl-4'-methyl-2,2'-bipyridine)ruthenium(II) on an electrode by electroreduction of the monomeric complex.

Diaz et al.³⁹ reported the electropolymerization of pyrrole on a platinum electrode surface as the first example of a one-step preparative procedure for a conducting film. The polymer film prepared by the electrochemical oxidation of pyrrole was durable and adhered strongly to the electrode surface. The procedure is fairly general and has been used to prepare conducting polymers based on the following monomers⁵: alkyl- and phenyl-N-substituted pyrroles, thiophene, aniline and naphthylamine.

Two approaches have been taken to chemically graft polymers onto high surface area solids in solution. It has been reported that living

polyisoprene and polystyrene can be grafted to carbon black containing ester groups.⁴⁰ The grafting reaction was restricted by the accessibility of the living polymer to the carbon surface. Consequently, the yield of the grafting reaction was dependent on both the surface area of the solid and the molecular weight of the polymer. This method was also used to graft living polystyrene onto silica.⁴¹ The silica was heat treated (750°C) to condense the silanol groups to siloxane bridges. The siloxane bond was broken by nucleophilic attack of the living polystyryl anion. Polystyrene samples with $M_w = 4,000$ and 27,800 were grafted to silica by this procedure. The extent of grafting reaction was determined by weighing the solid before and after exposure to the living polymer.

The second approach was to initiate polymerization at the surface. Carbon black containing alkali metal carboxylate groups was used to initiate the anionic ring-opening polymerization of β -propiolactone.⁴² The observation that the product produced a stable colloidal dispersion in a good solvent for the polyester was given as proof that the polymer was grafted to the carbon black surface.

Vapor phase polymerization has been used to graft polymer films to metal surfaces. Toy⁴³ has reported the surface-polymerization of tetrafluoroethylene on fluorine-activated metal substrates including copper, nickel, aluminum, titanium, titanium alloy and stainless steel. Fluorination of the metal samples converted the oxide film on the surface to a metal fluoride film. Under anhydrous conditions the fluoride films were very adherent and did not easily detach from the

substrate metal after mechanical flexing or thermal shock. The fluoride films were used as in-situ catalysts to affect surface polymerization of tetrafluoroethylene. An infrared spectrum of the polydifluoromethylene coating was obtained after removing the film by cross-sectioning the sides with exposed interfaces followed by soaking the edge-exposed samples in aqua-regia. The author proposed an insertion mechanism for the polymer initiation of tetrafluoromethylene by the high-valency fluorides on the metal surface.

Grunze and Lamb⁴⁴ used vapor phase polymerization to form ultra-thin polyimide films on polycrystalline silver substrates. 4,4'-Oxydianiline (ODA) and 1,2,3,5-benzenetetracarboxylic anhydride (PMDA) were sublimed, mixed in a vapor mixing chamber and then deposited on a metal substrate in the preparation chamber of an XPS system. The authors reported that PMDA and ODA chemisorbed on the clean surface under partial fragmentation and polymerized upon heating of the substrate. Their data indicated that adhesion of the polyimide film to the surface involved chemical bonding to fragmented PMDA and/or ODA chemisorbed on the surface.

Surface Analytical Techniques

Fourier Transform Infrared Spectroscopy. There are several techniques available for investigating surfaces, but many of these techniques use high energy probes that can damage the organic material being analyzed. Infrared spectroscopy on the other hand, is a photon-

intensive technique which is nondestructive; it does not alter the chemical, crystal or morphological structure of organic films. It is therefore desirable to use infrared spectroscopy to study polymers adsorbed on surfaces.

Unfortunately, there are intrinsic problems in using a transmission technique when you are only interested in obtaining information about an outer adsorbed layer. Transmission infrared spectroscopy provides information about the entire bulk material being analyzed and cannot provide information specific to the surface or interface. The problem is particularly severe in studying adsorption on metals, where the free electrons, which characterize the metals, produce very high absorption in the infrared. Greenler⁴⁵ proposed a technique for obtaining the infrared spectrum of a layer of material situated on a metal surface by reflecting radiation from the surface. In contrast, the technique of attenuated total reflection infrared spectroscopy proposed by Harrick^{46,47} is limited to the study of surface layers on materials which are transparent to the infrared.

The grazing incidence reflection technique described in in Figure 1.1. If the polarization of the incoming beam is resolved into two components, one parallel (p-polarized) and one perpendicular (s-polarized) to the plane of incidence then, as schematically shown, the s-polarized component undergoes a phase shift approximately 180° upon reflection (almost independent of the angle of incidence), and hence the reflected beam will destructively interfere with the incident beam, producing a node at the reflective surface. The p-polarized component,

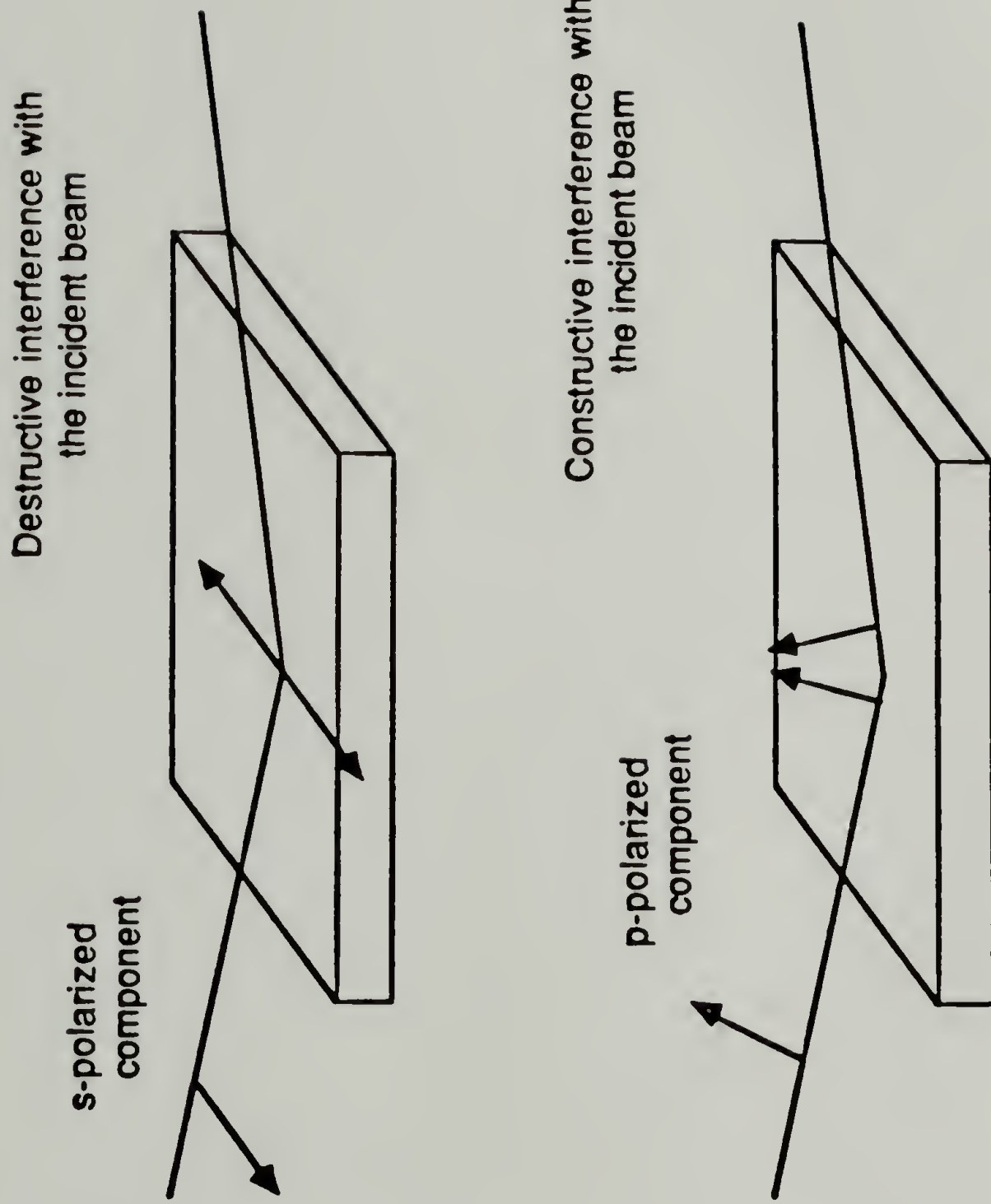


Figure 1.1 Grazing incidence reflection infrared technique

on the other hand, experiences some phase change upon reflection, varying from near zero degrees at small incident angles and approaching 180° at large angles, but the net result is an electric field component polarized normal to the reflecting surface.

The significant point of this technique is that the light reflected from the metal surface combines with the incident light to produce a standing wave electric field, into which the thin adsorbing layer is introduced, at the metal surface. The optimum arrangement is that which yields the greatest standing wave amplitude at the location of the absorbing layer. The absorption factor for infrared radiation polarized parallel to the plane of incidence typically has a maximum at an incident angle of about 88° , which varies slightly with the various optical constants of the metal surface under investigation. The absorption of a thin layer by the reflection technique, at optimum conditions, has been calculated to be about 25 times greater than by transmission through the unsupported film at normal incidence.⁴⁵

Three different experimental conditions were used to obtain IR spectra in the work described in this dissertation. All samples were analyzed on a nitrogen-purged IBM-38 Fourier transform spectrometer. A deuterated triglycine sulfate (DTGS) detector was used with a cut off at $\sim 400\text{ cm}^{-1}$. Spectra were taken at 2 cm^{-1} resolution and the interferograms were Fourier transformed using triangular apodization. Transmission IR spectra of polystyrene grafted onto platinum were taken using a similar procedure to that reported by Mosher et al.^{48,49} Samples were dispersed in KBr (0.5% w/w) by agitation for 2 minutes

using a Wig-L-Bug. The dispersions were dried under vacuum and disks were pressed in a nitrogen atmosphere. Reference spectra were obtained on pressed KBr disks.

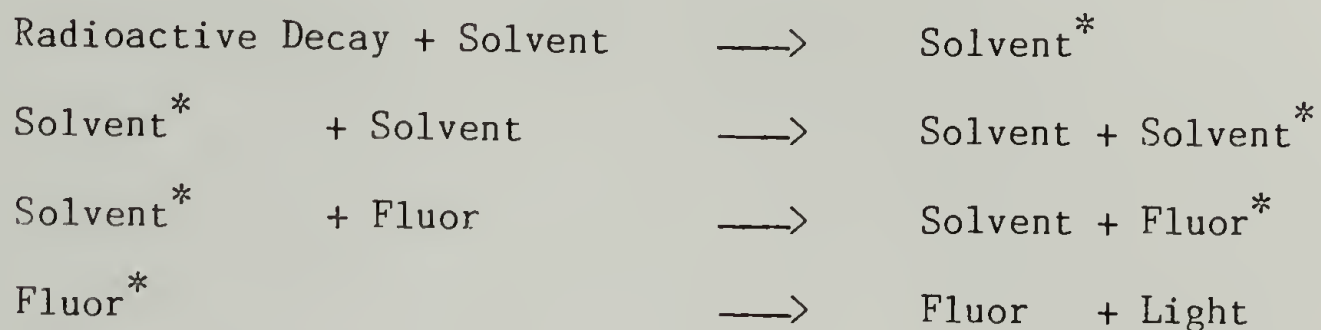
Model sulfur-functionalized polystyrene samples were synthesized for the investigation of polymer adsorption. These polymers were characterized by infrared prior to using them in the adsorption experiments. IR spectra were obtained in transmission mode of thin films cast from solution onto sodium chloride disks. Reference spectra were obtained of clean sodium chloride disks.

External reflectance infrared measurements were taken of the sulfur-functionalized polystyrene samples adsorbed to gold substrates using Greenler's reflection technique.^{45,50} Infrared spectra were taken by reflection of the incident beam at an angle of incidence of 86° using p-polarized radiation. Spectra were taken at 2 cm^{-1} resolution. Typically, 1,000 scans were averaged to yield spectra with acceptable signal-to-noise ratios. Reference spectra were obtained of freshly evaporated gold substrates.

Radioisotopic Labelling. Radioisotopic labelling was used in this dissertation to determine the amount of polymer adsorbed on a gold surface. Polymers were prepared from tritiated styrene and adsorbed from solution onto gold surfaces. Using liquid scintillation counting (LSC) the relative radioactivity of the sample was determined.

Liquid scintillation involves the detection and counting of radioactive decay. The radioactive sample to be counted is combined with a "scintillation cocktail" which usually contains a solvent, an

emulsifier and a fluor. This cocktail serves to convert the energy of the particle emitted during the radioactive decay process into light which is detected by the LS counter. The light produced is the result of the following interactions:



* = excited molecule

Part of the energy of the emitted radioactive decay is absorbed by the molecules of the solvent causing them to become excited. The number of solvent molecules that become excited is proportional to the energy of the radioactive decay being measured. The energy is transferred between solvent molecules since they are the predominant species in the cocktail. Eventually, the excited solvent molecules transfer their energy to a fluor molecule. This entire process occurs in less than 10^{-12} seconds. The fluor is now in the excited state and the solvent molecules return to the ground state. The excited fluor molecules return to the ground state by emitting light. The light emitted from the vial is directed to photomultiplier tubes, which convert it into a measurable electrical pulse. These pulses are analyzed, converted to digital form and stored in a multichannel analyzer. This data is used to determine the rate (counts per minute, CPM) of the radioactive decay in the sample.

The observed decay (CPM) is directly proportional to the actual disintegrations per minute (DPM).

$$\text{DPM} = E(\text{CPM})$$

The E is the experimentally determined detection efficiency for the radioassay method. The efficiency can be divided into an energy transfer term (quench) which is an intrinsic property of the scintillation cocktail and a geometric factor which depends upon the angle between the source and the detector as well as the geometry of the sample.

In this work only tritium was used so there was no complication of other isotopes contributing to the energy analyzed in the channel for ^3H . The radioactive polymers adsorbed to gold substrates were counted directly, after washing with clean solvent, in a xylene-based scintillation cocktail using a Beckam 3801 scintillation counter. The radioactivity (in CPM) of every polymer used was measured in dilute solution and a Beer's Law plot of mass versus CPM was drawn. It was determined that adding a 11 x 22 mm glass cover slip coated with ~150 nm of gold, to a solution of radiolabelled polystyrene decreased counting efficiency by 20%. A correction was also made to account for the geometry of the solid sample. ^3H emits low energy beta particles (28.3 keV) that cannot penetrate the gold coated glass cover slip. Therefore, it was assumed that for every 2 disintegrations that occurred only one was detected. The following is an example of how the mass of the polymer adsorbed to the substrate was determined from the scintillation results:

CPM x (Corrections for Efficiency and Geometry) = Corrected CPM

Corrected CPM => Mass, from Beer's Law relationship

Mass ÷ Area of Sample = Adsorbance (g/cm^2)

X-Ray Photoelectron Spectroscopy. X-ray photoelectron spectroscopy (XPS), also known as electron spectroscopy for chemical analysis (ESCA), provides information about approximately the outer 10 – 100 Å of a surface. In this technique samples are irradiated with monochromatic x-rays which interact with atoms in the surface region by the photoelectric effect, causing electrons to be emitted. The emitted electrons have kinetic energies given by:

$$KE = h\nu - BE - \phi_s$$

where $h\nu$ is the energy of the photon, BE is the binding energy of the atomic orbital from which the electron originates, and ϕ_s is the spectrometer work function. The emitted electrons are energy-analyzed and the results are reported in a spectrum in which the number of emitted electrons per energy interval is plotted against their kinetic energy. The kinetic energy identifies the type of element present and also something about the chemical bonding of the atom from which it came. The chemical state of an element alters the kinetic energy of the photoelectron. The effective depth of the XPS analysis depends on the mean free path of the photoelectrons and the angle of the sample relative to the analyzer axis (Figure 1.2). Consequently, one can investigate various depths of the surface in question by simply varying the angle of the sample stage. The surface sensitivity of XPS is due to

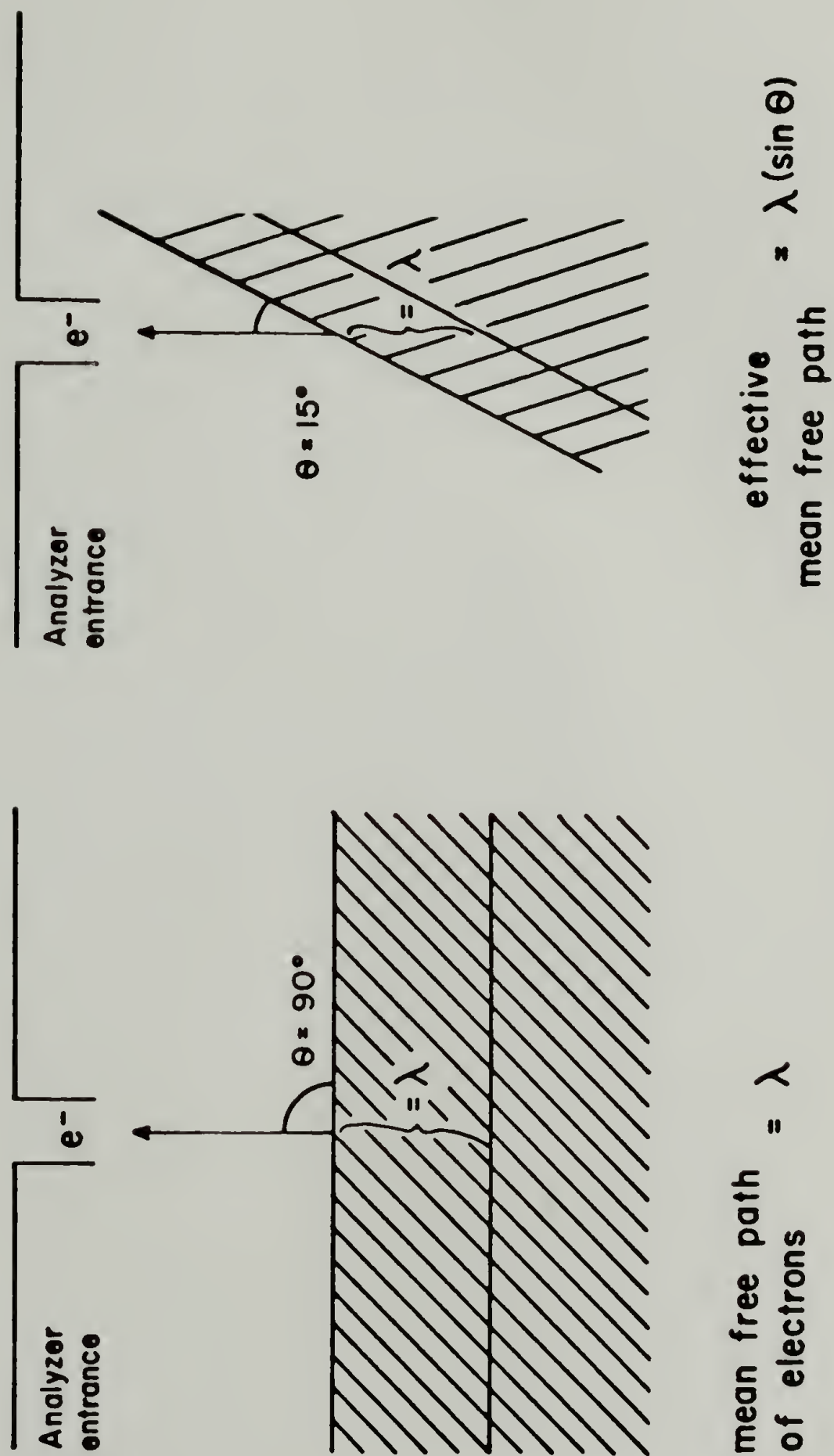


Figure 1.2 Angle-resolved XPS

the short mean free paths of photoelectrons. Even though x-rays interact with material deeper in the bulk (on the order of 1-10 micrometers), those photoelectrons generated deep in the sample are inelastically scattered. They are either self-absorbed by the sample or lose part of their kinetic energy and contribute to the spectral background.

The mean free path of photoelectrons in solids has been determined by the overlayer technique, from LEED data, and by several other techniques.⁵¹ The overlayer technique was pioneered for XPS by Siegbahn et al.⁵² and for Auger electron spectroscopy (AES) by Palmberg and Rhodin.⁵³ In this type of experiment, the intensities of photoelectrons or Auger electrons from a substrate and an overlayer film are monitored as a function of overlayer thickness. These intensities show an exponential dependence on overlayer thickness. Using the XPS overlayer technique for poly(p-xylyene) polymer films on gold substrates Clark and Thomas⁵⁴ determined the attenuation length for C_{1s} (~969 eV) to be ~14Å and for Au_{4f} (~1170 eV) to be ~22Å. These values vary slightly depending on the polymer film and the angle between the sample and analyzer, but the relative difference between the two values remains approximately the same.

The XPS spectra presented in this dissertation were obtained with a Perkin-Elmer PHI 5100 spectrometer utilizing a concentric hemispherical analyzer. The instrument resolution was ~1.8 eV for survey spectra and ~1.4 eV for multiplex spectra, a 4 mm mechanical aperture was used in conjunction with the x-ray source. The base operating pressure was

$<5 \times 10^{-9}$ torr. Samples were irradiated with monochromatic Mg K_{α} x-rays (1253.6 eV). The angle between the source and the analyzer was fixed at 45° , but the angle of the sample holder with respect to the analyzer was variable. Spectra were recorded at two angles: the sample surface 15° and 75° from the analyzer. To aid in the interpretation, the spectra obtained in these experiments were compared to standard spectra and charts listing photoelectron lines specific to each pure element.⁵⁵ Quantitative analysis of the XPS measurements were made using peak area sensitivity factors to determine the atomic composition of the sample. The computer software from the PHI 5000 series ESCA uses the following equation to calculate the atomic percentage of any element in the sample:⁵⁶

$$\% \text{ AC for element X} = \frac{I_X/S_X T_X}{\sum_{i=0}^N I_i/S_i T_i} \times 100$$

where N = number of regions (elements) surveyed

I = peak area of the 5 point smooth, baseline corrected data

S = peak area sensitivity factor

T = total acquisition time per data point

The values obtained for carbon (C_{1s}) and gold (Au_{4f}) from the atomic composition were used as a measure of the relative thickness (C/Au) of polymer films adsorbed to gold substrates.

References

1. Napper, D. Polymer Stabilization of Colloidal Dispersions; Academic Press: London, 1983.
2. Bregman, J.I. Corrosion Inhibitors; MacMillan: NewYork, 1963.
3. Epoxy Resins and Composites II; Dusek, K., Ed; Advances in Polymer Science 75; Springer-Verlag: New York, 1986.
4. Chidsey, C.E.D.; Murray, R.W. Science 1986, 231, 25.
5. Diaz, A.F. Chemica Scripta 1981, 17, 145.
6. Bowden, F.P.; Tabor, D. The Friction and Lubrication of Solids; Oxford University Press: London, 1968.
7. Murray, R.W. Acc. Chem. Res. 1980, 13, 135.
8. Park, J.B Biomaterials Science and Engineering; Plenum Press: New York, 1984.
9. Frisch, H.L.; Simha, R.; Eirich F. R. J. Chem. Phys. 1953, 21, 365.
10. Silberberg, A. J. Phys. Chem. 1962, 66, 1872.
11. DiMarzio, E.A. J. Chem. Phys. 1965, 42, 2101.
12. DiMarzio, E.A.; McCrackin, F.L. J. Chem. Phy. 1965, 43, 539.
13. Hoeve, C.A.J. J. Chem. Phys. 1965, 43, 3007.
14. Hoeve, C.A.J. J. Chem. Phys. 1966, 43, 1505.
15. Hoeve, C.A.J. J. Polym. Sci., Polym. Phy. Ed. 1970, 30, 361.
16. Hoeve, C.A.J. J. Polym. Sci., Polym. Phy. Ed. 1971, 34, 1.
17. Silberberg, A. J. Chem. Phys. 1968, 48, 2835.
18. Scheutjens, J.M.H.M.; Fleer G.J. J. Phys. Chem. 1979 83, 1619.
19. Scheutjens, J.M.H.M.; Fleer G.J. J. Phys. Chem. 1980 84, 178.
20. de Gennes, P.G. J. Phys. 1976, 37, 1445.

21. de Gennes, P.G. Scaling Concepts in Polymer Physics Cornell University: Ithaca, NY, 1979; p35.
22. Gebhard, H.; Killman, E. Ange. Makromol. Chem. 1976, 53, 171.
23. Takahashi, A.; Kawaguchi, M.; Hirota, H.; Kato, T. Macromolecules 1980, 13, 884.
24. Kawaguchi, M.; Takahashi, A.; J. Polym. Sci., Polym. Phys. Ed. 1980, 18, 2069.
25. Kawaguchi, M.; Takahashi, A.; Macromolecules 1983, 16, 631, 1465.
26. Fontana, B.J.; Thomas, J.R. J. Phys. Chem. 1961, 65, 480.
27. Kawaguchi, M.; Hayakawa, K.; Takahashi, A. Polym. J. 1980, 12, 265.
28. Kawaguchi, M.; Takahashi, A. Macromolecules 1983, 16, 635.
29. Israelachvili, J.N.; Adams, G.E. Nature (London) 1976, 262, 774.
30. Klein, J.; Nature, 1980, 288, 248.
31. Israelachvili, J.N.; Tirrell, M.; Klein, J.; Almog, Y. Macromolecules 1984, 17, 204.
32. Klein, J.; Pinus, P.; Macromolecules 1982, 15, 1129.
33. Ingersent, K.; Klein, J.; Pinus, P. Macromolecules 1986, 19, 1374.
34. Klein, J.; Luckham, P. Macromolecules 1984, 17, 1041.
35. Klein, J.; Luckham, P. Macromolecules 1985, 18, 721.
36. Klein, J.; Luckham, P. Macromolecules 1986, 19, 2007.
37. Hadziioannou, G.; Patel, S.; Granick, S.; Tirrell, M. J. Am. Chem. Soc. 1986, 108, 2869.
38. Murray, R.W.; Pickup, P.G. J. Electrochem. Soc. 1984, 131, 833.
39. Diaz, A.F.; Kanazawa, K.K.; Gardini, G.P. J. Chem. Soc. Chem. Comm. 1979, 635.
40. Papirier, E.; van Tao, Nguyen; Donnet, J.-B. J. Polym. Chem., Polym. Lett. Ed. 1971, 9, 195.
41. Papirier, E.; van Tao, Nguyen J. Polym. Chem., Polym. Lett. Ed. 1972, 10, 167.

42. Tsubokawa, N.; Fumaki, A.; Hada, Y.; Sone, Y J. Polym. Sci., Polym. Chem. Ed. 1982, 20, 3297.
43. Toy, M.S. J. Polym. Sci.: Part C 1971, 34, 273.
44. Grunze, M.; Lamb, R.N. Chem. Phys. Lett. 1987, 133, 283.
45. Greenler, R.G. J. Chem. Phys. 1966, 44, 310.
46. Harrick, N.J. J. Opt. Soc. Am. 1965, 55, 851.
47. Harrick, N.J. Internal Reflection Spectroscopy; Wiley Interscience: New York, 1967.
48. O'Reilly, J.M.; Mosher, R.A. Carbon 1983, 21, 47.
49. Prest, W.M., Jr.; Mosher, R.A. In Reprographic Technology; ACS Symposium Series 200; American Chemical Society; Washington, DC, 1982, pp 225-247.
50. Greenler, R.G. J. Vac. Sci. Technol. 1975, 12, 1410.
51. Powell, C.J. Surface Science 1974, 44, 29.
52. Siegbahn, K.; Nordling, C.; Fahlman, A.; Nordberg, R.; Hamrin, J.; Hedman, J.; Johansson, G.; Bergmark, T.; Karlsson, S. -E.; Lingren, I.; Lindberg, B ESCA-Atomic, Molecular and Solid State Structure Studied by Means of Electron Spectroscopy Almqvist and Wiksells: Uppsula, 1967.
53. Palmberg, P.W.; Rhodin, T.N. J. Appl. Phys. 1968, 39, 2425.
54. Clark, D.T; Thomas, H.R. J. Polym Sci., Polym. Chem. Ed. 1977, 15, 2843.
55. Wagner, C.D.; Riggs, W.M.; Moulder, J.F.; Muilenberg, G.E., Ed. Handbook of X-Ray Photoelectron Spectroscopy; Perkin-Elmer: Eden Prairie, MN, 1979.
56. Technical Manual: 5000 Series ESCA Systems; Perkin-Elmer Physical Electronics Division; Perkin-Elmer: Eden Prairie, MN, 1980.

Chapter II

EXPERIMENTAL

Synthetic Methods

This section describes the apparatus and the glassware used to synthesize materials and perform the experiments discussed in later sections. It also includes the purification of all materials used in this dissertation.

Material Handling and Purification Techniques

Most of the compounds used and the materials synthesized in this dissertation are sensitive to air and water therefore necessitating the use of inert atmosphere techniques.^{1,2,3} All experiments and transfers described in this dissertation were performed under an atmosphere of prepurified nitrogen unless specified.

The gas lines were constructed out of 1/4 inch copper tubing with brass Swagelock fittings. For nitrogen, connections were made to the gas line with 1/4 inch Tygon tubing. Syringe needles held in male Luerlocks were connected to the end of the Tygon tubing. For hydrogen, a flexible coil of 1/8 inch copper tubing was connected to the 1/4 inch tubing. An 18 gauge needle was attached to the 1/8 inch tubing by a stainless steel Swagelock fitting.

The transfer of liquids via cannula was performed by applying a positive pressure of nitrogen through the septum of the source flask and allowing excess nitrogen pressure in the receiving flask to pass out through a needle in the septum which was connected to a bubbler. For

quantitative transfers a gastight syringe was employed; larger quantities were transferred to a septum-capped graduated cylinder, which had been evacuated and filled with nitrogen. Solids which are sensitive to water and/or oxygen were manipulated in a Vacuum Atmospheres glove box.

The vacuum line used to perform the experiments described in this dissertation is depicted in Figure 2.1. The line, along with the other custom-made glassware described below, was crafted by the glassblowers of the University of Massachusetts Glass Shop. The vacuum line was connected to a Precision vacuum pump through a liquid nitrogen cooled trap. Typical base operating pressure for the vacuum line was 0.05 mm Hg as measured by a Teledyne-Hastings vacuum gauge and meter.

Custom-made Schlenk glassware was used as reaction flasks and for the storage of purified solvents and reagents under nitrogen. A typical storage flask is shown in Figure 2.2. It has only one opening in which a 14/20 F female connection is attached to a 4 mm straightbore Teflon stopcock. The 14/20 connection is used to temporarily attach the flask to the vacuum manifold where it is evacuated and filled with nitrogen. After the stopcock is closed, the flask is removed from the manifold. The 14/20 opening is covered with a septum and secured with copper wire. Nitrogen is blown via needles through the headspace above the stopcock; the needles are removed leaving a positive pressure of nitrogen. This headspace allows one to open and close the flask repeatedly while always maintaining a nitrogen atmosphere. Anionic polymerizations were performed in 50-mL Schlenk tubes (Figure 2.3) using magnetic stirbars

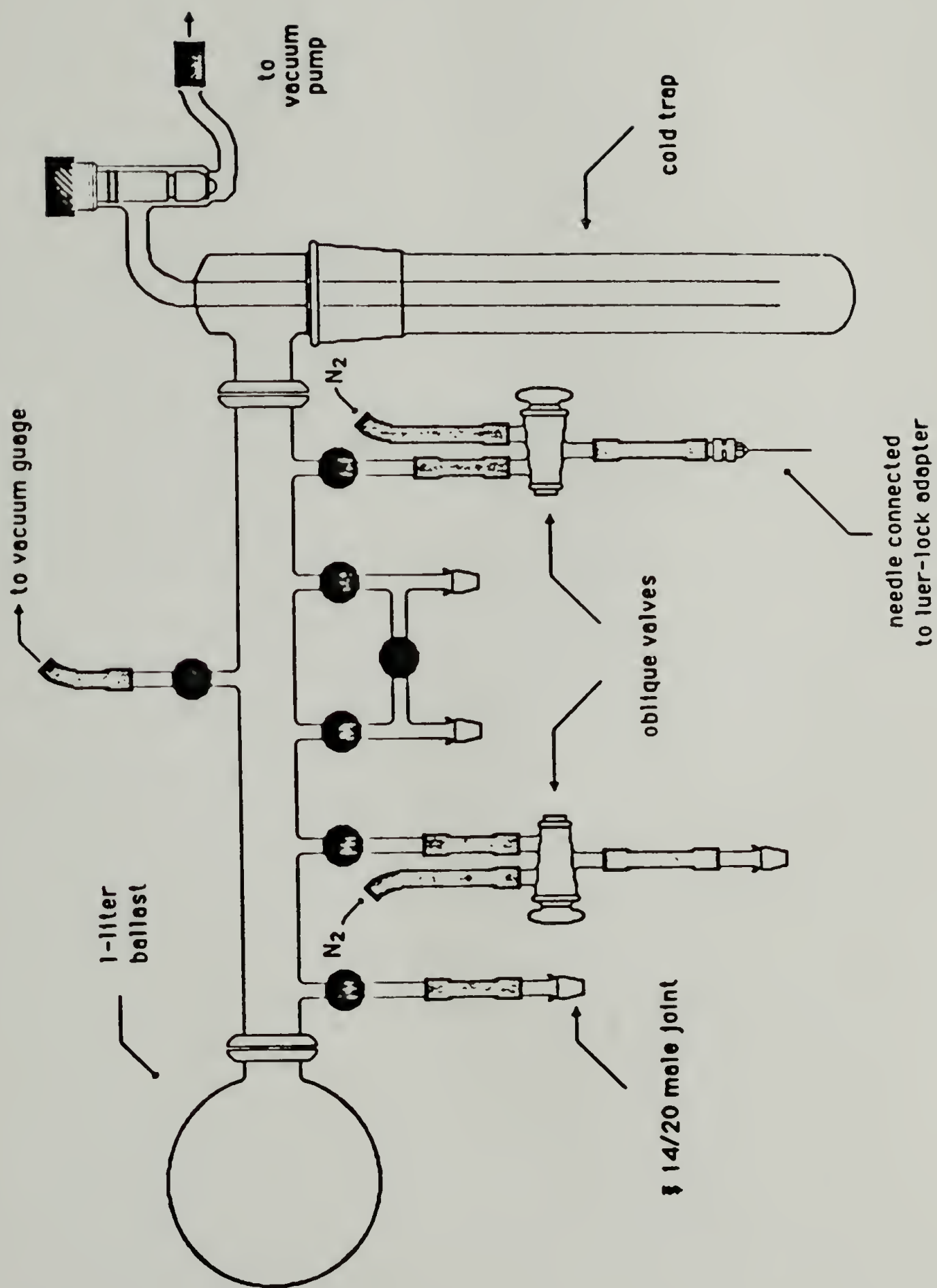


Figure 2.1 Vacuum manifold

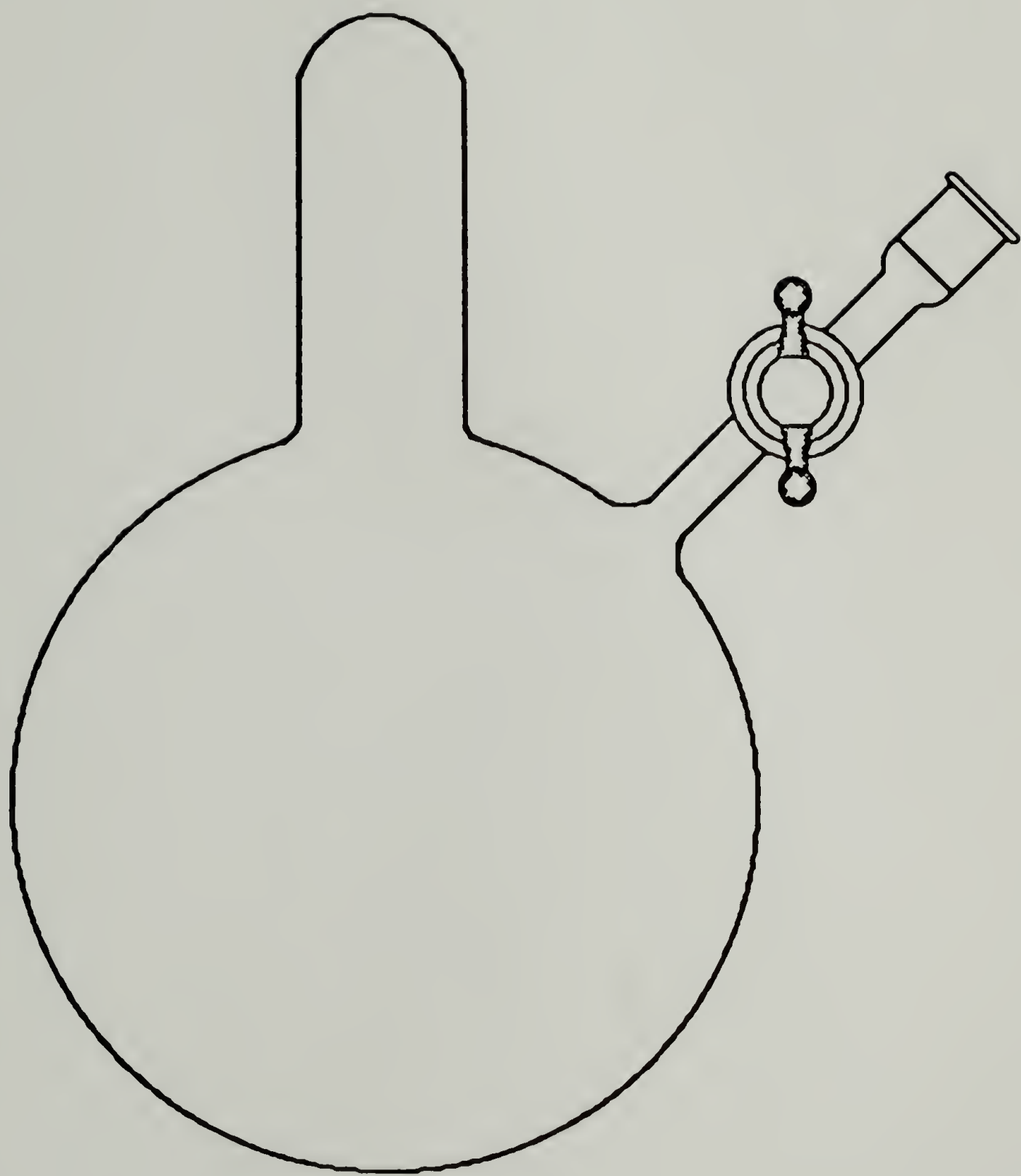


Figure 2.2 Storage flask



Figure 2.3 Schlenk tube for polymerizations

small enough to fit through the stopcock. For polymer adsorption experiments a substrate had to be placed in the tube so the original design was modified to include a wide opening (Figure 2.4). This opening terminated in a #25 O-ring with a matching cap which was held in place with a #35 Thomas clamp. Using this tube the substrate was placed in the flask prior to evacuation, then all subsequent additions and removals of liquids were performed via cannula through the stopcock.

The purifications described below were those employed in the work described in this dissertation. Other procedures could have been used to produce clean, dry material and the reader is referred to Perrin and Perrin⁴ for such examples. Distillations were run through a 10 cm Vigreux column. Continuous distillations were run under nitrogen using the distillation head shown in Figure 2.5 which was attached to a reservoir containing the drying agent. Distillations run at reduced pressure were monitored with a mercury manometer and regulated with a Manowatch (I²R Company). Trap-to-trap distillations were performed using the apparatus shown in Figure 2.6. The solution was frozen with liquid nitrogen (-196°C), the frozen solution was opened to the vacuum until minimum pressure was observed, the liquid nitrogen was removed from the frozen solution and placed under the trap and the solution was allowed to warm to room temperature. Solutions were degassed by repeated freeze-pump-thaw cycles in which the solution was frozen with liquid nitrogen in a round bottom flask attached to the vacuum manifold; the frozen solution was opened to the vacuum until minimum pressure was observed, then the stopcock was closed and the solution was allowed to thaw.

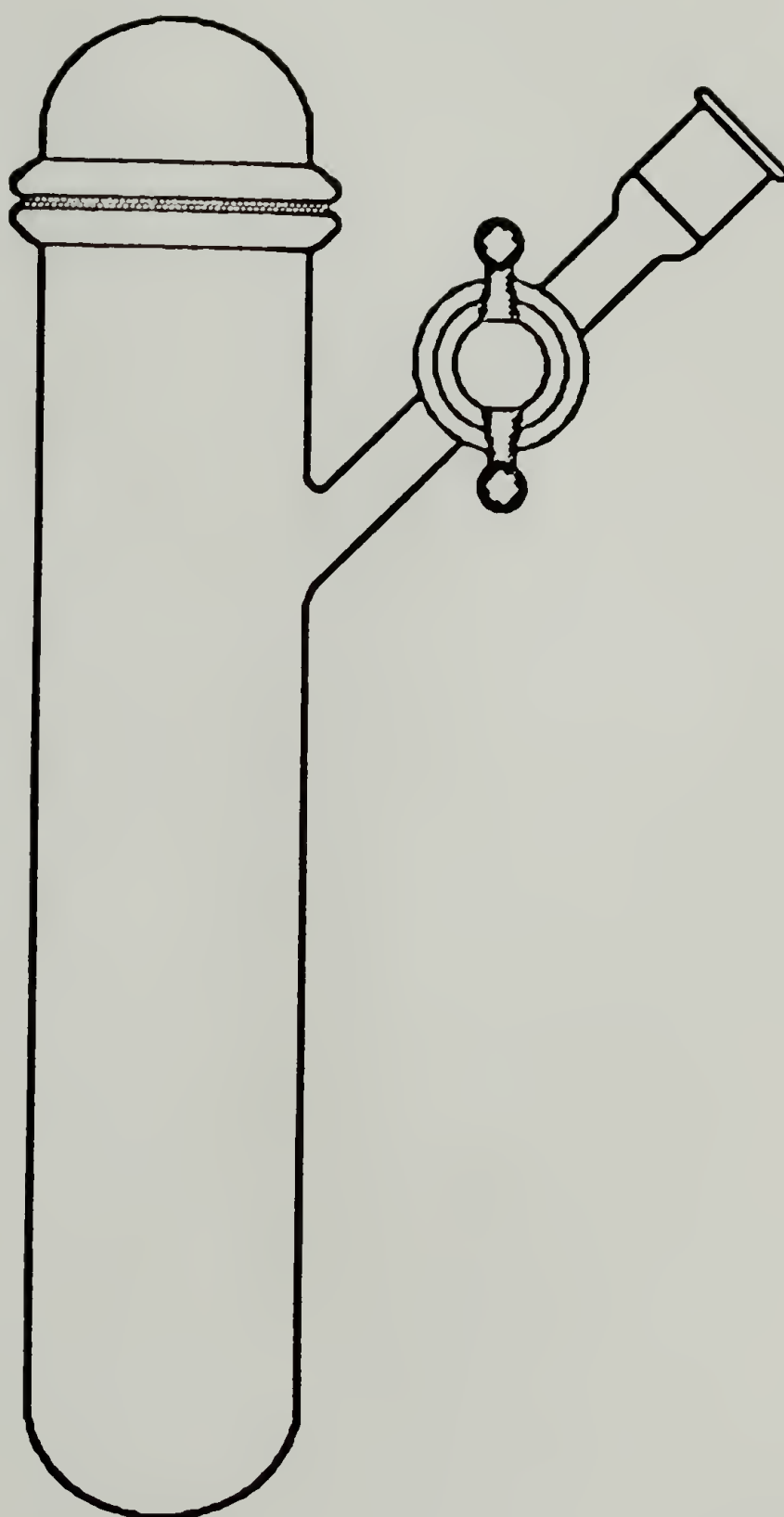


Figure 2.4 Schlenk tube for polymer adsorption

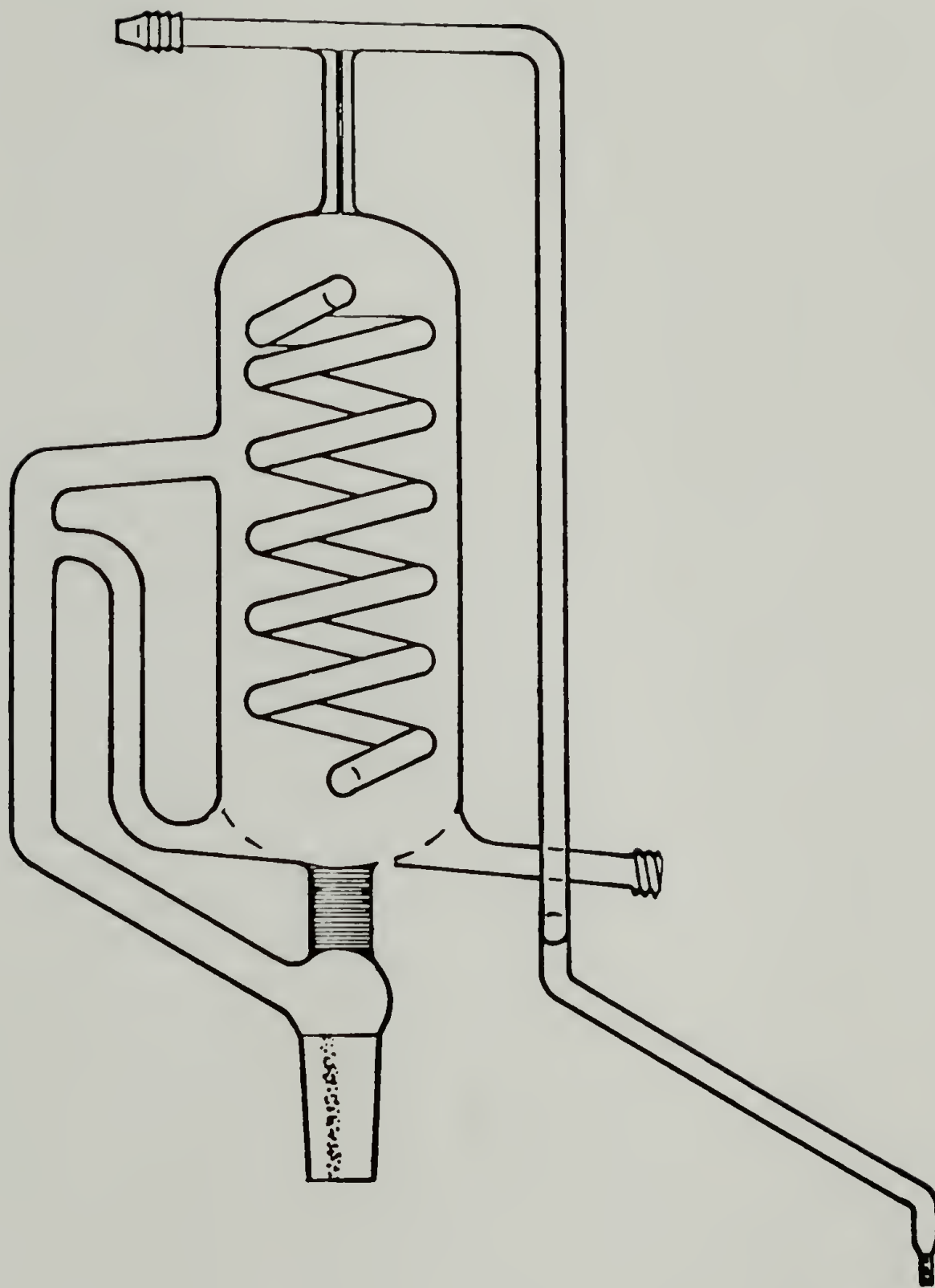


Figure 2.5 Continuous distillation apparatus

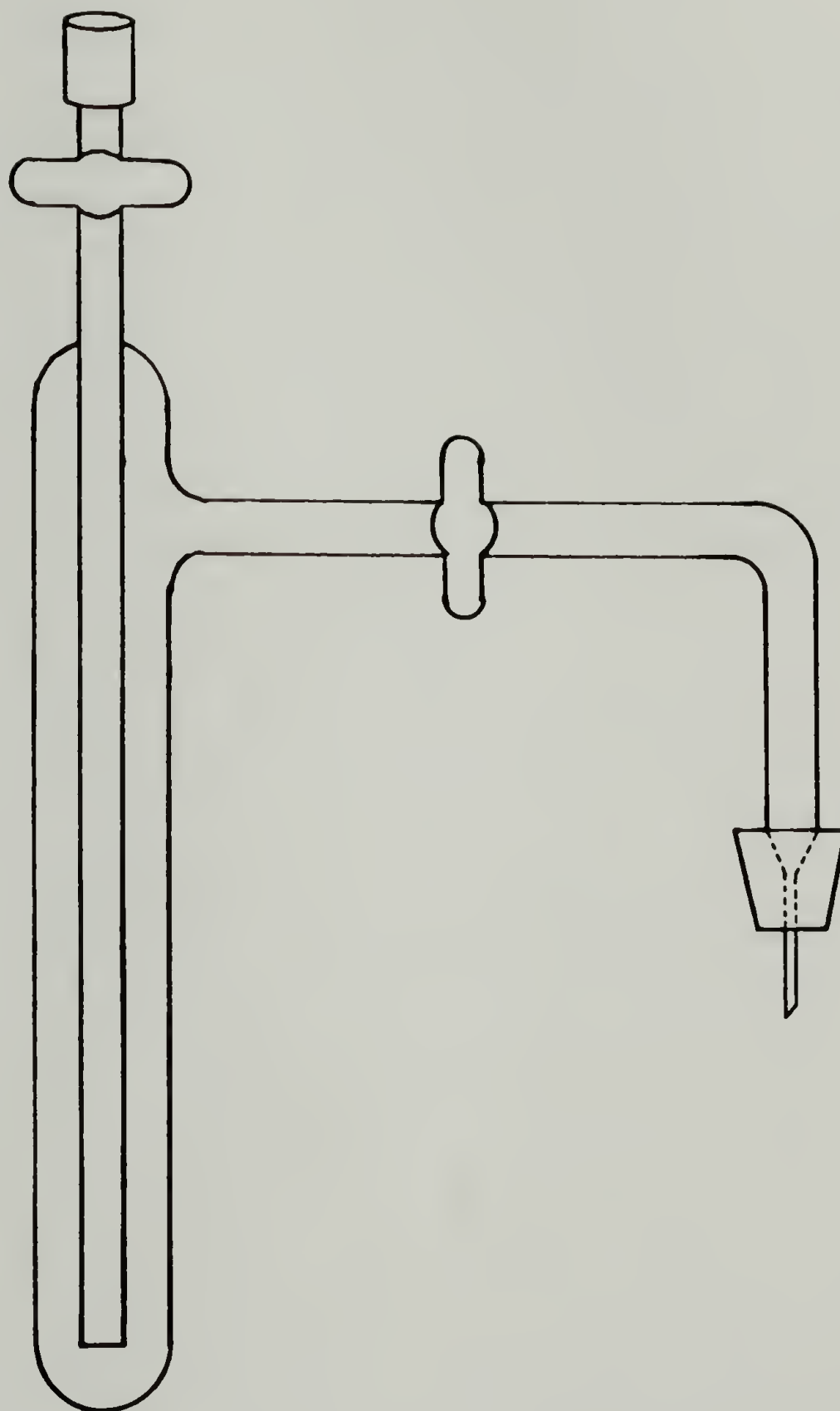


Figure 2.6 Trap-to-trap distillation apparatus

Purification of Solvents

Benzene (Fisher, bp 80.2°C) was distilled from sodium benzophenone dianion and stored under nitrogen.

Cyclohexane (Aldrich, bp 80.7–81°C) was distilled from calcium hydride and stored under nitrogen.

Pentane (Fisher, bp 35–36°C) was deolefinated by stirring over concentrated sulfuric acid for 24 hours and distilled from lithium aluminum hydride and stored under nitrogen.

Tetrahydrofuran (American Burdick and Jackson, spectrophotometric grade containing no inhibitors, bp 67°C) was continuously distilled from sodium benzophenone dianion and stored under nitrogen.

Toluene (Fisher, bp 111°C) was distilled from calcium hydride and stored under nitrogen.

To obtain the deep purple color of the sodium benzophenone dianion necessary for dry, oxygen-free distillations the following procedure was used. A bottle of HPLC grade solvent (uninhibited) was capped with a septum and secured with copper wire. A septum stoppered Schlenk flask containing a magnetic stirbar was purged with nitrogen. The solvent was transferred to the flask via cannula and sparged with nitrogen for 1 hour. Benzophenone (2 g/L) and freshly cut sodium (1 g/L) were added to the flask under a stream of nitrogen. The mixture was stirred under a static positive pressure of nitrogen until the deep purple color was obtained.

Purification of Reagents

Benzenethiol (Aldrich, bp 169°C) was distilled from calcium sulfate at reduced pressure (20 mm Hg) and stored under nitrogen.

Cyclohexene (Aldrich, bp 83°C) was distilled from sodium sulfate and stored under nitrogen.

Ethanethiol (Aldrich, bp 35°C) was distilled from calcium sulfate and stored under nitrogen.

Ethyl bromide (Aldrich, bp 37-40°C) was distilled from phosphorous pentoxide and stored under nitrogen.

Ethylene sulfide (Aldrich, bp 55-56°C) was distilled from calcium hydride and stored under nitrogen at 4°C.

1-Pentene (Aldrich, bp 29.9-30.1°C) was distilled from calcium hydride and stored under nitrogen.

Phenylacetylene (Aldrich, 142-144°C) was distilled from calcium hydride at reduced pressure (20 mm Hg) and stored under nitrogen at 4°C.

4-Picoline (Aldrich, bp 145°C) was distilled from calcium hydride at reduced pressure (20 mm Hg) and stored under nitrogen.

Propylene sulfide (Aldrich, bp 72-75°C) was distilled from calcium hydride and stored under nitrogen at 4°C.

Pyridine (Aldrich, bp 115°C) was distilled from calcium hydride and stored under nitrogen.

Styrene (Fisher, bp 145-146°C) was distilled from calcium hydride at reduced pressure (20 mm Hg) and stored under nitrogen at -20°C.

4-Vinylpyridine (Aldrich, bp 62-65°C (15 mm Hg)) was distilled from calcium hydride at reduced pressure (15 mm Hg) and stored under nitrogen

at 4°C.

³H-Water (New England Nuclear, 1 mL of 100 mCi/mL) was degassed by freeze-pump-thaw cycles repeated three times and stored under nitrogen.

The following reagents were used as received:

4-Biphenylmethanol (Aldrich, mp 99-101°C)

Bis(1,2 di-p-tolylphosphino)ethane (Strem, mp 145-148°C)

n-Butyllithium (Aldrich, 1.6M or 2.5M in hexanes)

sec-Butyllithium (Aldrich, 1.6M in hexanes)

Calcium hydride (Aldrich)

Calcium sulfate (Aldrich)

4,4'-Dimethyl-2,2'-bipyridine (Strem, mp 171-175°C)

Gold, 0.5 mm wire (Alfa, >99.999% pure)

Lithium aluminum hydride (Aldrich)

Methanol (Fisher, bp 64.6°C)

OCS scintillation cocktail (Amersham)

Palladium on calcium carbonate poisoned with lead, 5% Pd,
Lindlar's Catalyst (Aldrich)

Phosphorous pentoxide (Aldrich)

Platinum black, 24 m²/g (Aldrich)

Platinum on alumina support, 5% Pt (Aldrich)

Potassium bromide (Aldrich, Gold Label)

Sodium sulfate (Aldrich)

Sulfuric acid, concentrated (Fisher)

Triethylphosphine (Strem, bp 126-128°C)

Triphenylphosphine (Strem, mp 79–81°C)

Tri-p-tolylphosphine (Strem, mp 145–148°C)

Methods and Instrumentation

This section will discuss only those methods not already covered in detail in the Introduction.

Elemental Analysis. Elemental analyses for carbon, hydrogen, nitrogen and sulfur were determined in the Microanalytical Laboratory at the University of Massachusetts by Dr. G. Dabkowski and Dr. M.E. DeCheke. A complete discussion of the procedures employed by this laboratory can be found in Modern Organic Elemental Analysis.⁵ Carbon and hydrogen were determined by the Pregl-Lieb procedure using a Perkin-Elmer 240 Elemental Analyzer. The organic material (1–3 mg) was decomposed by oxidation at ~1000°C converting the carbon to carbon dioxide and the hydrogen to water. The same instrument was used to determine nitrogen by the Dumas method in which organic nitrogen is oxidized to nitrogen oxides then reduced with copper to N₂. Organic sulfur was combusted in a closed Schoeniger flask under static oxygen to produce sulfates; elemental sulfur was determined by titration of an alcohol solution of the sulfates.

Gas Chromatography and Kinetic Analysis. Gas chromatographic analyses were performed with a Hewlett Packard 5790A gas chromatograph and 3390A recorder-integrator. The platinum-catalyzed olefin hydrogenation of cyclohexene to cyclohexane in a pentane solution was monitored by GC on a 6ft x 1/8in column packed with 15%

tris(cyanoethoxy)propane on 80/90 F-1 alumina. The column temperature was 100°C, the injection port was 200°C and the detector was at 250°C. The carrier gases were at the following pressures: nitrogen 60 psig (30.0 mL/min), hydrogen 15 psig and air 27 psig. A one microliter sample was injected and the compounds eluted with retention times of: pentane in 1.53 minutes, cyclohexane in 3.02 minutes and cyclohexene in 3.68 minutes. The percentage of cyclohexene was determined from the relative peak areas of cyclohexane and cyclohexene; identical molar response factors were assumed.

| Example: | <u>Compound</u> | <u>Relative Areas (Time t)</u> |
|----------|-----------------|--------------------------------|
| | Cyclohexane | 0.5 |
| | Cyclohexene | 3.6 |

$$\% \text{ Cyclohexene} = \frac{0.5}{0.5 + 3.6} = .878$$

$$[\text{Cyclohexene}] \text{ at time } t = (.878)(\text{Initial Concentration})$$

Kinetic analysis of the rate of platinum catalyzed olefin hydrogenation was performed by monitoring the decrease in concentration of olefin over time. The concentration of olefin at time t during the progress of the reaction was determined by GC as described above. The concentration of olefin was plotted as a function of time.

Gel Permeation Chromatography. The molecular weight distributions of the polymers were determined by GPC using a Rainin Rabbit-HP pump with Polymer Laboratories 5 μ m PL gel columns (10², 10³, 10⁴ Å) and a Knauer refractive index detector. The solvent was toluene which was

continuously distilled and supplied directly to the instrument. The GPC had been interfaced to an Apple IIe computer and molecular weight calculations were made relative to polystyrene molecular weight standards using IMI Chromatix GPC software. Samples were prepared by dissolving the polymer in freshly distilled toluene (2 mg/mL). The polymer solution was filtered and a sample was injected into the instrument through a second filter.

Gravimetric Analysis. Gravimetric measurements were made using a Cahn 29 Electrobalance with an ultimate sensitivity of 1×10^{-7} g. The balance was stabilized against static charging with a polonium source.

Proton Nuclear Magnetic Resonance. ^1H -NMR spectra were obtained using a Varian XL-200. Samples were dissolved in CDCl_3 or C_6D_6 containing 1% TMS.

Ultraviolet-Visible Light Spectrophotometry. UV-vis spectra were recorded using a Perkin-Elmer Lambda 3A spectrophotometer. The instrument was zeroed with pentane in the sample and reference cells. The cells were modified with tops containing small ground glass stopcocks and septa to avoid evaporation of the pentane. The spectra were recorded from 430 to 190 nm at 120 nm/min with the absorbance range set at 0.000 to 1.000 absorbance units.

Platinum-Catalyzed Hydrogenation of Olefins

This section describes experiments which were performed to investigate the coordination chemistry of platinum. By monitoring the reaction rate of olefin hydrogenation over platinum we were able to

determine if a ligand added to the reaction mixture would bind to the platinum surface. Initially a series of potential catalyst poisons were surveyed to determine which were good candidates to be coordinating ligands. Once a single poison was chosen, its effect on the platinum-catalyzed hydrogenation of cyclohexene and its coordination with platinum were studied in detail.

Hydrogenation of Cyclohexene to Cyclohexane over a Platinum

Supported Catalyst. (1:49, 50, 55) Platinum supported on alumina ($\text{Pt}/\text{Al}_2\text{O}_3$) 5% Pt (0.15 g, 3.85×10^{-5} mole Pt) was placed in a 20-mL pressure tube containing a small magnetic stir bar. A rubber seal and a metal cap with two holes, were placed on top of the tube which was capped with a bottle capper. The tube was evacuated and filled with nitrogen. A solution of cyclohexene in pentane (3 mL, 0.247 M, 7.41×10^{-4} mole cyclohexene) was added by syringe. The stirred system was charged with hydrogen (15 psig) and kinetic samples were taken at 15, 30 and 60 minutes. A control reaction of the same solution with no catalyst was run simultaneously.

Platinum on Alumina-Catalyzed Olefin Hydrogenation Poisoned with Tris(2-cyanoethyl)phosphine and Tri-*p*-tolylphosphine. (1:63)

Hydrogenations were carried out in five, 20-mL pressure tubes fitted with rubber seals and bottle caps. Platinum on alumina (0.15 g, 3.85×10^{-5} mole Pt) was placed in each tube along with a magnetic stir bar. A control reaction contained no poison. Tris(2-cyanoethyl)phosphine was added to two of the tubes: 7.4 mg (3.85×10^{-5} mole) to one and 14.8 mg (7.70×10^{-5} mole) to another. Tri-*p*-tolylphosphine was placed in the

remaining tubes (0.0120g, 3.85×10^{-5} mole and 24.0 mg, 7.70×10^{-5} mole). The tubes were capped, evacuated and filled with nitrogen. A solution of cyclohexene in pentane (3 mL, 0.247M, 7.41×10^{-4} mole cyclohexene) was added by syringe. The stirred system was charged with hydrogen (15 psig) and kinetics samples were taken after 15 and 30 minutes.

Platinum on Alumina-Catalyzed Olefin Hydrogenation Poisoned with various Concentrations of Tris(2-cyanoethylphosphine). (1:69)

Hydrogenations, were run and sampled as described above. Five tubes were prepared with catalyst (3.85×10^{-5} mole Pt), one without any poison and four with various amounts of tris(2-cyanoethylphosphine): 0.01 g (5.18×10^{-5} mole), 0.02 g (1.04×10^{-4} mole), 0.03 g (1.55×10^{-4} mole) and 0.04 g (2.07×10^{-4}).

Platinum on Alumina-Catalyzed Olefin Hydrogenation Poisoned with Pyridine, 4-Picoline, Benzenethiol and Bis(1,2 di-p-tolylphosphino)ethane. (1:75) Platinum on alumina (0.10 g, 2.56×10^{-5} mole Pt) was placed in five pressure tubes. Bis(1,2 di-p-tolylphosphino)ethane (0.01 g, 2.20×10^{-5} mole) was added to one of the tubes, then all of the tubes were capped, evacuated and filled with nitrogen. A solution of cyclohexene in pentane (3 mL, 0.247 M, 7.41×10^{-4} mole cyclohexene) was added to each. To three of the tubes the following liquid poisons were added by syringe: pyridine (0.1 mL, 1.24×10^{-3} mole), 4-picoline (0.1 mL, 1.03×10^{-3} mole), benzenethiol (0.1 mL, 9.74×10^{-4} mole). The stirred systems were charged with hydrogen (15 psig) and kinetics samples were taken after 15 and 30

minutes.

Platinum on Alumina-Catalyzed Olefin Hydrogenation Poisoned with Pyridine, Benzenethiol, Triethylphosphine and Dimethyl-bipyridine.

(1:87) Platinum on alumina (0.10 g, 2.56×10^{-5} mole Pt) was placed in five pressure tubes. 4,4'-Dimethyl-2,2'-bipyridine (5.0 mg, 2.71×10^{-5} mole) was added to one of the tubes. All of the tubes were capped, evacuated and filled with nitrogen. A solution of cyclohexane in pentane (3 mL, 0.247 M, 7.41×10^{-4} mole cyclohexene) was added by syringe to each tube. To three of the tubes the following liquid poisons were added by syringe: pyridine (0.002 mL, 2.48×10^{-5} mole), benzenethiol (0.002 mL, 1.95×10^{-5} mole) and triethylphosphine (0.0026 mL, 2.73×10^{-5} mole). The stirred systems were charged with hydrogen and kinetics samples were taken after 1, 2, 3 and 10 minutes.

Platinum on Alumina-Catalyzed Olefin Hydrogenation Poisoned with Ethanethiol, Benzenethiol, Triethylphosphine, Triphenylphosphine, Pyridine and 4-Picoline. (1:125) Platinum on alumina (0.10 g, 2.56×10^{-5} mole Pt) was placed in seven pressure tubes. Triphenylphosphine (6.7 mg 2.55×10^{-5} mole) was added to one of the tubes. All of the tubes were capped, evacuated and filled with nitrogen. A solution of cyclohexene in pentane (3 mL, 0.247 M, 7.41×10^{-4} mole cyclohexene) was added by syringe to each tube. The following liquid poisons were added by syringe: ethanethiol (0.002 mL, 2.73×10^{-5} mole), benzenethiol (0.002 mL, 1.91×10^{-5} mole), triethylphosphine (0.0026 mL, 2.73×10^{-5}), 4-picoline (0.0026 mL, 2.68×10^{-5} mole). The stirred systems were charged with hydrogen (15 psig) and kinetics samples were taken

after 2 1/2, 5 and 10 minutes.

Hydrogenation of Cyclohexene to Cyclohexane Using Various Concentrations of a Platinum Black Catalyst. (1:149; 2:13, 19, 23)

Platinum black (5 mg, 2.56×10^{-5} mole; 10 mg, 5.13×10^{-5} mole; 26 mg, 1.43×10^{-4} mole) and a magnetic stir bar were placed in a three pressure tubes; the tubes were capped, evacuated and filled with nitrogen. A solution of cyclohexene in pentane (3 mL, 0.247 M, 7.41×10^{-4} mole cyclohexene) was added by syringe to each tube. The stirred systems were charged with hydrogen (15 psig) and kinetics samples were taken after 1, 2, 4 and 8 minutes.

Platinum-Catalyzed Hydrogenation of Cyclohexene Using Various Concentrations of Olefin. (2:31,37) Platinum black (5 mg, 2.56×10^{-5} mole) and a magnetic stir bar were placed in pressure tubes; the tubes were capped, evacuated and filled with nitrogen. Solutions of cyclohexene in pentane (6 mL, 0.247 M, 1.48×10^{-3} mole cyclohexene; 6 mL, 0.123 M, 7.41×10^{-4} mole cyclohexene) were added by syringe. The stirred systems were charged with hydrogen (15 psig) and kinetics samples were taken after 1, 2, 4 and 8 minutes.

The same procedure was run using only 3 mL of the pentane solutions of cyclohexene (3 mL, 0.123 M, 3.69×10^{-4} mole cyclohexene; 3 mL, 0.247 M, 7.41×10^{-4} mole cyclohexene; 3 mL, 0.494 M, 1.48×10^{-3} mole cyclohexene) (2:45, 51, 57).

Platinum-Catalyzed Olefin Hydrogenation Poisoned with 4-Picoline. (2:81, 85, 93, 101) Hydrogenations were carried out in 20-mL pressure tubes fitted with rubber seals and bottle caps. Platinum black

(10 mg, 5.13×10^{-5} mole) was placed in a tube with a magnetic stir bar; the tube was capped, evacuated and filled with nitrogen. A solution of cyclohexene in pentane (5.9 mL, 0.247 M, 1.46×10^{-3} mole cyclohexene) was added by syringe. If the catalyst was to be poisoned, 0.1 mL of a solution of 4-picoline in pentane (0.513 M, 5.13×10^{-5} mole 4-picoline) was added. The stirred system was charged with hydrogen (15 psig) and kinetics samples were taken every 60 seconds.

Adsorption of 4-Picoline on Platinum

This section describes experiments used to quantitate the adsorption of 4-picoline on platinum. Once 4-picoline was adsorbed, the strength of the interaction was investigated.

Dilute Solutions of 4-Picoline in Pentane for Beer's Law

Justification. (3:121; 5:105) A stock solution of 4-picoline in pentane (5×10^{-5} v/v) was prepared by adding 0.01 mL of 4-picoline to a storage flask by syringe, then diluting this to 200 mL with pentane. A specific volume of this pentane solution was added to a 10-mL volumetric flask by syringe, then diluted to the mark with pentane. Seven solutions were prepared and the UV-vis absorbance spectra were obtained. The absorbance at 254 nm was plotted against concentration.

UV-vis Analysis of 4-Picoline Adsorbed to Platinum Black. (3:123, 127, 129, 149; 4:11, 13, 15) Platinum black (10 mg, 5.13×10^{-5} mole) was placed in a pressure tube which was subsequently capped, evacuated and filled with nitrogen. A control experiment was performed along side which did not contain platinum. A solution of 1-pentene in pentane (6.0

mL, 0.046 M, 2.74×10^{-4} mole 1-pentene) was introduced to each tube via cannula and the tubes were pressurized with hydrogen (15 psig). The tubes were agitated using a Fisher Vortex Genie. GC analysis indicated that 1-pentene was being reduced in the tube containing platinum. (Platinum black agglomerates while reducing olefins and in practice, this is a convenient indication of an active platinum catalyst.) The olefin solutions were removed via cannula and the platinum was dried with a slow stream of nitrogen. A solution of 4-picoline in pentane (6.0 mL, 5.13×10^{-4} M, 3.02×10^{-6} mole 4-picoline) was introduced to each tube, the tubes were agitated using the Vortex Genie and the platinum was allowed to settle. The solutions were transferred via cannula to UV-vis cells which were modified with a stopcock and ground glass joint.

Attempted Removal of 4-Picoline from Platinum with Solvent. (5:15, 17) 4-Picoline was adsorbed to platinum black as described above. All of the 4-picoline solution was removed from the pressure tube by cannula and the platinum was dried under a slow stream of nitrogen. 6.0 mL of fresh pentane was added to the tube and agitated using the Vortex Genie. After 12 hours the solutions were transferred to UV-vis cells.

Gravimetric Analysis of 4-Picoline Adsorbed to Platinum Black. (3:91, 93, 105, 107, 109, 117, 131, 133, 139, 141, 143, 145, 147, 151; 4:35, 43, 45, 53, 57, 67, 69) A Teflon "envelope" container was prepared by heat-sealing two filters together with a soldering pencil. An open container was weighed, platinum was added and the container was reweighed. The container was completely heat-sealed and weighed again.

A control container (no platinum) was prepared and weighed. The containers were placed in a flask which was subsequently evacuated and filled with nitrogen. A solution of 1-pentene in pentane (6.0 mL, 0.046 M, 2.74×10^{-4} mole 1-pentene) was added and the flask was pressurized with hydrogen (15 psig). After 10 minutes, the olefin solution was removed and the containers were dried at 0.02 mm Hg for 24 hours. The containers were exposed to 4-picoline vapor (generated by allowing a frozen sample to thaw in a chamber connected to the evacuated flask) for 60 minutes. Excess vapor was removed and the containers were dried under vacuum to constant weight.

Synthesis of a Platinum-Polystyrene Interface

This section describes the synthesis of a platinum-polystyrene interface in which the graft polymerization of styrene from the platinum surface was initiated by picolyl carbanions bound to the platinum. The synthesis of picolyl anion-initiated polystyrene in the absence of platinum is also described.

Picolyl Anion-Initiated Polymerization of Styrene. (4:29, 33, 37, 39, 49, 63, 81; 5:83, 85, 93, 95; 6:87) Reactions were carried out in 50-mL Schlenk tubes containing small magnetic stir bars. The tubes were evacuated and filled with nitrogen. THF (10 mL) and 4-picoline (0.038 mL, 3.9×10^{-4} mole) were added and the tubes were cooled to -78°C . n-Butyllithium (3.1 mL, 0.123 M, 3.8×10^{-4} mole) was added dropwise to the stirred solution and allowed to react for 2 hours. Styrene (0.1 - 2.0 mL, 8.73×10^{-4} - 1.75×10^{-2} mole, depending on desired molecular

weight) was introduced and the tube was removed from the cold bath and allowed to warm to room temperature, at which temperature it was held for 30 minutes. The reaction was quenched with a small amount of methanol. High molecular weight polymer ($M_n > 2,000$) was precipitated in methanol and collected on a Buchner funnel; low molecular weight polymer was isolated as an oil and dried under vacuum.

Platinum-Polystyrene Interface Synthesis. (4:17, 19, 21, 23, 25, 27, 31, 75, 77, 79, 83, 91, 93, 95, 97, 99, 100, 101, 103, 113, 125, 141, 149; 5:21, 63, 77, 87, 89, 99, 101, 103, 119, 127, 131, 137, 139; 6:27, 31, 41, 43, 45, 47, 51, 55, 75, 77, 85, 97, 99, 101, 107, 109) Platinum (30 mg, 1.54×10^{-4} mole) and a small magnetic stir bar were added to a Schlenk tube which was subsequently evacuated and filled with nitrogen. A pentane solution of 1-pentene (10 mL, 0.046 M, 4.6×10^{-4} mole 1-pentene) was charged with hydrogen (15 psig). After the platinum had agglomerated, the stirring was stopped and the platinum was allowed to settle. The 1-pentene solution and hydrogen atmosphere were removed and a THF solution of 4-picoline (1.0 mL, 0.205 M, 2.05×10^{-4} mole 4-picoline) was introduced. The solution was stirred and the platinum became dispersed. THF (10 mL) was added and the mixture was cooled to -78°C . n-Butyllithium (1.5 mL, 0.133 M) was added dropwise to the stirred reaction mixture. After 2 hours, styrene (1.5 mL, 1.31×10^{-2} mole) was added, the mixture was allowed to warm to room temperature and the reaction was quenched with a small amount of methanol. The platinum was allowed to settle and the resulting grey suspension was transferred via cannula to centrifuge tubes. The soluble polystyrene was removed

from the grey solid by repeated washing (THF) and centrifugation until no polystyrene was present (by UV-vis) in the washes. The grey solid samples were dried under vacuum.

Sulfur-Containing Polymers for Adsorption Studies

This section describes the synthesis of thiol-terminated polystyrene and poly(styrene)/poly(propylene sulfide) block copolymers. The synthesis of tritiated styrene, which was used to make radiolabelled polystyrene, is also included. The procedure for adsorbing these polymers to a gold surface is discussed.

^3H -Styrene Synthesis. (7:111-113, 126-129) A 250-mL pressure flask containing a magnetic stir bar was evacuated and filled with nitrogen. *n*-Butyllithium (9.6 mL, 2.5 M, 2.4×10^{-2} mole) was added dropwise to the stirred solution of phenylacetylene (2.6 mL, 2.4×10^{-2} mole) in 60 mL of pentane. The reaction was quenched with ^3H -water (0.43 mL, 10 mCi/mL, 2.4×10^{-2} mole). The ^3H -phenylacetylene solution was distilled (trap-to-trap) from the lithium salts and transferred to a 250-mL pressure flask containing a magnetic stir bar and 0.35 g of Lindlar's Catalyst. The flask was connected to a hydrogen manifold (22 psig) and the hydrogenation was allowed to proceed for 21 minutes. The solvent was removed under reduced pressure and the ^3H -styrene was distilled trap-to-trap from calcium hydride.

Synthesis of Thiol-Terminated Polystyrene. (7:15, 49, 55, 57, 59, 61, 67, 83, 85, 89, 101, 123) Polystyrene endcapped with propylene sulfide (PSSH) was prepared by anionic polymerization under nitrogen in

50-mL Schlenk tubes containing small magnetic stir bars. The tubes were evacuated and filled with nitrogen, and then benzene and sec-butyllithium were added by cannula. Styrene was added and allowed to polymerize to completion (exhaustion of styrene monomer, determined by gas chromatographic analysis) while maintaining the active polystyryl anion. A small sample of the reaction mixture was removed at this point, terminated with methanol, and used to determine the molecular weight of the PS block. The relative amounts of initiator and monomer determined the molecular weight. The polystyryl anions were endcapped using propylene sulfide and the polymer was protonated with acidic methanol which produced thiol terminated polystyrene. High molecular weight polymer ($M_n > 2,000$) was precipitated in methanol and collected on a Buchner funnel; low molecular weight polymer was isolated as an oil and dried under vacuum.

Synthesis of Polystyrene/Poly(propylene sulfide) Block Copolymers.

(7:19, 23, 25, 37, 45, 53, 45, 53; 8:9, 13, 27)

Polystyrene/poly(propylene sulfide) (PS/PPS) block copolymers were polymerized anionically in THF. A 50 ml Schlenk tube containing a small magnetic stir bar was evacuated and filled with nitrogen. Styrene and solvent were added and cooled to -78°C . sec-Butyllithium was added and the orange solution was stirred until no styrene monomer could be detected by GC. A sample was taken for GPC characterization of the PS block. The relative amounts of initiator and monomers determined the molecular weights of the blocks. Propylene sulfide monomer of the appropriate amount was added to the reaction tube and the polymerization

was allowed to proceed at room temperature until no propylene sulfide was detected by GC. The polymer was protonated with acidic methanol. The polymer was precipitated in methanol and collected on a Buchner funnel.

Synthesis of Poly(propylene sulfide). (6:17, 29, 31, 87)

Poly(propylene sulfide) was prepared anionically in THF. A 50-mL Schlenk tube containing a small magnetic stir bar was evacuated and filled with nitrogen. The solvent and sec-butyllithium were added and cooled to -78°C . Propylene sulfide monomer was added and the reaction mixture was stirred for 30 minutes. The polymerization was allowed to warm to room temperature and it was stirred until no monomer could be detected by GC. The polymer was protonated with acidic methanol and isolated by precipitation in methanol.

Synthesis of Radiolabelled Polymers. (7:115, 131, 135, 139, 143, 145, 147; 8:33, 43, 47, 51) ^3H -polymers were made under similar reaction conditions using ^3H -styrene. The radioactive reaction could not be monitored directly so an identical "cold" reaction was run simultaneously (with the same amounts of initiator, solvent and "cold" monomer) from which samples were taken for GC and GPC analysis. The yields from the syntheses of the radioactive polymer were determined directly.

Dilute Solutions of Radiolabelled Polymers for Beer's Law

Justification. (8:3., 35, 37, 41, 45) Radiolabelled polymer (0.040 g) was placed in a 50-mL round bottom flask stoppered with a rubber septum and secured with copper wire. The flask was evacuated and filled with

nitrogen. THF (20 mL) was added to the flask and the polymer was allowed to dissolve. 2.0 Microliters of the polymer solution was transferred to a 10 mL volumetric flask using a 10 L syringe, and then diluted to the mark with OSC scintillation cocktail. 4.0 Milliliters of the solution from the first volumetric flask were transferred to a second 10-mL volumetric flask and diluted to the mark with OSC scintillation cocktail. 4.0 Milliliters of solution were taken from the second flask and diluted to 10-mL in a third volumetric flask with scintillation cocktail. 4.0 Milliliters of solution were taken from the second flask and diluted to 10 mL in a third volumetric flask with scintillation cocktail. 4.0 Milliliters of solution were taken from the third flask and diluted to 10 mL in a fourth volumetric flask with scintillation cocktail.

Adsorption of Polymers on Gold. (7:63, 69, 78, 109, 117, 119, 125, 133, 137, 141, 149, 151; 8:11, 15, 17, 21, 23, 25, 39, 41, 49, 55, 59) Freshly evaporated gold substrates were placed in Schlenk tubes which were then evacuated and filled with nitrogen. Polymer solutions (2.0 mg/mL) were prepared by placing the polymer (0.040 g) in a 50-mL round bottom flask capped with a septum and secured with copper wire. The flask was evacuated and flushed with nitrogen. 20 Milliliter of solvent was added using a cannula. The polymer dissolved and the solution was transferred to the Schlenk tube covering the gold substrate. After a specified time, usually several hours, the polymer solution was removed via cannula under positive nitrogen pressure and the substrate was rinsed with fresh solvent until no polystyrene could be detected by UV-

vis analysis of the rinsing solvent. The substrates were dried under vacuum prior to subsequent analysis.

References

1. Shivers, D.F. The Manipulation of Air Sensitive Compounds; McGraw-Hill: New York, 1969.
2. Handling Air-Sensitive Compounds; Technical Information Bulletin Number AL-134; Aldrich Chemical Company: Milwaukee, WI, 1983.
3. How to Use Ace No-Air Glassware; Bulletin Number 570; Ace Glass Incorporated: Vineland, NJ, 1983.
4. Perrin, D.D.; Armarego, W.L.F.; Perrin, Dawin R. Purification of Laboratory Chemicals, 3rd ed.; Pergamon Press: New York, 1980.
5. Ma, T.S.; Rittner, R.C. Modern Organic Elemental Analysis; Marcel Decker: New York, 1979.

Chapter III

RESULTS AND DISCUSSION

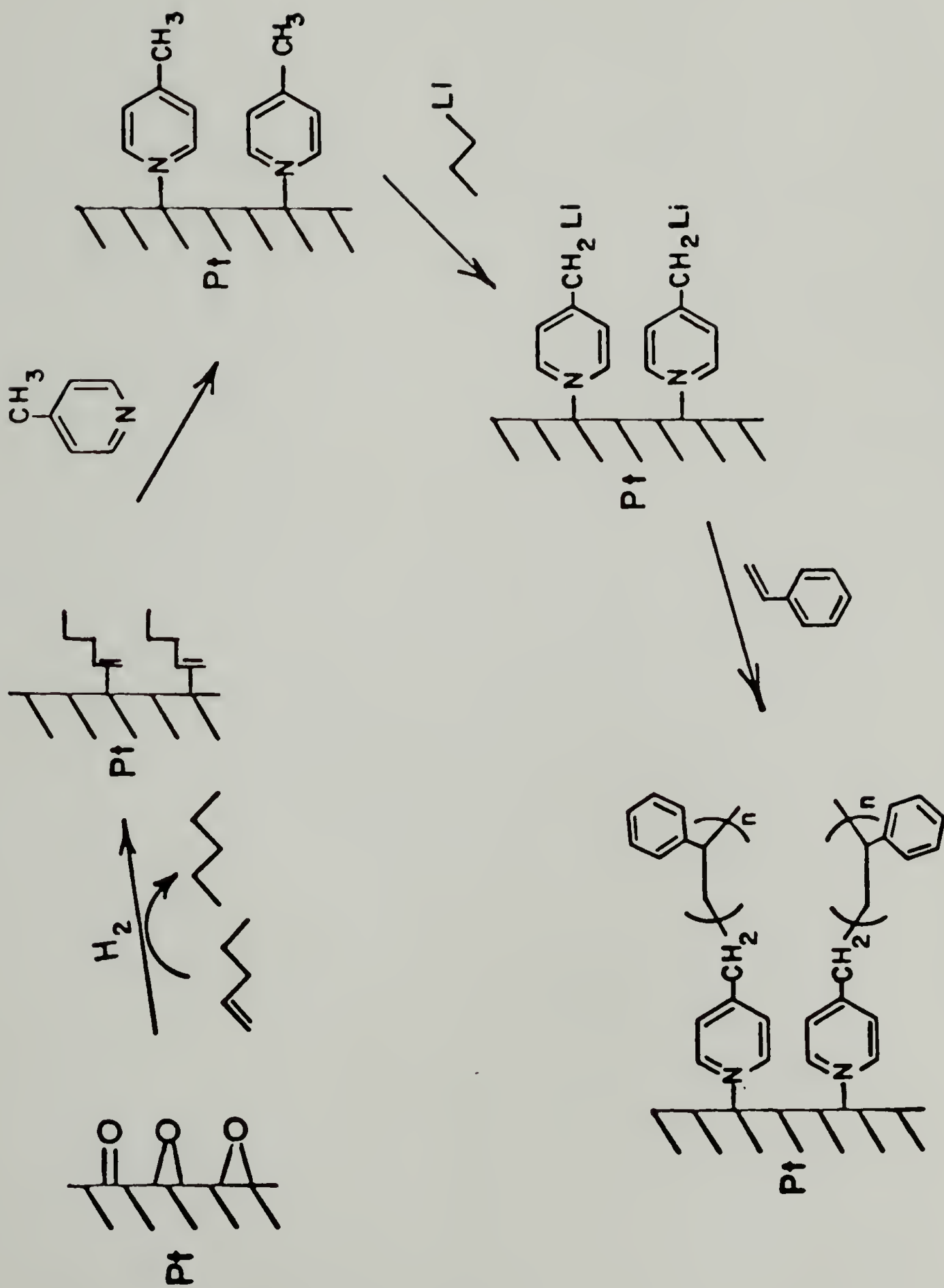
Platinum - Polystyrene Interface

Our general synthetic strategy for the stepwise synthesis of a metal-polymer interface is depicted in Scheme 3.1. A coordinating ligand is attached to clean metal which when activated initiates polymerization of monomer.¹ Platinum was chosen for the metal because it is available as a high surface area solid (platinum black) and it is easily cleaned of its oxide layer by using it as a catalyst for an olefin hydrogenation. 4-Picoline adsorbs irreversibly to the clean platinum surface and is deprotonated with *n*-butyllithium rendering surface confined pseudo-benzylic lithium reagents which are used to initiate the anionic polymerization of styrene.

Platinum-Catalyzed Olefin Hydrogenation

The coordination chemistry of a series of ligands was investigated by monitoring the rate of olefin hydrogenation over platinum: If ligands were bound to the surface, the catalyst was poisoned and the rate of olefin reduction would be effected.

Survey of Coordinating Ligands. The unpoisoned hydrogenation of cyclohexene to cyclohexane was run over a platinum catalyst supported on alumina. GC analysis of the reaction mixture after 15 minutes showed that all of the olefin had been reduced. Several catalyst poisons (thiols, phosphines and pyridines) were surveyed to determine their effect on the rate of olefin hydrogenation.



Scheme 3.1 General synthetic strategy for the stepwise synthesis of a platinum-polystyrene interface

The catalyst poisons were added to the olefin hydrogenation system in a 1:1 mole ratio of poison to platinum. Samples of the reaction mixture were taken at various time intervals during the hydrogenation for GC analysis to monitor the disappearance of cyclohexene. Table 3.1 lists the poisons surveyed and their relative effect on the rate of the platinum catalyzed hydrogenation of cyclohexene. The relative strength

Table 3.1 Effect of Poisons on Platinum Catalyzed Hydrogenations

| <u>Poison</u> | <u>% Cyclohexene^a</u> |
|---|----------------------------------|
| Ethanethiol | 100 |
| Benzenethiol | 100 |
| Triethylphosphine | 100 |
| Bis(1,2 di- <i>p</i> -tolylphosphino)ethane | 95 |
| Tris(2-cyanoethylphosphine) | 60 |
| Tri- <i>p</i> -tolylphosphine | 50 |
| Triphenylphosphine | 40 |
| Pyridine | 15 |
| 4-Picoline | 10 |
| Control, no poison | 0 |

^a Determined after 15 minutes by GC

of the poison was determined by the percentage of cyclohexene still present after 15 minutes. Ethanethiol, benzenethiol and triethylphosphine completely inhibited olefin hydrogenation, while only

a small amount (5%) of olefin was hydrogenated after 15 minutes in the presence of the bidentate ligand bis(1,2 di-p-tolylphosphino)ethane. The monodentate phosphine ligands tris(2-cyanoethylphosphine), tri-p-tolylphosphine and triphenylphosphine caused the rate of olefin hydrogenation to be suppressed but not completely inhibited. The pyridine-based ligands pyridine and 4-picoline interfered with the rate of hydrogenation, but with enough time all of the of the olefin was hydrogenated in the presence of these ligands.

These data reflect the strength of the platinum-ligand interaction relative to the platinum-cyclohexene interaction under a hydrogen atmosphere. The strongest interaction was exhibited by the thiols and triethylphosphine. Bidentate ligands usually exhibit very strong interactions; the bulkiness of bis(1,2 di-p-tolylphosphino)ethane could have reduced its effectiveness relative to triethylphosphine. The electron-withdrawing cyano groups caused tris(2-cyanoethylphosphine) to interact less strongly with the platinum than triethylphosphine. The bulky nature of tri-p-tolylphosphine and triphenylphosphine reduced their effectiveness as coordinating ligands to the platinum surface. Pyridine and 4-picoline lost their effectiveness with time because under the reaction conditions they were hydrogenated.

Effect of 4-Picoline on the Rate of Olefin Hydrogenation. 4-Picoline was chosen as a ligand for two reasons: (1) It has been shown that pyridine adsorbs irreversibly² and perpendicularly³ to Pt(111). We assume that 4-picoline behaves analogously; this has been demonstrated for Ni(100).⁴ (2) The pseudo-benzylic hydrogens of 4-picoline are

acidic and can be removed to form an anionic polymerization initiator.

To observe the effect of 4-picoline on the rate of the hydrogenation of cyclohexene to cyclohexane over platinum black we initially investigated the unpoisoned hydrogenation system. The rate of hydrogenation depends on the effective surface area of platinum. During the hydrogenation process clean platinum was exposed and the platinum black tended to agglomerate. This is a common problem in industry for unsupported catalysts.⁵ When the hydrogenation system was agitated by sonication, agglomeration was prevented; whereas the same amount of platinum black in a stirred system agglomerated. Consequently, even with the same amount of catalyst the rate of reaction is faster for a sonicated system (Table 3.2). The rate of hydrogenation increases as the amount of platinum increases until there is so much platinum present that it readily agglomerates. When the platinum agglomerates it decreases its effective surface area, thus decreasing the rate.

Table 3.2 Effect of Agitation on the Rate of Hydrogenation

| <u>Sample</u> | <u>Agitation</u> | <u>Weight(mg)</u> | <u>Rate(mole/L-min)</u> |
|---------------|------------------|-------------------|-------------------------|
| 121-B | Sonicated | 0.613 | -0.025 |
| 127-C | Stirred | 0.615 | -0.006 |

Figure 3.1 shows a plot of the concentration of cyclohexene against time. The slope of this line (-0.025 mole/L-min) is the kinetic rate constant for this reaction. The concentration of cyclohexene was doubled and halved and the rate constant remained the same (Figure 3.2).

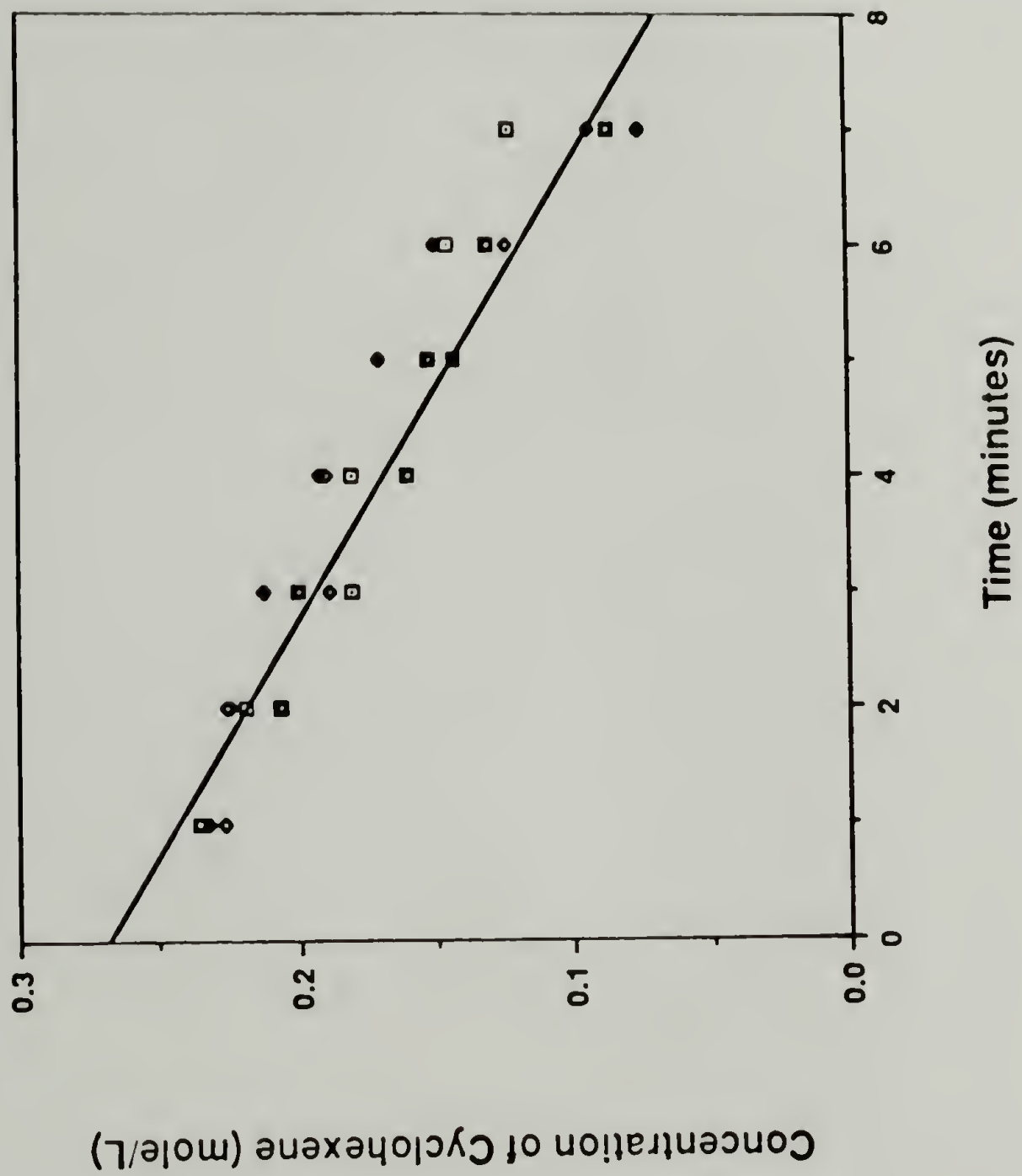


Figure 3.1 Disappearance of cyclohexene over time in a platinum catalyzed hydrogenation

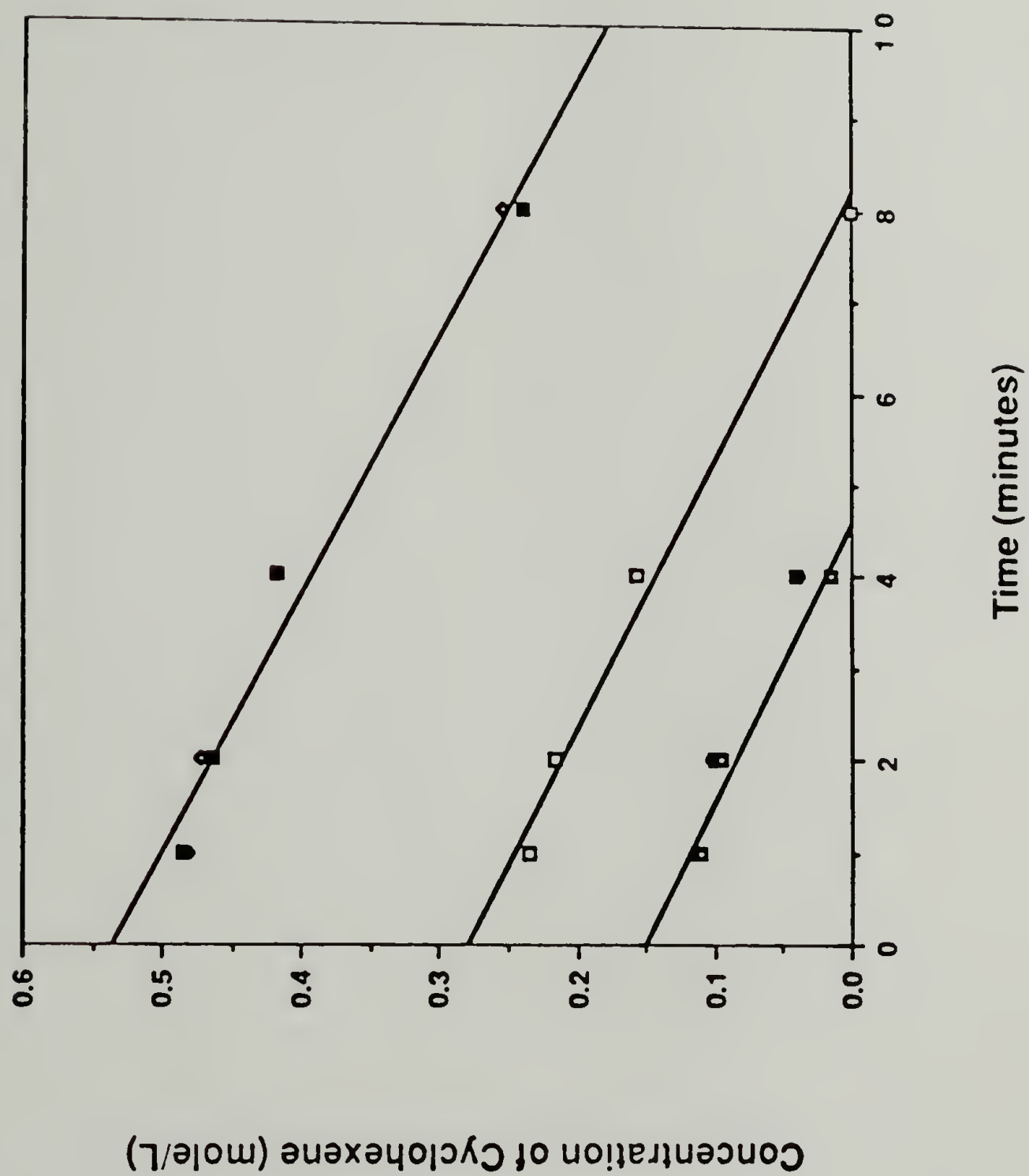


Figure 3.2 Effect of cyclohexene concentration on the rate of hydrogenation

These data show that the disappearance of cyclohexene is zero order under these conditions, indicating a surface saturated with cyclohexene.⁶ Under these conditions, surface oxygen is not stable and is removed as water.⁷

The addition of 4-picoline to the hydrogenation system at a one-to-one mole ratio of 4-picoline to platinum suppressed the rate as seen in Figure 3.3 and as listed below:

| <u>System</u> | <u>Rate (mole/L-min)</u> |
|---------------|--------------------------|
| Unpoisoned | -0.025 |
| 4-Picoline | -0.007 |

Adsorption of 4-Picoline on Platinum

The amount of 4-picoline adsorbed to platinum black (that had been cleaned via olefin hydrogenation) was determined by three independent methods: UV-vis, gravimetric and elemental analyses. The 4-picoline could not be removed from the platinum by washing with clean solvent.

UV-vis Analysis. The UV-vis absorption spectrum of 4-picoline in pentane has a maxima at 254 nm. The absorbance at this wavelength for dilute solutions of 4-picoline in pentane exhibits a linear Beer's Law relationship with concentration as seen in Figure 3.4. The analytical expression obtained from linear regression is:

$$\text{Concentration} = \frac{\text{Absorbance} - 0.0055}{17,500 \text{ (mL/g)}}$$

A pentane solution of 4-picoline was exposed to cleaned platinum. The UV-vis spectrum of the solution showed a decrease in absorbance at 254 nm

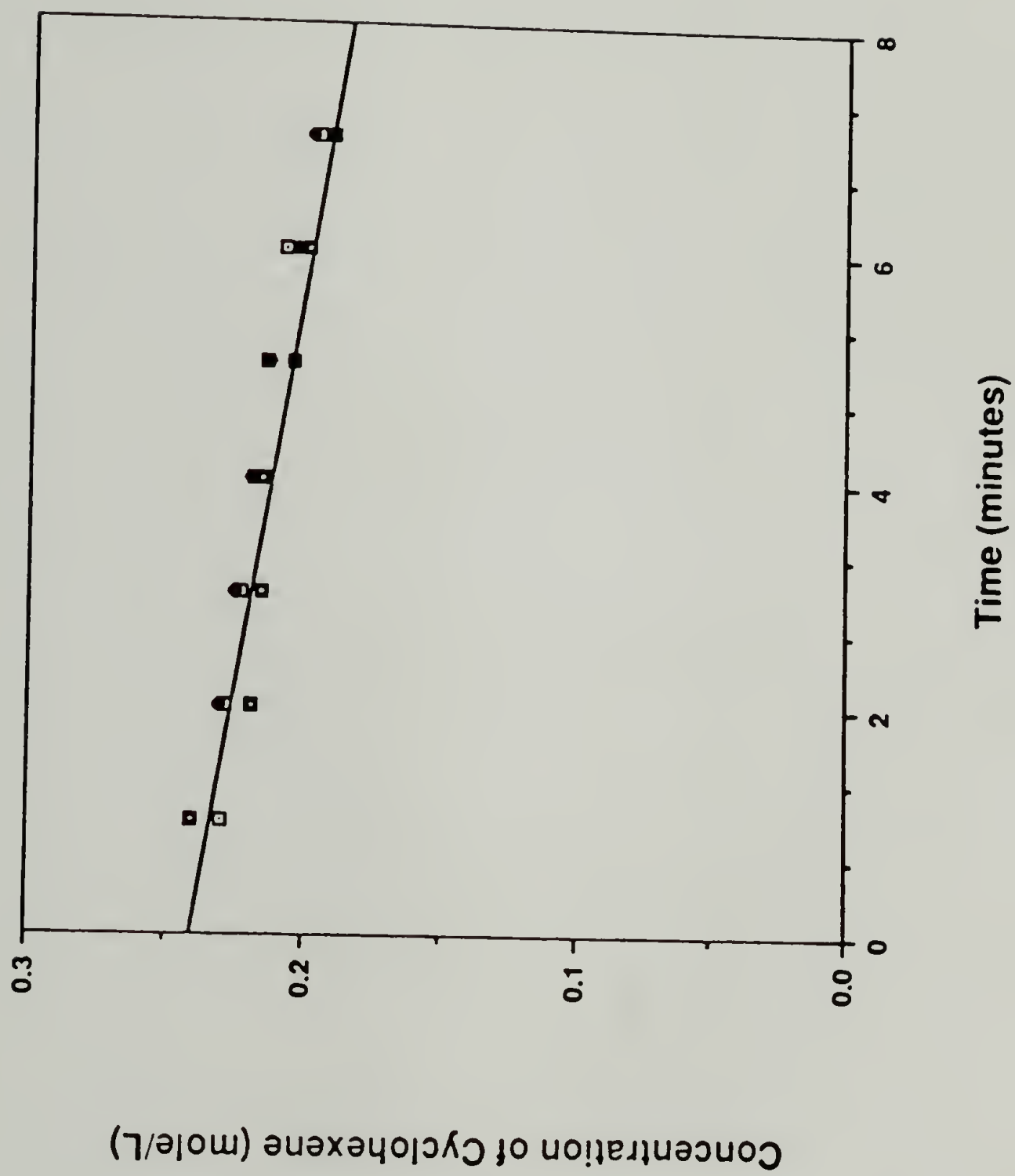


Figure 3.3 Effect of 4-picoline on the rate of olefin hydrogenation

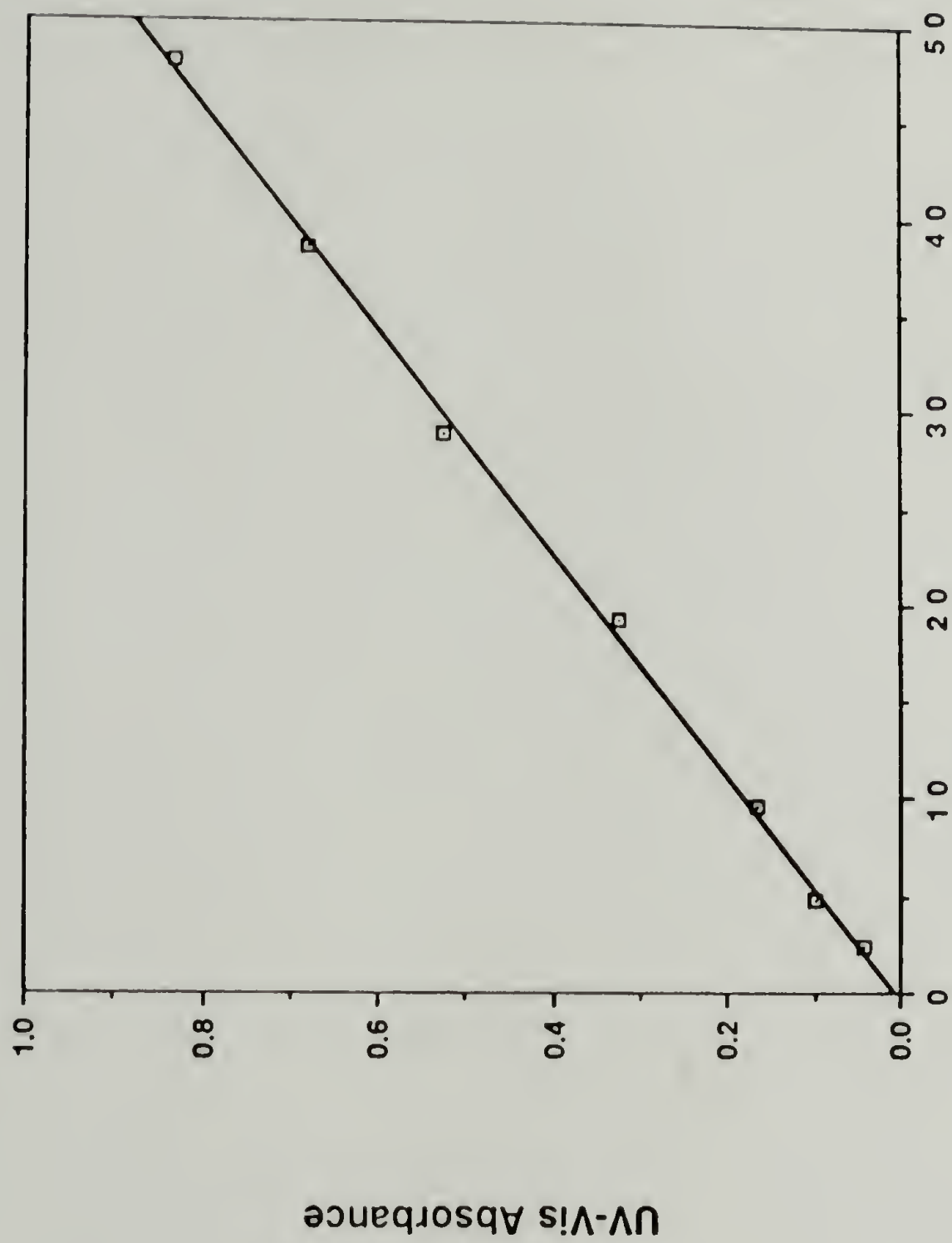


Figure 3.4 Beer's Law plot of dilute solutions of 4-picoline

compared to the original 4-picoline solution (Figure 3.5). The measurement of the absorbance at 254 nm for several solutions before and after exposure to platinum is listed in Table 3.3. The observed decrease was 0.123 ± 0.008 absorbance units. From the Beer's Law relation this corresponds to $4.0 \pm 0.1 \times 10^{-5}$ g of 4-picoline per 10 mg of platinum or $8.5 \pm 0.05 \times 10^{-3}$ moles of 4-picoline adsorbed per mole of platinum.

Table 3.3 UV-vis Absorbance at 254 nm for 4-Picoline Solutions Before and After Exposure to Platinum Black

| <u>Sample</u> | Absorbance at 254 nm | |
|---------------|----------------------|--------------|
| | <u>Before</u> | <u>After</u> |
| Control | 0.991 | 0.991 |
| A | 0.991 | 0.853 |
| B | 0.991 | 0.876 |
| C | 0.991 | 0.867 |
| D | 0.996 | 0.880 |
| E | 0.996 | 0.873 |
| F | 0.996 | 0.873 |

Gravimetric Analysis. The amount of 4-picoline vapor adsorbed on cleaned platinum was quantitated by gravimetric analysis. Platinum contained in a Teflon "envelope" was weighed before and after exposure to 4-picoline. Table 3.4 shows the weight gain due to irreversibly adsorbed 4-picoline. This change corresponds to $1.2 \pm 0.2 \times 10^{-2}$ moles of 4-picoline adsorbed per mole of platinum black.

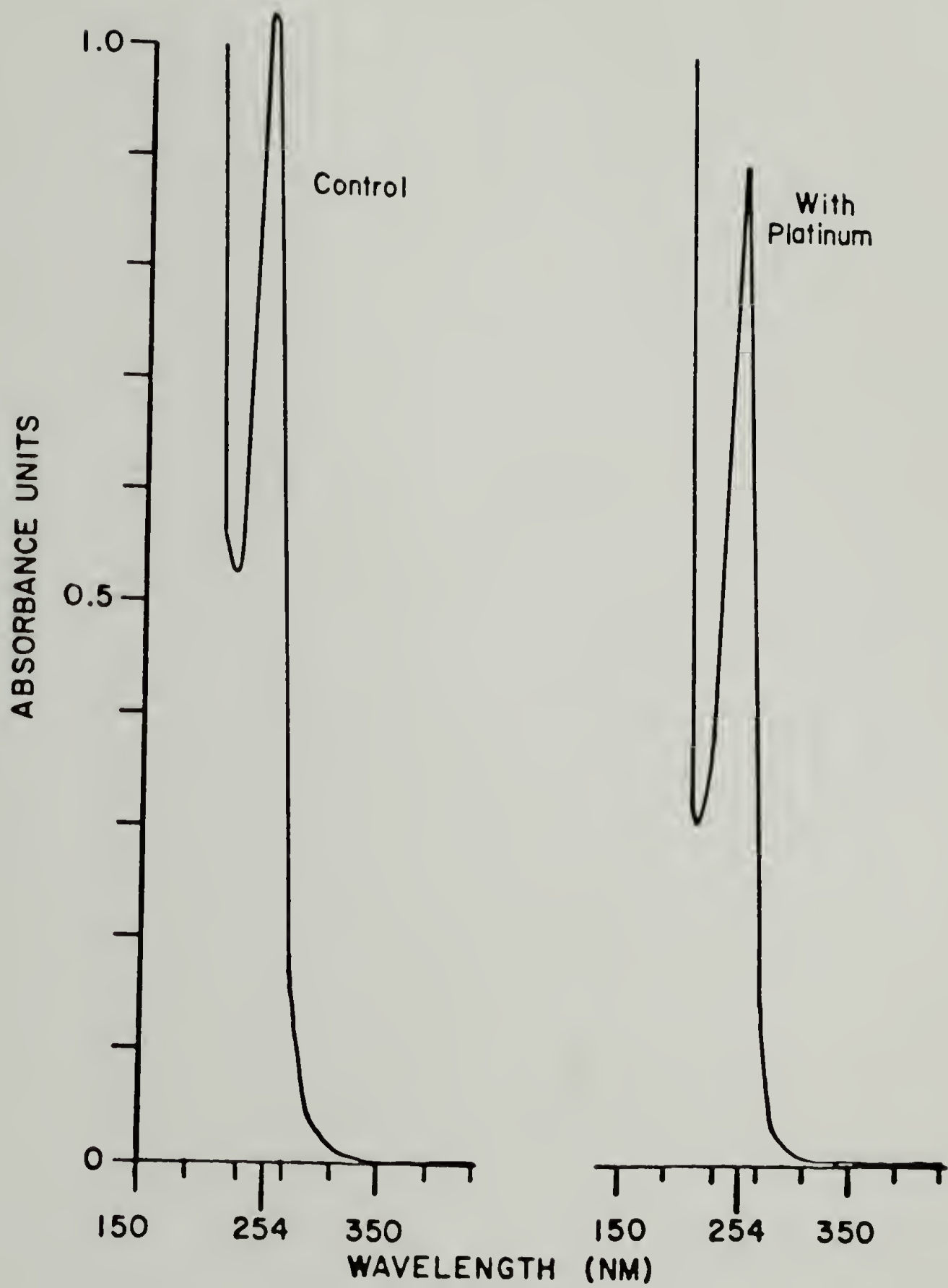


Figure 3.5 UV-vis spectra of 4-picoline solutions before and after exposure to platinum black

Table 3.4 Gravimetric Analysis of 4-Picoline Adsorbed to Platinum Black

| <u>Sample</u> | <u>Initial Weight(mg)</u> | <u>Final Weight(mg)</u> | <u>Weight Gain(mg)</u> |
|---------------|---------------------------|-------------------------|------------------------|
| Control | 0.9445 | 0.9451 | 0.0006 |
| A | 1.8368 | 1.8460 | 0.0092 |
| B | 0.9501 | 0.9554 | 0.0053 |
| C | 0.5712 | 0.5752 | 0.0040 |

Elemental Analysis. The amount of 4-picoline adsorbed to platinum black was determined indirectly in the UV-vis analysis by monitoring the disappearance of 4-picoline from solution. The platinum black used in these experiments was analyzed for elemental nitrogen which showed 0.12 ± 0.02 percent nitrogen by weight. Assuming that all of the nitrogen comes from the adsorbed 4-picoline this corresponds to 0.73 percent 4-picoline or $1.5 \pm 0.2 \times 10^{-2}$ moles of 4-picoline adsorbed per mole of platinum.

The amount of 4-picoline adsorbed to platinum black determined by these three methods is shown in Table 3.5. These data indicate that about 1 mole of 4-picoline is adsorbed for every 100 moles of platinum used. Given that the surface area of platinum black is $24 \text{ m}^2/\text{g}$ and using 1.39 \AA as the atomic radius for Pt one can calculate a value of 5.14×10^{-4} surface moles per gram (5.13×10^{-3} mole) of platinum. This means that there is one mole of platinum surface exposed for every ten

moles of platinum used. Therefore, for the adsorption of 4-picoline on a platinum surface there is one 4-picoline molecule adsorbed for every 10 atoms of platinum.

Table 3.5 Determination of the Amount of 4-Picoline Adsorbed to Platinum Black

| <u>Method</u> | <u>Moles of 4-Picoline Adsorbed per Mole of Platinum</u> |
|---------------|--|
| UV-vis | $0.85 \pm 0.05 \times 10^{-2}$ |
| Gravimetric | $1.2 \pm 0.2 \times 10^{-2}$ |
| Elemental | $1.5 \pm 0.2 \times 10^{-2}$ |

4-Picoline that had been adsorbed to cleaned platinum could not be removed by rinsing with solvent. Figure 3.6 shows the UV-vis absorbance spectra for a pentane solution of 4-picoline (A), and pentane (B) after exposure to cleaned platinum. After removal of the original solutions, fresh pentane was added to the tubes containing the platinum. If 4-picoline was physisorbed to the platinum in tube A then some of it would have desorbed into the pentane and would have been detected by an absorbance in the UV-vis spectrum at 254 nm. The UV-vis spectra of the pentane used to wash the platinum samples are shown in Figure 3.7. Spectrum AW exhibits the same level of absorbance at 254 nm as does the control BW, therefore no 4-picoline was displaced from the platinum black by solvent. These samples of platinum black were used as catalysts in the hydrogenation of cyclohexene. The rate of hydrogenation using the 4-picoline-platinum catalyst was suppressed

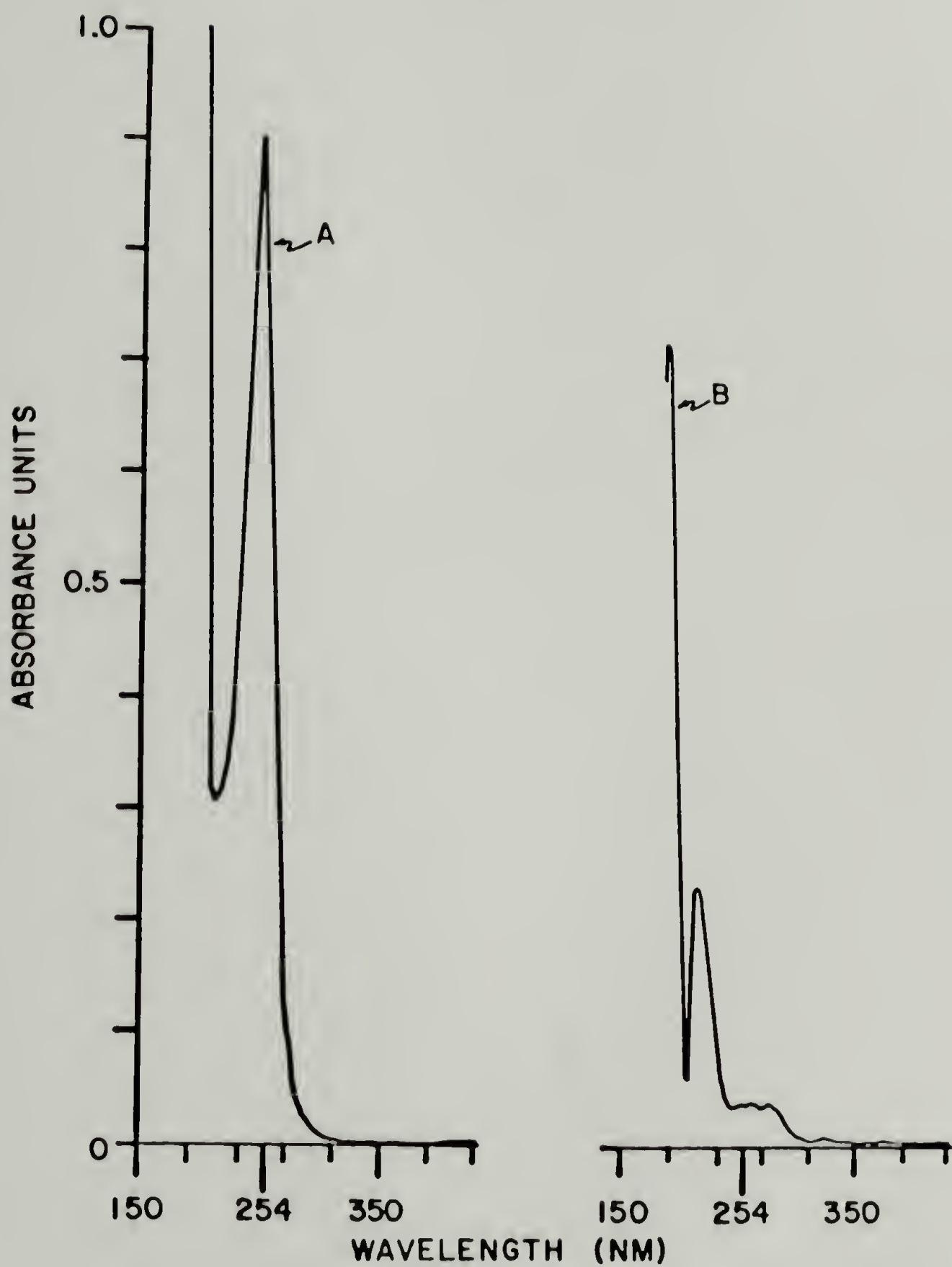


Figure 3.6 UV-vis spectra of pentane (B) and a pentane solution of 4-picoline (A) after exposure to platinum black

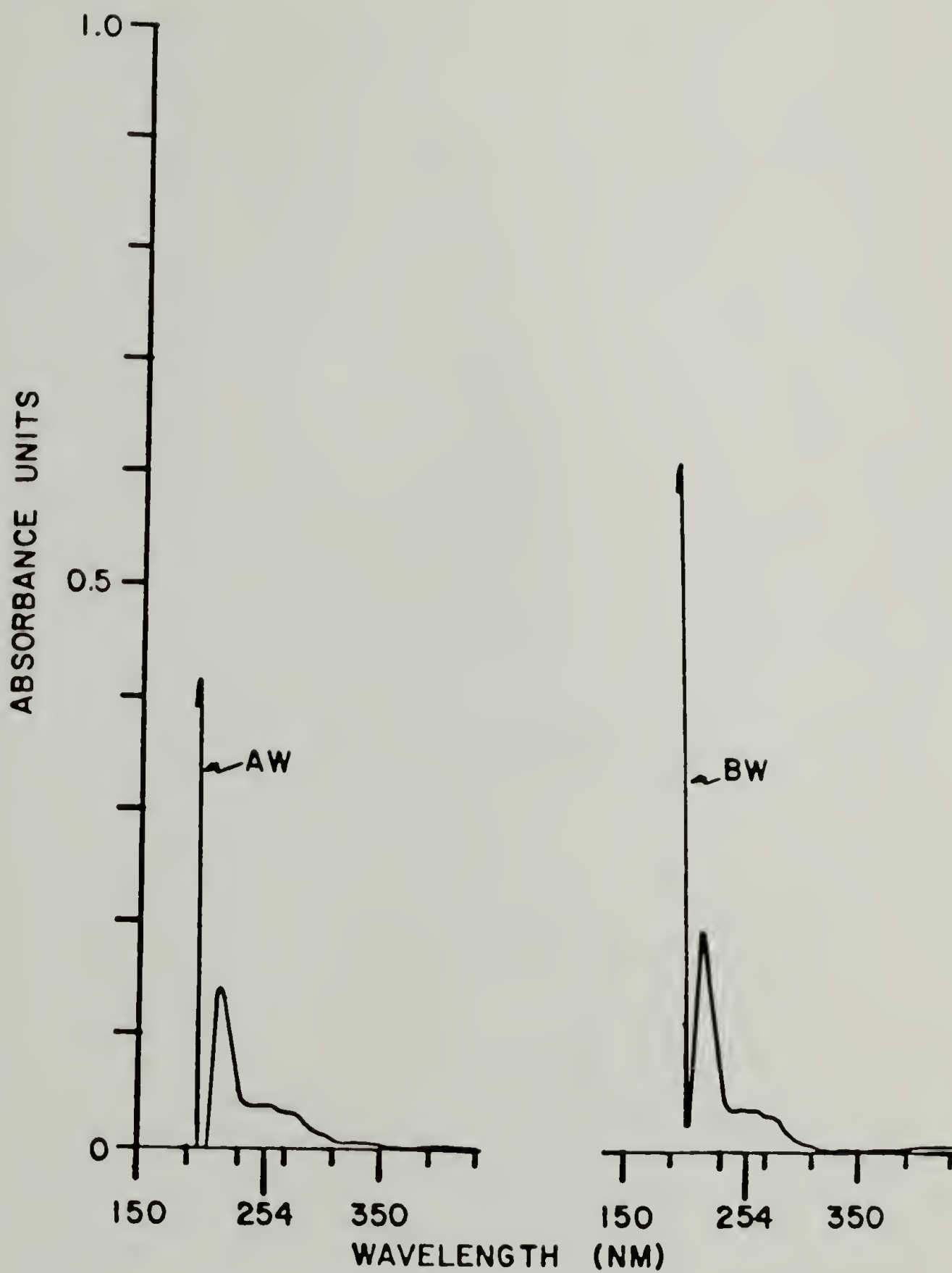


Figure 3.7 UV-vis spectra of pentane washings of platinum black AW: platinum exposed to 4-picoline, BW: control platinum

relative to the platinum catalyst (Figure 3.8). This was the same result as the system investigated earlier in which a solution of 4-picoline was added to the hydrogenation system.

The platinum black that was used in the gravimetric experiment was also tested under hydrogenation conditions. The platinum black sealed inside two Teflon filters was used as a catalyst for the hydrogenation of pentene. Figure 3.9 shows that the rate was suppressed for the platinum that had adsorbed 4-picoline vapor, relative to the unexposed platinum sample.

Synthesis of a Platinum-Polystyrene Interface

Our general synthetic strategy for the stepwise synthesis of a platinum-polystyrene interface is depicted in Scheme 3.1. The oxide layer from high surface area platinum (platinum black) was removed by chemical reduction and the surface was deliberately poisoned with 4-picoline. Deprotonation of the 4-picoline with n-butyllithium rendered surface confined pseudo-benzylic lithium reagents which were used to initiate the anionic polymerization of styrene.

Picolyl Anion-Initiated Polymerization of Styrene. Our stepwise synthesis involves initiating styrene polymerization with surface-confined carbanions produced by deprotonating the adsorbed 4-picoline. This initiation (in solution) has been reported⁸, but only as a side reaction of the attempted mono-alkylation of lithiopicoline with styrene. Addition of alkylolithium reagents to the 2-position of 4-picoline (Ziegler alkylation) is a side reaction of this deprotonation, but conditions, (n-butyllithium, THF, -78°C, 2 hours.) have been

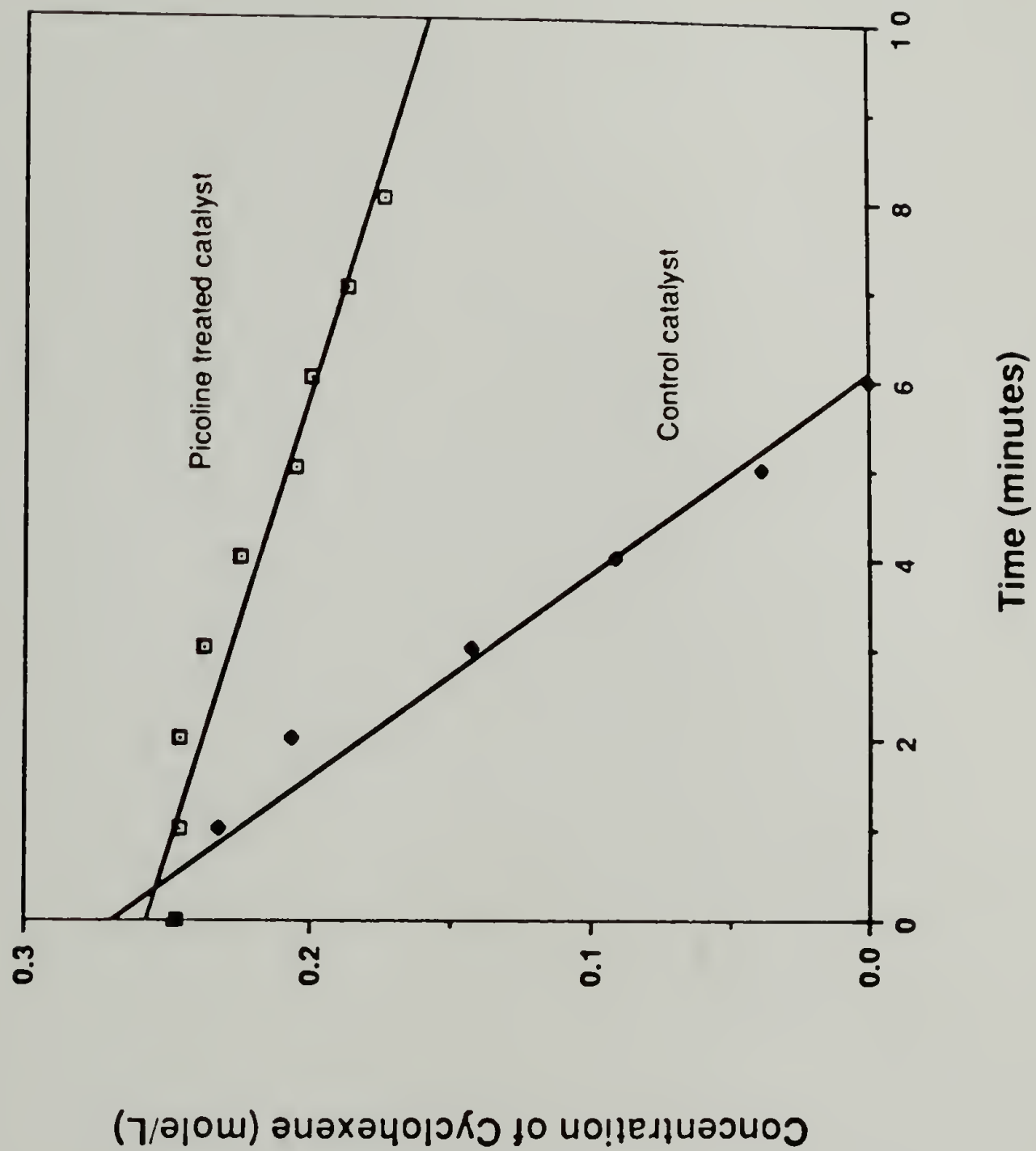


Figure 3.8 Effect of 4-picoline-poisoned-platinum catalyst on the rate of olefin hydrogenation

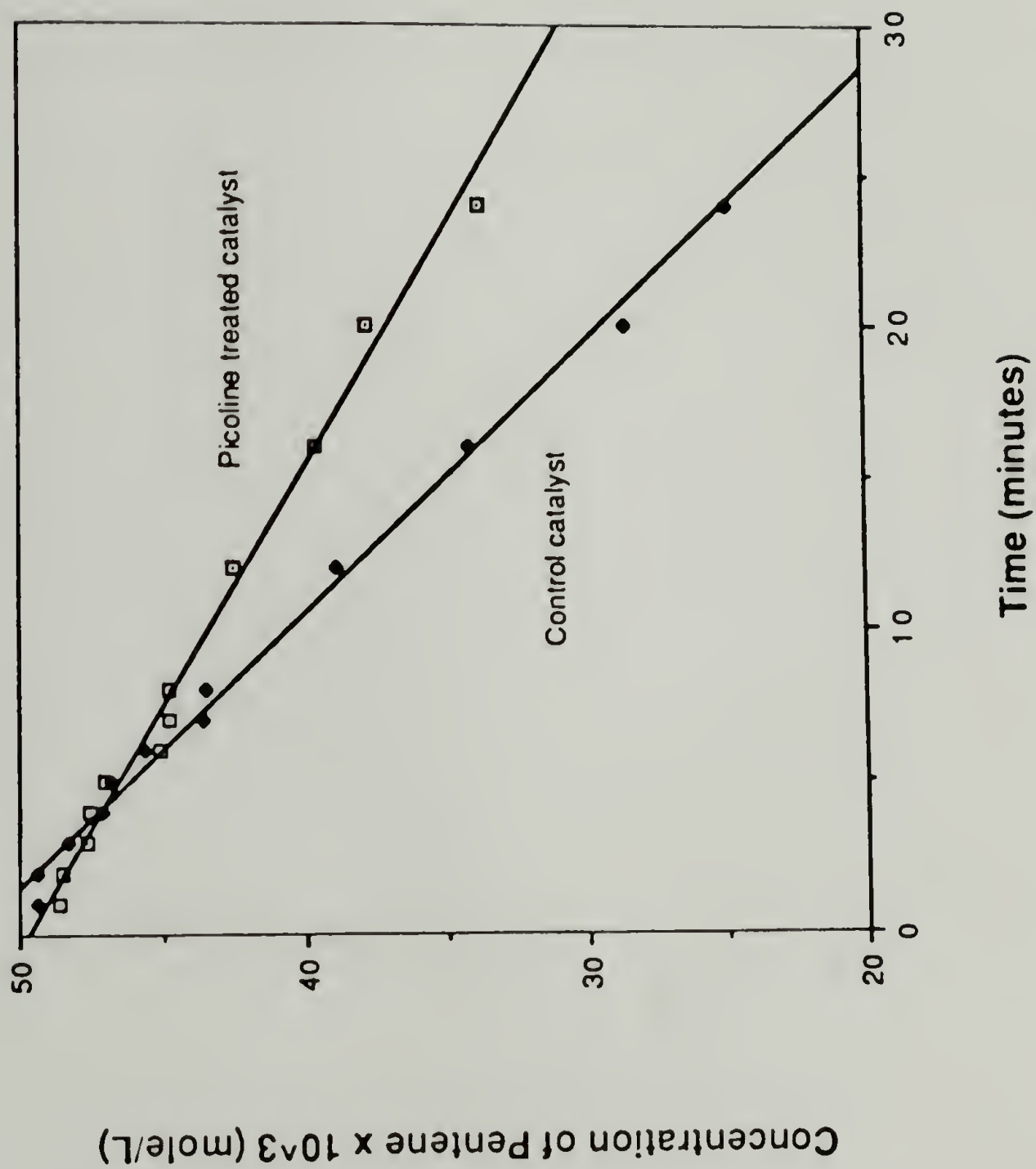


Figure 3.9 Effect of 4-picoline-poisoned-platinum catalyst sealed inside teflon filters on the rate of olefin hydrogenation

reported⁸ that produce lithiopicoline quantitatively. We used these conditions to generate the lithium initiator, and prepared a range of molecular weight samples. Picolyllithium was compared to n-butyllithium as an initiator to anionically polymerize styrene in THF at -78°C. The GPC characterization of the polystyrene made from these initiators is shown in Table 3.6. For comparison, equimolar amounts of the initiators

Table 3.6 GPC Characterization of Polystyrene Initiated by Picolyllithium and n-Butyllithium

| <u>Initiator</u> | <u>Sample</u> | <u>M_n</u> | <u>M_w</u> | <u>PDI</u> |
|------------------|---------------|----------------------|----------------------|------------|
| Picolyl | 5-89D | 8,119 | 13,990 | 1.72 |
| Picolyl | 5-93A | 9,580 | 16,037 | 1.67 |
| <u>n</u> -Butyl | 5-93B | 7,099 | 9,203 | 1.30 |
| Picolyl | 5-95A | 11,919 | 13,468 | 1.13 |
| Picolyl | 5-99A | 13,814 | 18,610 | 1.35 |
| <u>n</u> -Butyl | 5-99B | 14,047 | 17,801 | 1.27 |
| Picolyl | 5-103A | 15,069 | 26,521 | 1.76 |
| Picolyl | 5-91A | 58,682 | 99,173 | 1.69 |

were used in reactions 99A, 99B, 93A and 93B; more styrene monomer was used in reactions 99A and 99B than 93A and 93B. n-Butyllithium produced polystyrene with a narrower molecular weight distribution, but otherwise picolyllithium was an acceptable anionic initiator.

The presence of the pyridine ring from the initiator was confirmed in low molecular weight samples. The ¹H-NMR spectrum obtained for the

picolyl anion-initiated polystyrene sample is shown in Figure 3.10. The spectra for polystyrene and poly(4-vinyl pyridine) are shown in Figures 3.11 and 3.12. The peak at 8.25 in the spectrum in Figure 3.10 is due to the protons α -to the nitrogen in the pyridine ring. In the infrared, vibrations at 980, 1225 and 1420 cm^{-1} are observed in the spectrum of polyvinylpyridine (Figure 3.13) but not in the spectrum of polystyrene (Figure 3.14). These absorbances resulting from the pyridine ring were also seen in the infrared spectrum of low molecular weight polystyrene initiated by picolyllithium (Figure 3.15).

Platinum-Polystyrene Interface Synthesis and Characterization. The anionic graft polymerization of styrene from the surface of platinum was initiated by a bound picolyl anion. A control experiment was run in which polystyrene was polymerized anionically in the presence of clean platinum. The platinum was cleaned via olefin hydrogenation as explained above, but no picoline was introduced to the system. The initiator was added, followed by styrene monomer. The system containing picoline produced a grey material after repeated washings, whereas the control reaction yielded a black powder.

FTIR spectroscopy was used to confirm the presence of polystyrene in the polymer-grafted platinum sample. We used the same procedure that O'Reilly and Mosher¹⁰ have reported to determine functional groups in carbon black. The grey, polymer-grafted-platinum showed vibrations characteristic of polystyrene in the C-H stretching region 3100 - 2800 cm^{-1} (Figure 3.16),¹¹ while the black control material showed no significant absorbance in the same region (Figure 3.17).

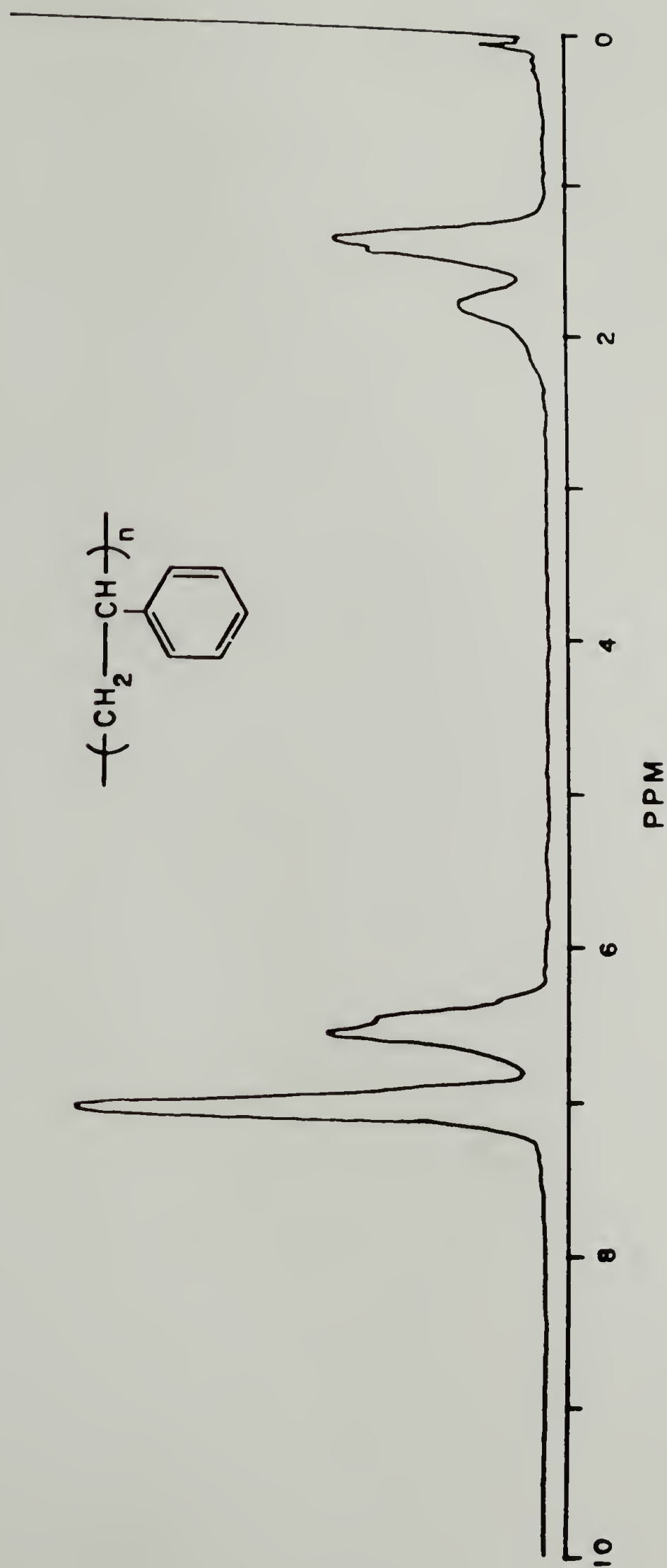


Figure 3.11 $^1\text{H-NMR}$ spectrum of polystyrene

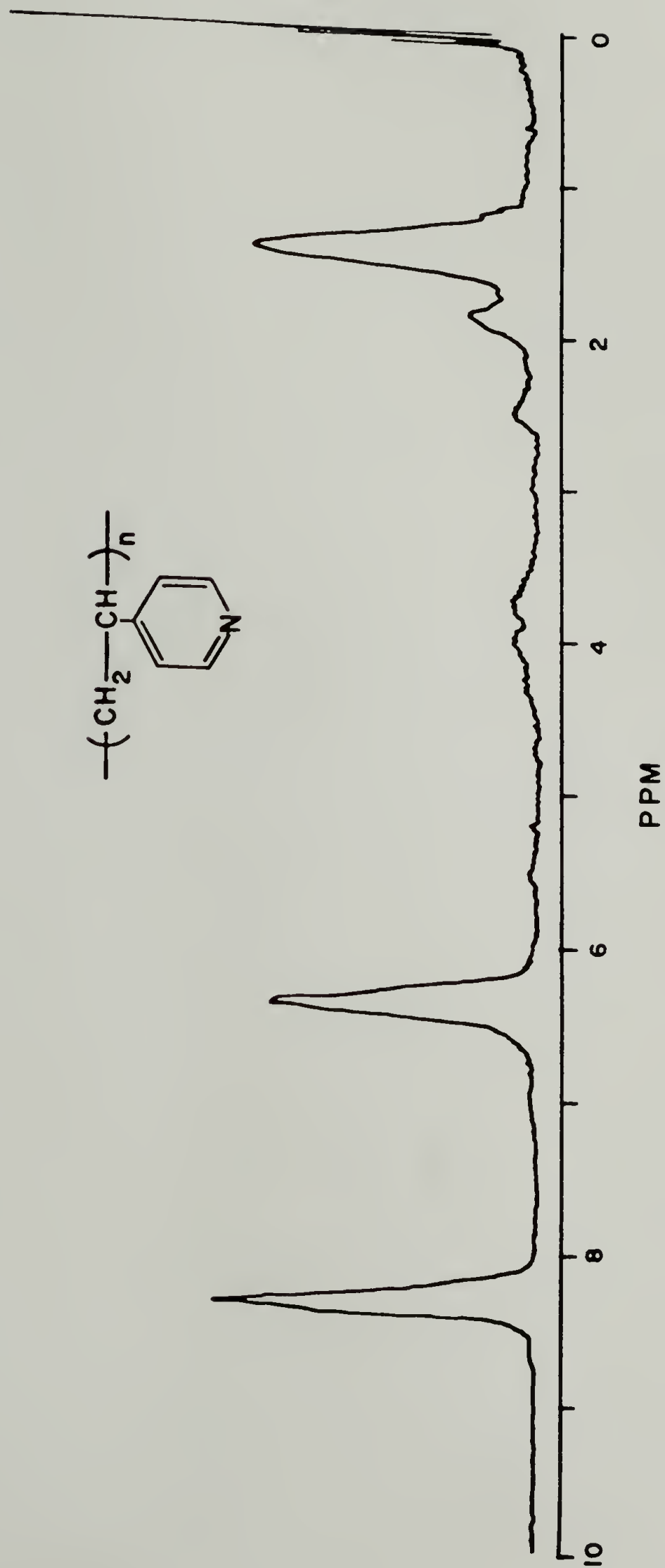


Figure 3.12 ^1H -NMR spectrum of poly(4-vinylpyridine)



Figure 3.13 Infrared spectrum of poly(4-vinylpyridine)

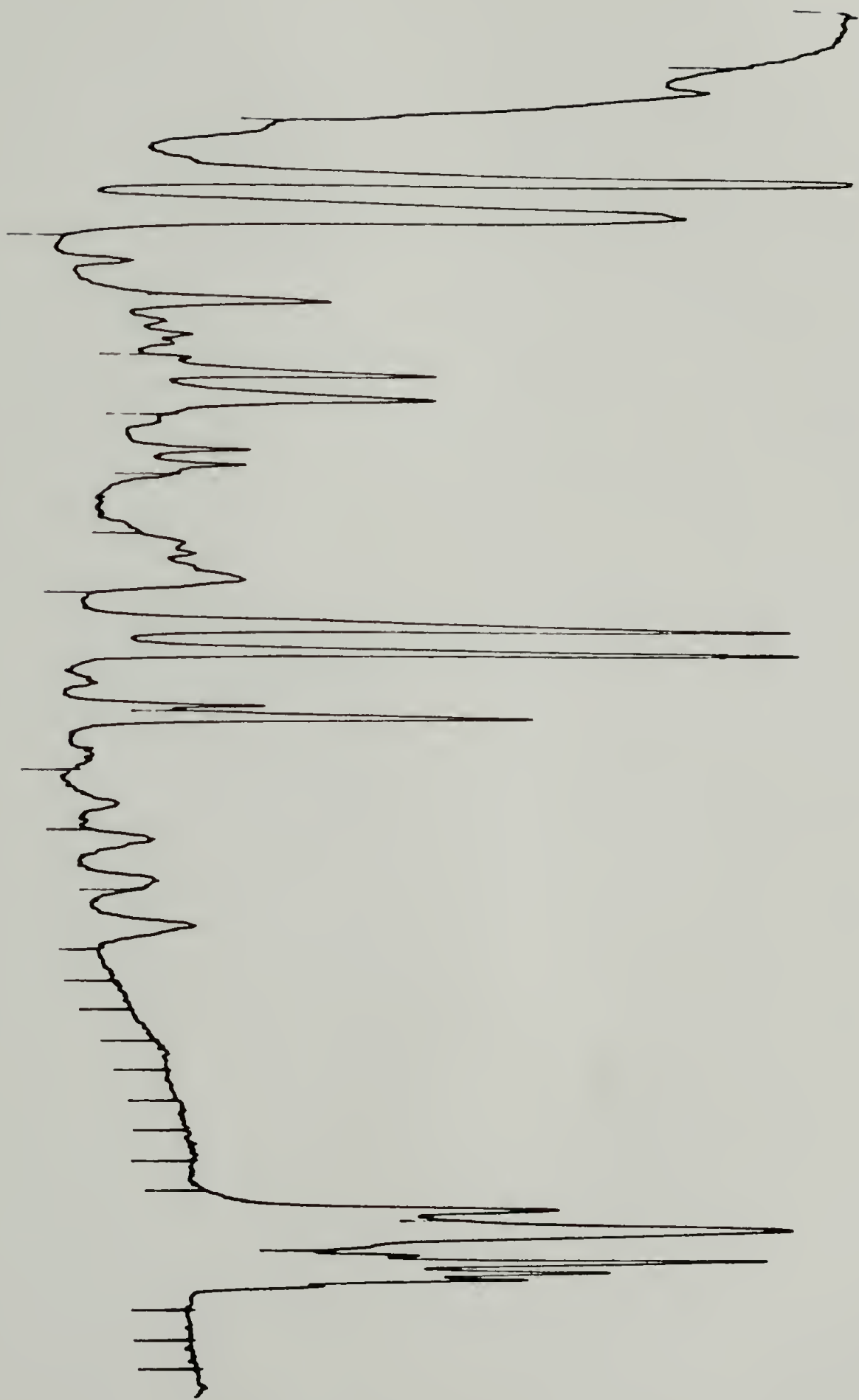


Figure 3.14 Infrared spectrum polystyrene



Figure 3.15 Infrared spectrum of picolyl anion-initiated polystyrene

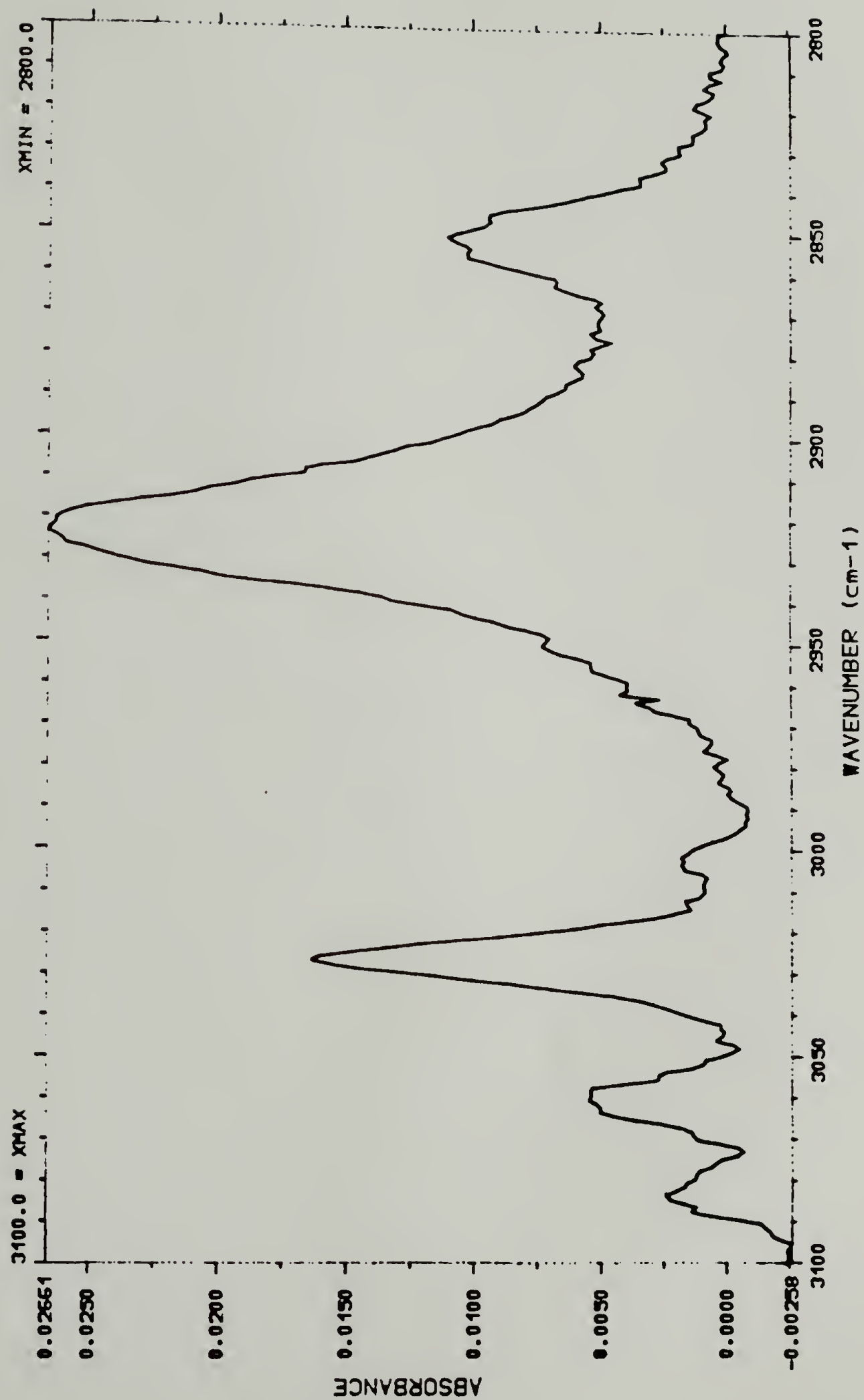


Figure 3.16 Infrared spectrum of polystyrene-grafted platinum

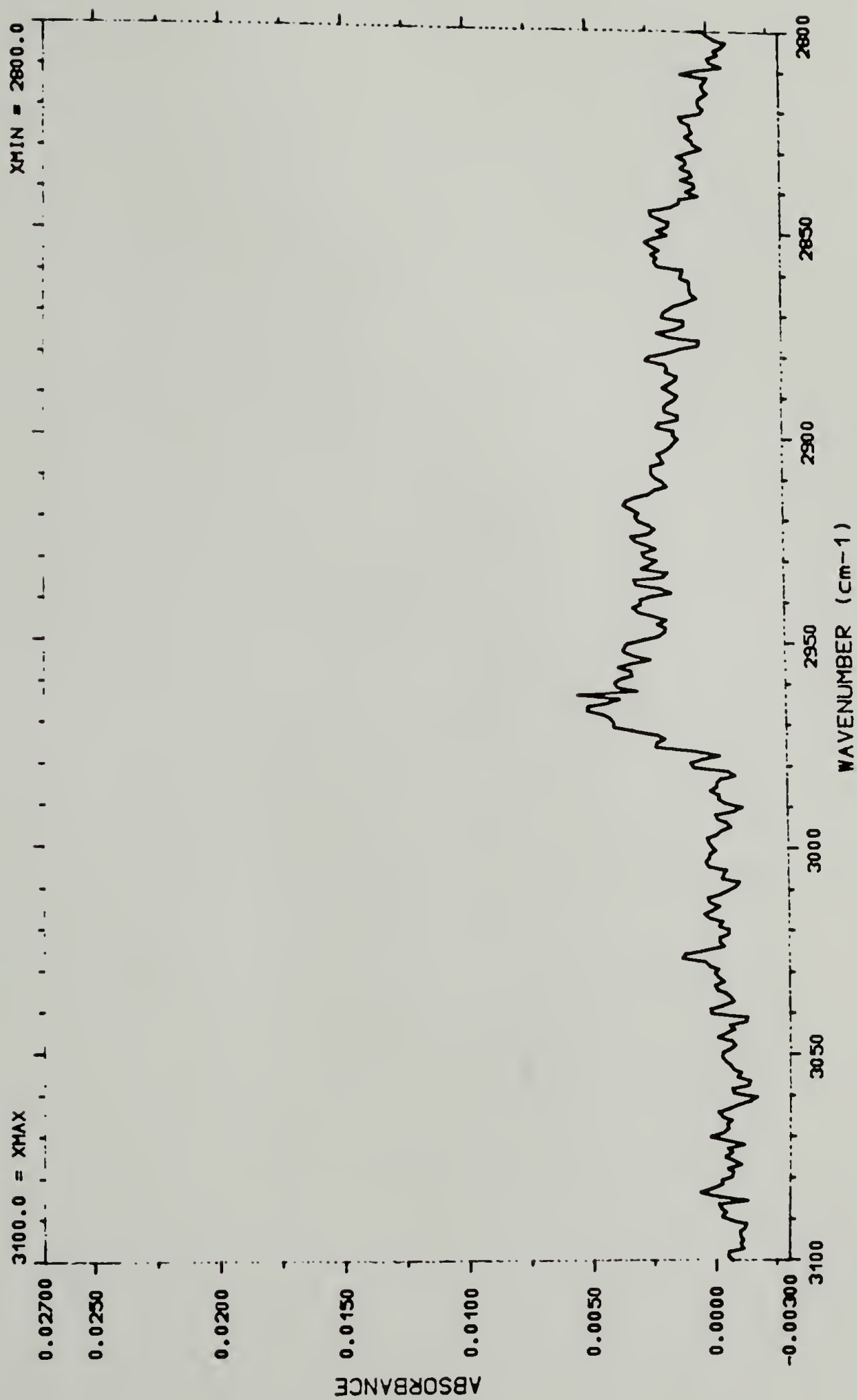


Figure 3.17 Infrared spectrum of control platinum

The samples listed in Table 3.7 were prepared from 2.05×10^{-4} mol 4-picoline, 2.05×10^{-4} mol initiator and the following amounts of styrene: 2.92×10^{-3} mol for 103-A, 1.75×10^{-2} mol in 131-A and 2.75×10^{-3} mol in 139-A and 139-B. Elemental analysis of the final samples showed that all of the polymer-grafted platinum samples contained higher amounts of carbon, hydrogen and nitrogen than the control sample (Table 3.7). We were able to increase the levels of carbon and hydrogen in the

Table 3.7 Elemental Analysis of Polystyrene-Grafted Platinum

| <u>Sample</u> | <u>Weight %</u> | | | <u>Moles</u> | | |
|--------------------------|-----------------|----------|----------|--------------|----------|----------|
| | <u>C</u> | <u>H</u> | <u>N</u> | <u>C</u> | <u>H</u> | <u>N</u> |
| 103-A | 19.27 | 1.88 | 0.20 | 1.61 | 1.88 | 0.014 |
| 131-A | 26.07 | 2.37 | 0.14 | 2.17 | 2.37 | 0.010 |
| 139-A | 6.18 | 0.47 | 0.11 | 0.51 | 0.47 | 0.008 |
| 139-B | 4.20 | 0.40 | 0.10 | 0.35 | 0.40 | 0.007 |
| Control | 1.15 | <0.10 | <0.10 | 0.09 | -- | -- |
| Polystyrene ^a | 92.31 | 7.69 | -- | 7.69 | 7.69 | -- |

^a Theoretical values for a high molecular weight sample neglecting endgroups.

final product by increasing the amount of monomer added to the reaction mixture. If we assume that every nitrogen detected in the compound was a site of initiation, we can calculate the expected molecular weight based on elemental analysis. The molecular weight was also calculated from the amount of styrene and initiator added to the system (Table 3.8). The molecular weight calculated from the nitrogen content was

lower than the theoretical molecular weight, indicating that some of the styrene added to the reaction mixture was polymerized by excess initiator in solution and was not grafted to the platinum. It is also possible that some of the picoline molecules bound to the platinum did not initiate

Table 3.8 Calculated Molecular Weight of Polystyrene-Grafted Platinum

| <u>Sample</u> | <u>Mn(elemental)^a</u> | <u>Mn(reagents)^b</u> |
|---------------|----------------------------------|---------------------------------|
| 103-A | 1,500 | 4,023 |
| 131-A | 4,040 | 8,891 |
| 139-A | 660 | 1,400 |
| 139-B | 570 | 1,400 |

^a Calculated from the elemental analysis of C and N. Assuming that each N is from one picoline molecule and therefore is a site of initiation. All the C is assumed to come from styrene.

^b Calculated from the moles of styrene and initiator added to the reaction.

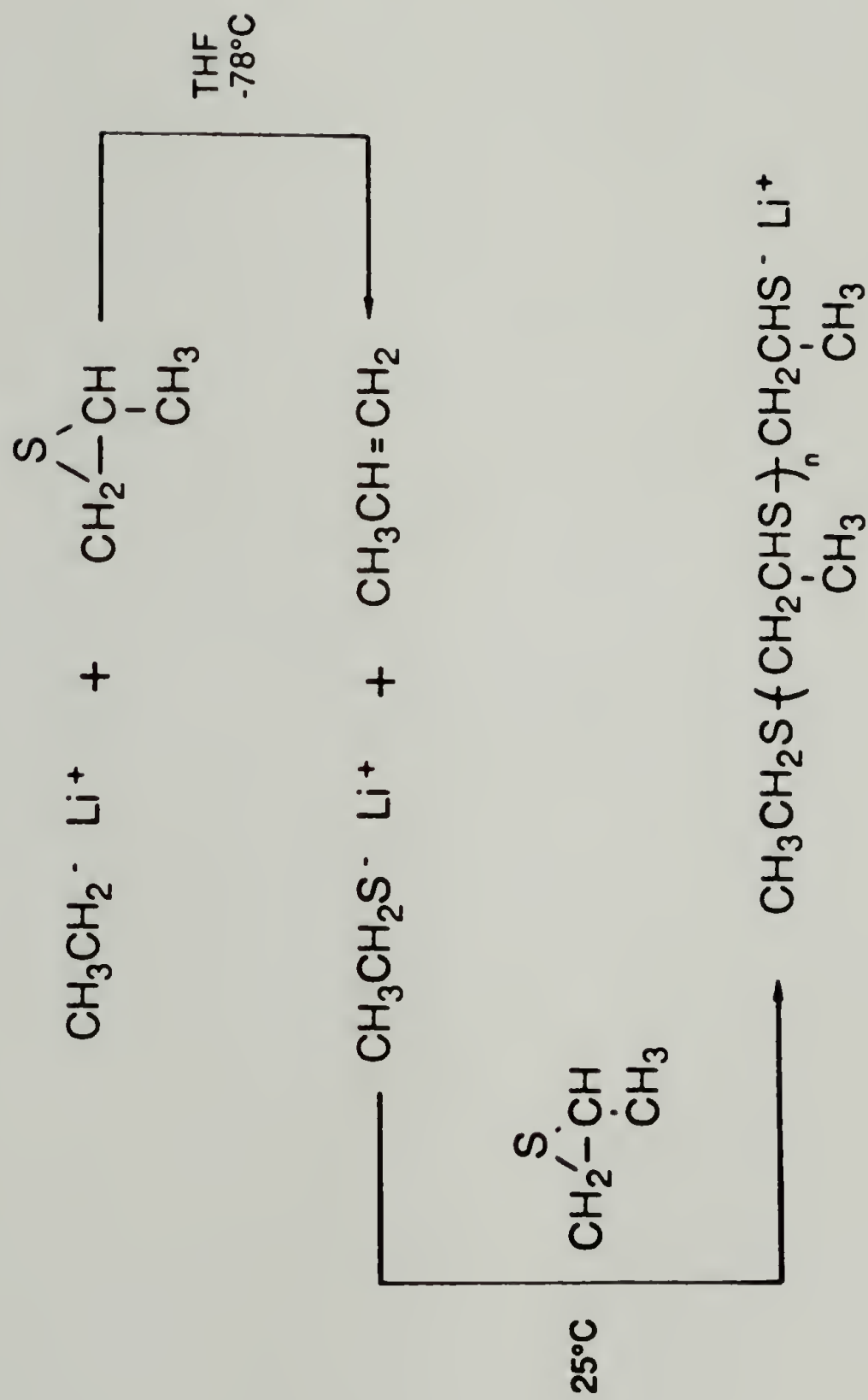
polymerization. It is quite probable that once polymer began to grow away from the surface it would sterically hinder monomer from reaching initiators bound to the surface and the growing polymer itself would react with the monomer.

Adsorption of Sulfur-Functionalized Polymers on Gold

We have investigated polymer monolayers prepared by the spontaneous adsorption of sulfur-functionalized polystyrene on gold surfaces.¹² Polymer monolayers were prepared by the adsorption of thiol-terminated polystyrenes (PSSH) and polystyrene/poly(propylene sulfide) block copolymers (PS/PPS) from solution onto glass-supported evaporated gold films. We use the term "polymer monolayer" to mean a thin film of polymer in which each polymer molecule is attached to the surface; no order in the polymer film is implied. The experiments which are discussed here were performed with the objective of determining what control of polymer film thickness could be exercised by changes in molecular weight, concentration, solvent composition and the number of sulfur atoms in the polymer chain.

Synthesis of Polymers

Thiol-Terminated Polystyrene. Living polystyrene was prepared by anionic polymerization of styrene. The living polystyryl anion was endcapped with propylene sulfide and the polymer was protonated with acidic methanol to produce thiol-terminated polystyrene (PSSH). The anionic polymerization of ethylene sulfide and propylene sulfide was originally reported by Boileau and coworkers.¹³⁻¹⁵ Unlike epoxide, the anionic polymerization of episulfides proceeds without chain transfer or termination so it is possible to synthesize high molecular weight polymers and block copolymers. Morton and Kammereck¹⁶ have investigated the initiation reaction of ethyllithium with propylene sulfide in THF at



Scheme 3.2 Polymerization of propylene sulfide initiated by ethyllithium

-78°C. They found that under stringent experimental conditions ethyllithium attacks propylene sulfide exclusively at the sulfur atom to form the lithium ethanethiolate which in the presence of excess propylene sulfide at room temperature produces a linear polymer with a carbon-carbon-sulfur backbone as shown in Scheme 3.2.

To obtain the thiol end group, thiolate anion was protonated with acidic methanol. Care was taken in the workup to avoid oxidation of the mercaptan. Even the oxygen in air oxidizes mercaptans on standing if a small amount of base is present.¹⁷ The polymer samples were stored under nitrogen. The presence of the thiol endgroup in low molecular weight polystyrene samples that had been endcapped with ethylenesulfide was seen by infrared spectroscopy. Figure 3.18 shows a weak absorbance at 2550 cm^{-1} characteristic of a S-H stretch; the ^1H -NMR spectrum of the low molecular weight thiol-terminated polystyrene showed a signal at $\sim 1.6\text{ ppm}$ which we attributed to the S-H proton. The two aliphatic signals seen for polystyrene fall at 1.4 and 1.8 ppm. When D_2O was shaken with the mercaptan product the ^1H -NMR spectrum showed a decrease in the intensity of the shift at 1.6 ppm while the other peaks remained unchanged. The adsorption experiments were performed using thiol-terminated polystyrene which had been endcapped with propylene sulfide. Table 3.9 shows the results from the GPC characterization of polymers before and after the endcapping reaction. Samples 67-A2 and 67-B2 show a slight increase in molecular weight due to the incorporation of the propylene sulfide (74.15 g/mole) and a little broadening of the narrow molecular weight distribution. The elemental composition of these

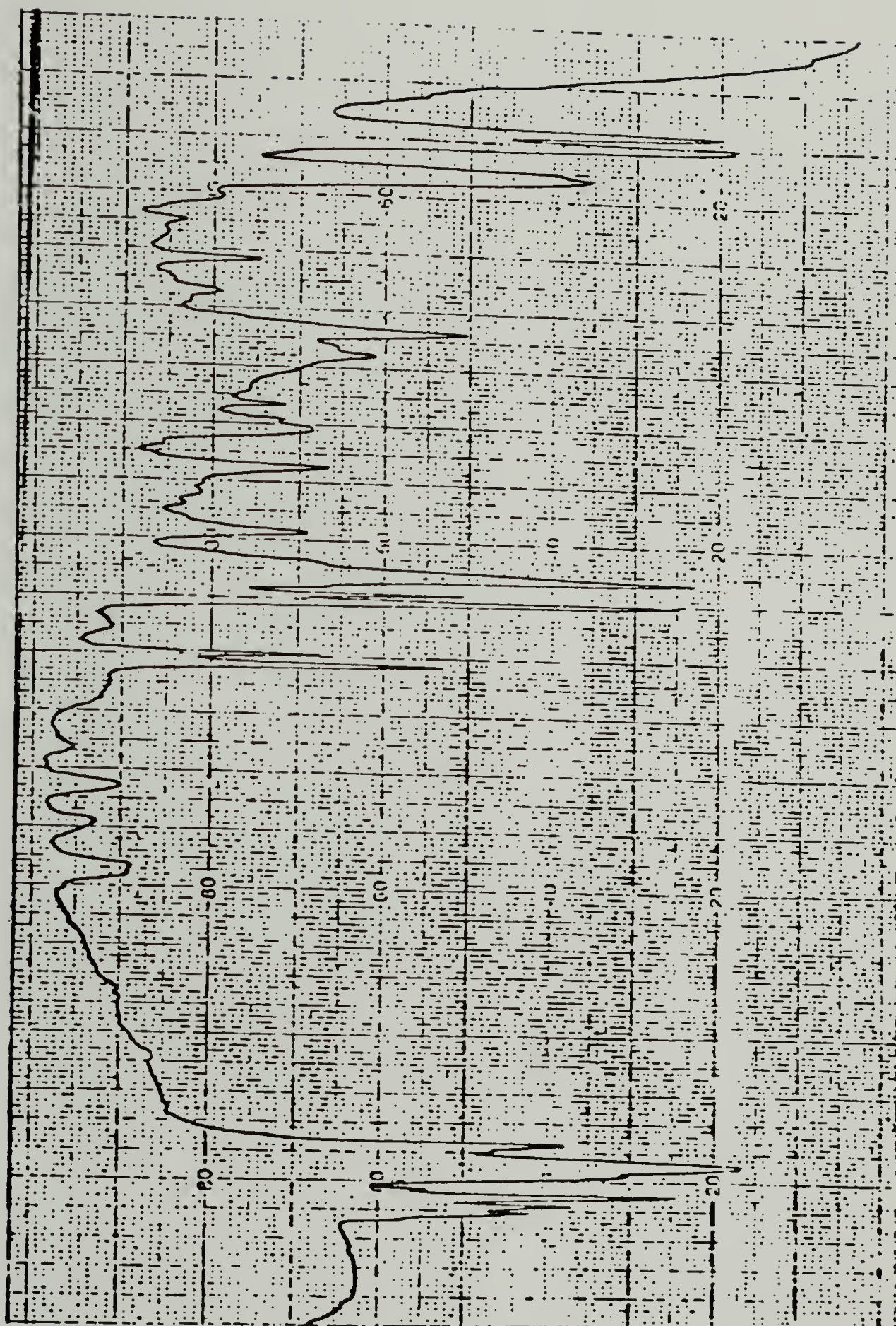


Figure 3.18 Infrared spectrum of thiol-terminated polystyrene

Table 3.9 GPC Characterization of Polystyrene Before and After Endcapping with Propylene Sulfide

| <u>Capping</u> | <u>Sample</u> | <u>Mn</u> | <u>Mw</u> | <u>PDI</u> |
|----------------|---------------|-----------|-----------|------------|
| Before | 67-A1 | 840 | 890 | 1.05 |
| After | 67-A2 | 910 | 960 | 1.06 |
| Before | 61-B1 | 11,400 | 11,800 | 1.04 |
| After | 61-B2 | 11,600 | 12,100 | 1.05 |

polymers is shown in Table 3.10. The GPC molecular weight characterization for all of the PSSH polymers used in the adsorption studies is listed in Table 3.11. Elemental analysis was not performed on the higher molecular weight samples because the sulfur content would have been below the detection limit.

Table 3.10 Elemental Analysis of Thiol-Terminated Polystyrene

| <u>Sample</u> | | <u>Weight Percent</u> | | |
|---------------|-------------|-----------------------|----------|-------------------|
| | | <u>C</u> | <u>H</u> | <u>S</u> |
| 67-A | Theoretical | 88.8 | 8.2 | 3.00 |
| | Determined | 88.48 | 8.46 | 3.06 |
| 61-B | Theoretical | 91.7 | 7.7 | 0.55 ^a |
| | Determined | 91.61 | 7.88 | 0.51 |

^a Value calculated for addition of two moles of propylene sulfide, one mole would have given 0.3 weight percent S.

Table 3.11 Characteristics of PSSH Polymers

| <u>Sample</u> | <u>Mn</u> | <u>Mw/Mn</u> | <u>CPM^a</u> |
|---------------|-----------|--------------|------------------------|
| 7-67A | 910 | 1.06 | -- |
| 7-123A | 5,057 | 1.04 | -- |
| 7-123B | 9,623 | 1.03 | -- |
| 7-83B | 57,029 | 1.04 | -- |
| 7-89A | 134,729 | 1.06 | -- |
| 7-89B | 203,175 | 1.03 | -- |
| 7-85A | 512,558 | 1.08 | -- |
| 7-143H | 5,544 | 1.06 | 784.9 |
| 7-135H | 17,682 | 1.06 | 516.1 |
| 7-131H | 57,970 | 1.06 | 270.0 |
| 7-145H | 194,993 | 1.08 | 287.2 |

^a Counts per minute of 2.4×10^{-7} g from THF solution.

Polystyrene/Poly(propylene sulfide) Block Copolymers. The synthetic strategy for making polystyrene/poly(propylene sulfide) block copolymer (PS/PPS) is depicted in Scheme 3.3. Following a procedure similar to the one reported by Nevin and Pearce¹⁸, styrene monomer was anionically polymerized with sec-butyllithium in THF at -78°C , propylene sulfide was added and the reaction was allowed to proceed at room temperature. The polymer was protonated with acidic methanol and precipitated in methanol. Propylene sulfide was used in the synthesis of block copolymers instead of ethylene sulfide because of the



Scheme 3.3 Synthesis of polystyrene/poly(propylene sulfide) block copolymers

insolubility of the poly(ethylene sulfide) block. Poly(propylene sulfide) is soluble in many of the same solvents that polystyrene is soluble in: acetone, THF, dioxane, benzene, chlorobenzene and carbon tetrachloride.

Table 3.12 Elemental Analysis for C, H, and S in Various Polymers Containing Styrene and Propylene Sulfide

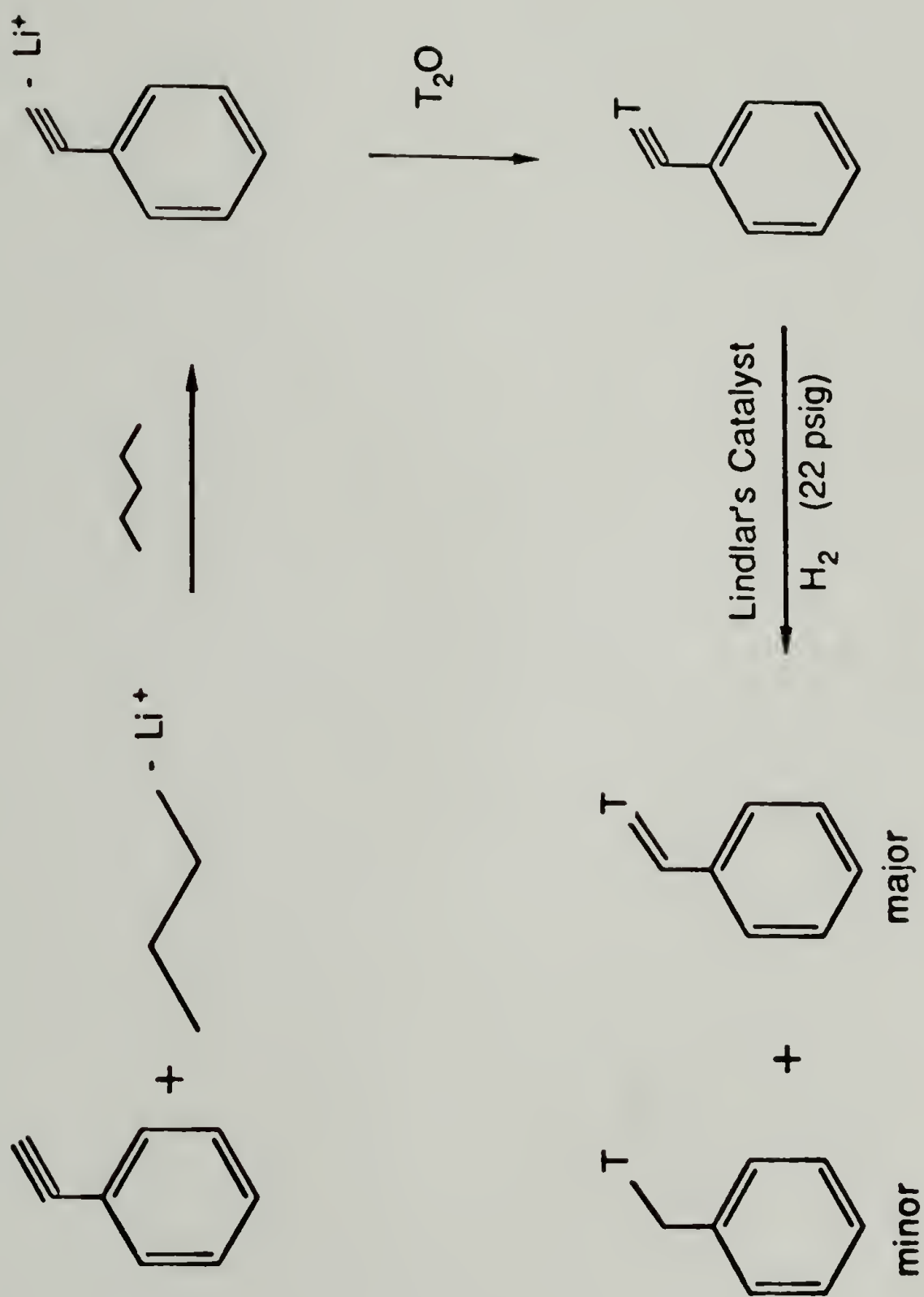
| <u>Sample</u> | | <u>C</u> | <u>H</u> | <u>S</u> | <u>Mn</u> ^b |
|---------------------|----------------|----------|----------|----------|------------------------|
| Polystyrene | T ^a | 92.31 | 7.69 | - | - |
| | D | 92.25 | 7.75 | - | 4,928 |
| PS/PPS 1/1 7-23A | T | 70.48 | 7.90 | 21.62 | - |
| | D | 73.73 | 8.25 | 18.02 | 4,106 |
| PS/PPS 3/1 7-25A | T | 81.40 | 7.80 | 10.81 | - |
| | D | 83.71 | 8.09 | 8.20 | 2,605 |
| PS/PPS 6/1 7-25B | T | 86.07 | 7.75 | 6.18 | - |
| | D | 87.50 | 8.38 | 4.12 | 2,114 |
| PPS 7-29A | T | 48.65 | 8.11 | 43.24 | - |
| | D | 47.44 | 8.26 | 41.29 | 2,129 |

^a T = Theoretical, D = Determined

^b Determined by GPC

Poly(ethylene sulfide) on the other hand, is insoluble in all common solvents. The elemental composition of low molecular weight samples listed in Table 3.12 shows that the expected amount of propylene sulfide was incorporated into the block copolymer with polystyrene.

Tritiated Styrene. The reported synthesis of β -deuteriostyrene (Hassner et al.¹⁹) was modified to prepare tritiated styrene as shown in Scheme 3.4. Phenylacetylene was deprotonated with *n*-butyllithium and then protonated with tritiated water. The ³H-phenylacetylene was



Scheme 3.4 Synthesis of tritiated styrene

reduced to ^3H -styrene using Lindlar's catalyst. This reduction produced a mixture of ^3H -styrene and ^3H -ethylbenzene. The ^1H -NMR spectrum for the final pentane reaction mixture dissolved in C_6D_6 is shown in Figure 3.19. All of the ^3H -phenylacetylene, which would have shown a proton signal at 3.1 ppm, was reduced. The relative amounts of ^3H -styrene and ^3H -ethylbenzene were determined from the integration of the expanded spectrum in Figure 3.20. The quartet at 6.5 ppm is due to the single proton on the carbon α to the ring in ^3H -styrene, and the quartet at 2.5 ppm is due to the two protons on the carbon α to the ring in ^3H -ethylbenzene.

$$\begin{array}{ll} \text{At 6.5 ppm} & \frac{27 \text{ mm of integration}}{1 \text{ proton}} = 27 \quad \text{from } ^3\text{H-styrene} \\ \text{At 2.5 ppm} & \frac{9 \text{ mm of integration}}{2 \text{ protons}} = 4.5 \quad \text{from } ^3\text{H-ethylbenzene} \end{array}$$

$$\frac{^3\text{H-styrene}}{^3\text{H-ethylbenzene}} = \frac{27}{4.5} = 6$$

From the ^1H -NMR data we see that our radiolabelled synthesis produced 86% ^3H -styrene and 14% ^3H -ethylbenzene. This radioactive mixture was diluted with "cold" styrene so that the ^3H -ethylbenzene was less than 1.5%, then purified prior to its use in an anionic polymerization.

Radiolabelled Polymers. The tritiated polymers were made under reaction conditions similar to those used for the "cold" polymers, but ^3H -styrene was used as the monomer. Since the radioactive product could not be characterized directly for molecular weight, an identical "cold" reaction was run simultaneously with the same amounts of

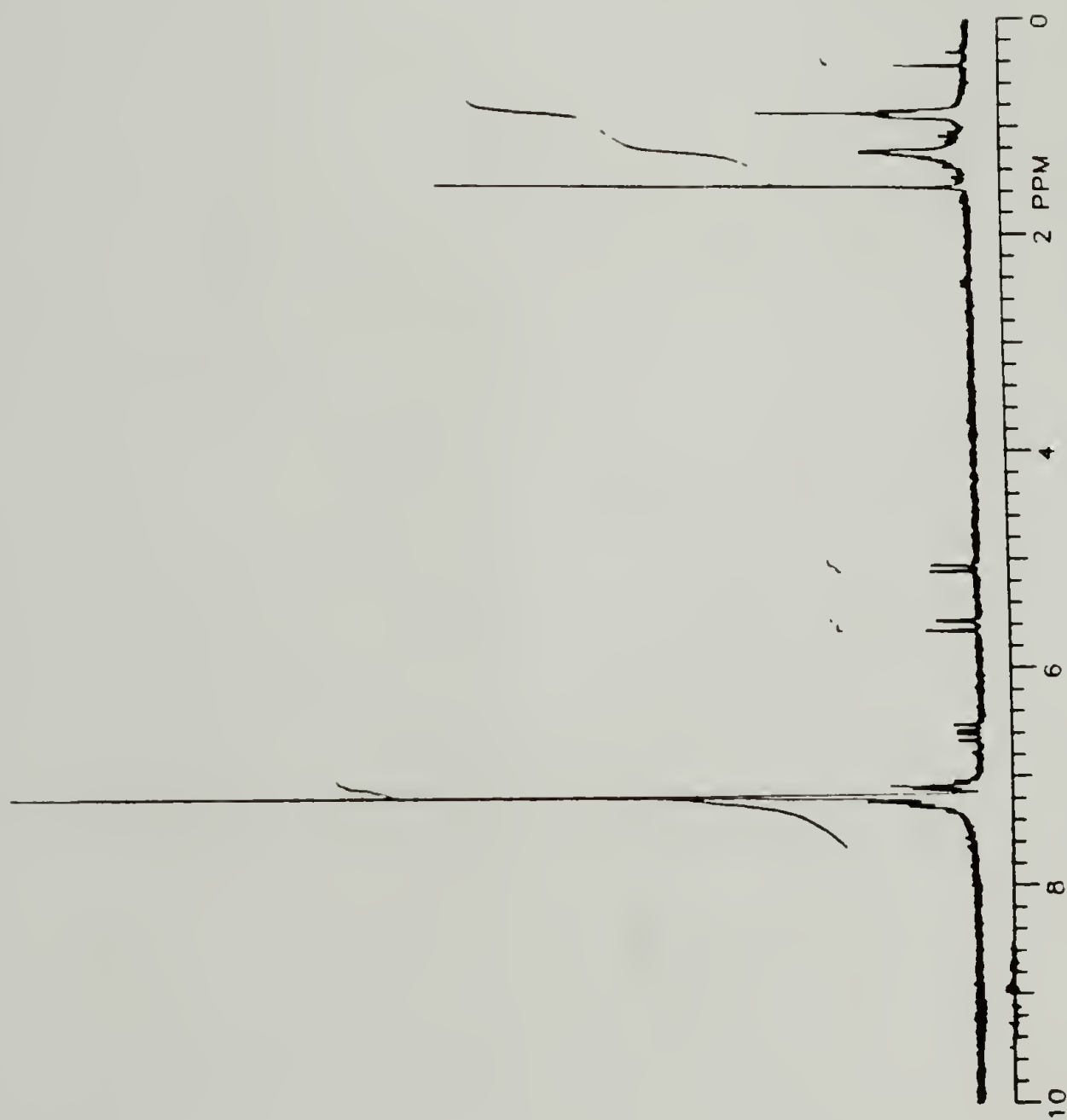


Figure 3.19 ^1H -NMR spectrum of the final reaction mixture from the tritiated styrene synthesis

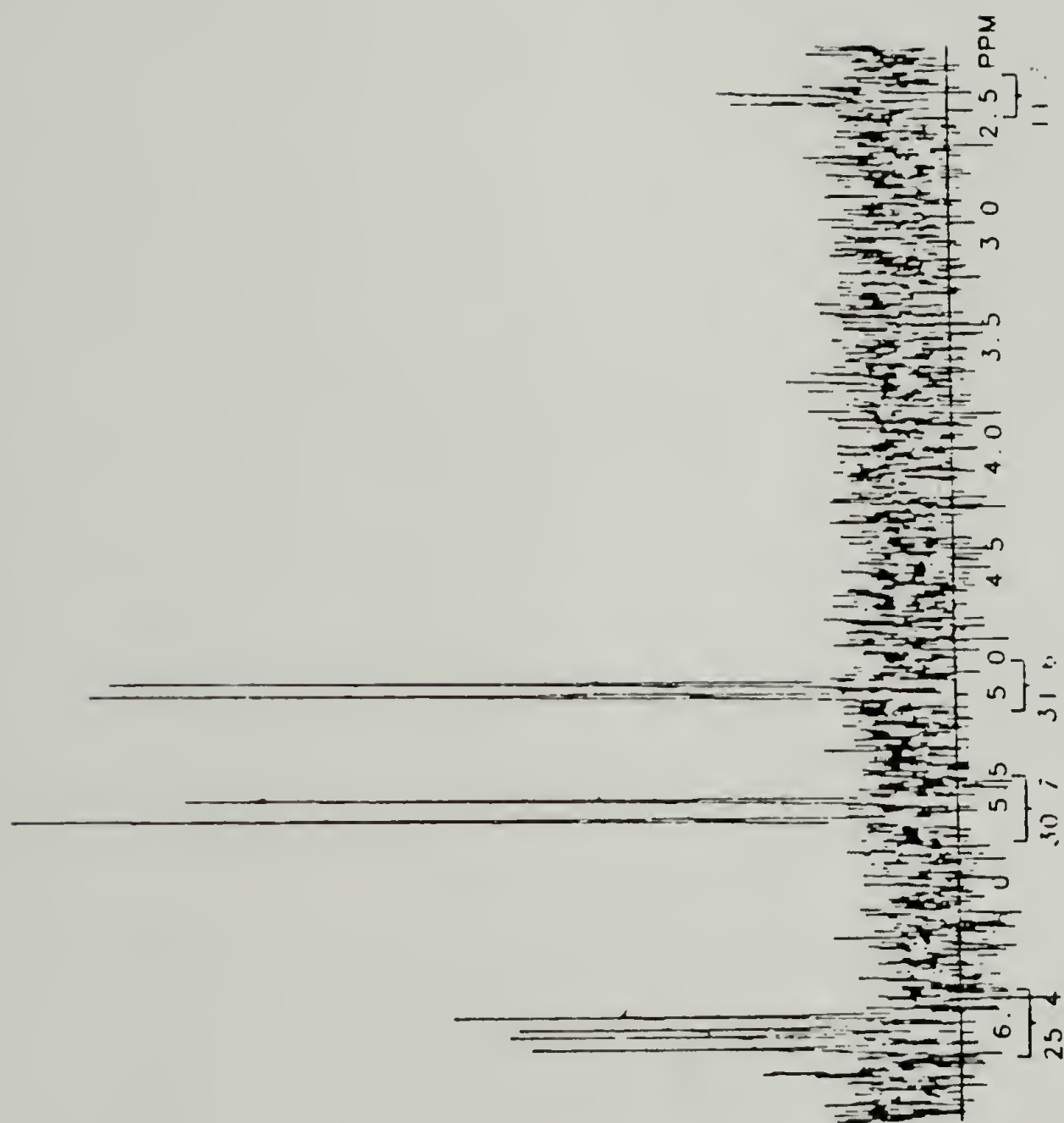


Figure 3.20 Expanded ^1H -NMR spectrum from the tritiated styrene synthesis

initiator, solvent and "cold" monomer from which samples were taken for GPC analysis. The yield from the synthesis of the radioactive polymer was determined directly. The characteristics for the thiol-terminated polystyrene polymers and the polystyrene/poly(propylene sulfide) block copolymers are listed in Tables 3.12 and 3.13.

Table 3.13 Characteristics of PS/PPS Block Copolymers

| <u>Sample</u> | <u>PS:PPS</u> | <u>Mn</u> | <u>Mw/Mn</u> | <u>CPM^a</u> |
|---------------|---------------|-----------|--------------|------------------------|
| 8-51H | 10:90 | 60,324 | 1.28 | 192.8 |
| 8-47H | 30:70 | 61,021 | 1.21 | 310.3 |
| 8-33H | 50:50 | 58,324 | 1.15 | 435.5 |
| 8-43H | 70:30 | 59,114 | 1.09 | 574.4 |
| 7-131H | 99:1 | 57,970 | 1.06 | 270.0 |

^a CPM of 2.4×10^{-7} g from THF solution.

Beer's Law Justification for Radiolabelled Polymers

For each radiolabelled polymer the level of radioactivity was determined for a series of dilute solutions. The concentration of the polymer solution was plotted against the radioactivity in CPM, as determined by liquid scintillation counting. All of the radiolabelled polymers showed a linear Beer's Law relationship between concentration and radioactivity (CPM) for dilute solutions. Figure 3.21 shows the Beer's Law plot for one of the radiolabelled polymers used in the adsorption experiments. Table 3.14 lists the analytical expressions for

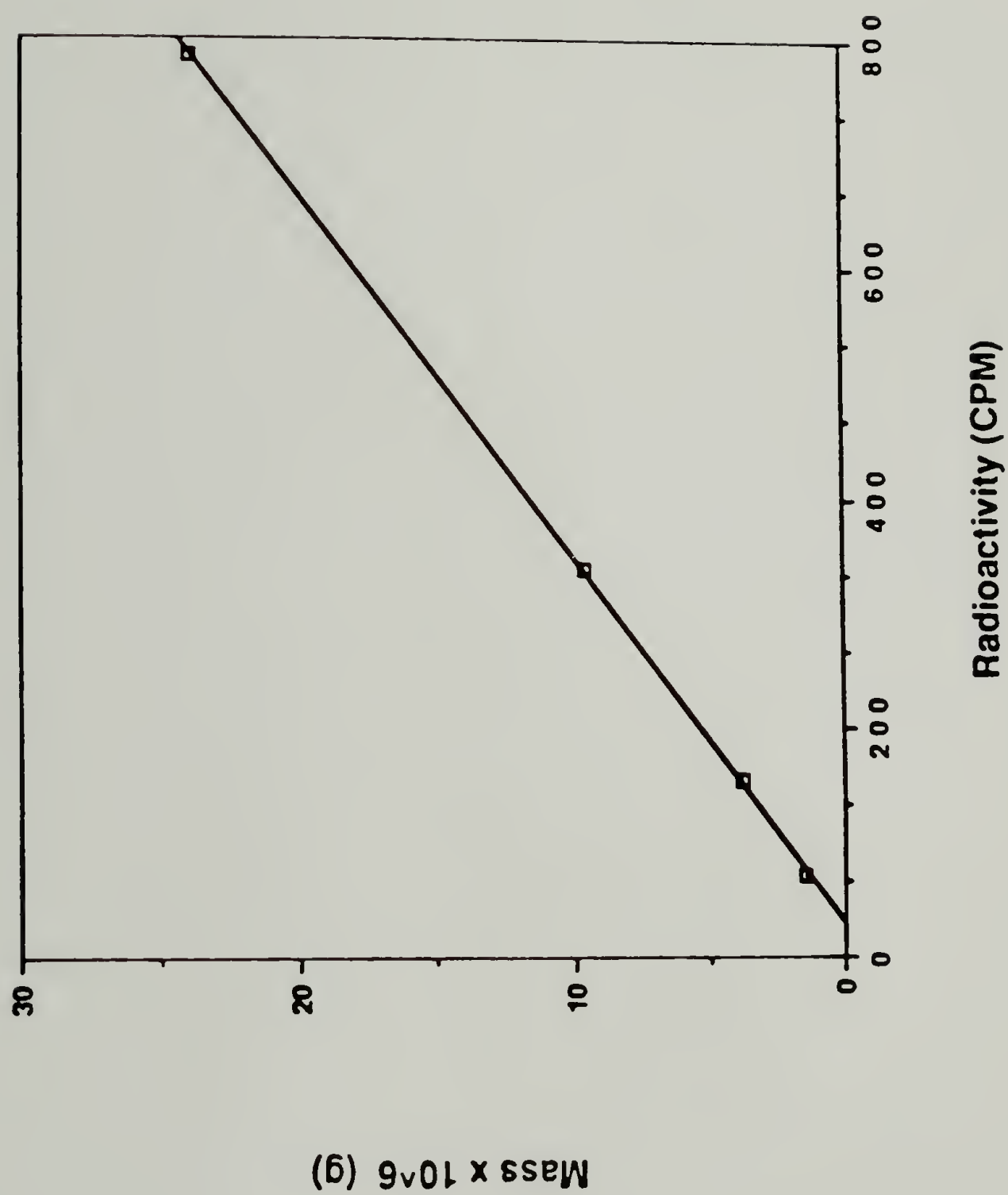


Figure 3.21 Beer's Law plot of mass versus radioactivity for PSSH 7-143H

the Beer's Law relationship of each radiolabelled polymer used. Data used to derive these expressions are listed in Table A.1 in the Appendix.

Table 3.14 Analytical Expressions for Beer's Law Relationships

| <u>Sample</u> | <u>Analytical Expression</u> |
|---------------|------------------------------|
| PSSH 7-143H | $y = -0.9540 + 0.0317x$ |
| PSSH 7-135H | $y = -1.4791 + 0.0494x$ |
| PSSH 7-131H | $y = -2.9302 + 0.0994x$ |
| PSSH 7-145H | $y = -2.8072 + 0.0933x$ |
| PS/PPS 8-51H | $y = -4.5793 + 0.1477x$ |
| PS/PPS 8-47H | $y = -2.6267 + 0.0860x$ |
| PS/PPS 8-33H | $y = -1.7799 + 0.0594x$ |
| PS/PPS 8-43H | $y = -1.3927 + 0.0446x$ |

Adsorption of Polymers on Gold

The mass of the polymer adsorbed to the gold surface was determined using tritiated polymers. The gold substrate was counted directly in the scintillation cocktail. The mass of the polymer adsorbed on the gold surface was calculated from the Beer's Law relationship of the polymer in dilute solution, the scintillation results were corrected for a 20% decrease in efficiency and absorption of half the low energy beta particles by the solid sample. A complete description of liquid scintillation counting and the corrections made for the solid samples

were discussed in the Introduction. A control experiment was run in which a glass cover slip, that had not been coated with gold, was exposed to a solution of tritiated, thiol-terminated polystyrene. The glass cover slip was counted and it did not show any increase in radioactivity indicating that no polymer adsorbed to the glass surface without a gold coating.

Factors Influencing the Adsorption of Polymers

The adsorption was followed and the resulting monolayers were characterized by various techniques. External reflectance FTIR spectroscopy (XR IR) was used to identify the polymer adsorbed to the gold surface. X-ray photoelectron spectroscopy (XPS) provided information about the elemental composition of the outer surface. Liquid scintillation counting (LSC) was used to determine the mass of the polymer adsorbed to the gold surface.

Adsorption Kinetics. Adsorption times were varied from several minutes to days. The adsorbance reached equilibrium for concentrations greater than 0.2 mg/mL after one hour, A in Figure 3.22. For extremely dilute solutions (0.02 mg/mL) equilibrium adsorbance was not reached until 24 hours, B in Figure 3.22. This same type of adsorption behavior was observed by Kawaguchi and Takahashi²⁰ in their study of the adsorption of polystyrene onto a chrome surface in good solvent conditions.

Molecular Weight Dependence. External reflectance FTIR (XR IR) spectroscopy showed that thiol-terminated polystyrene (PSSH) adsorbed to

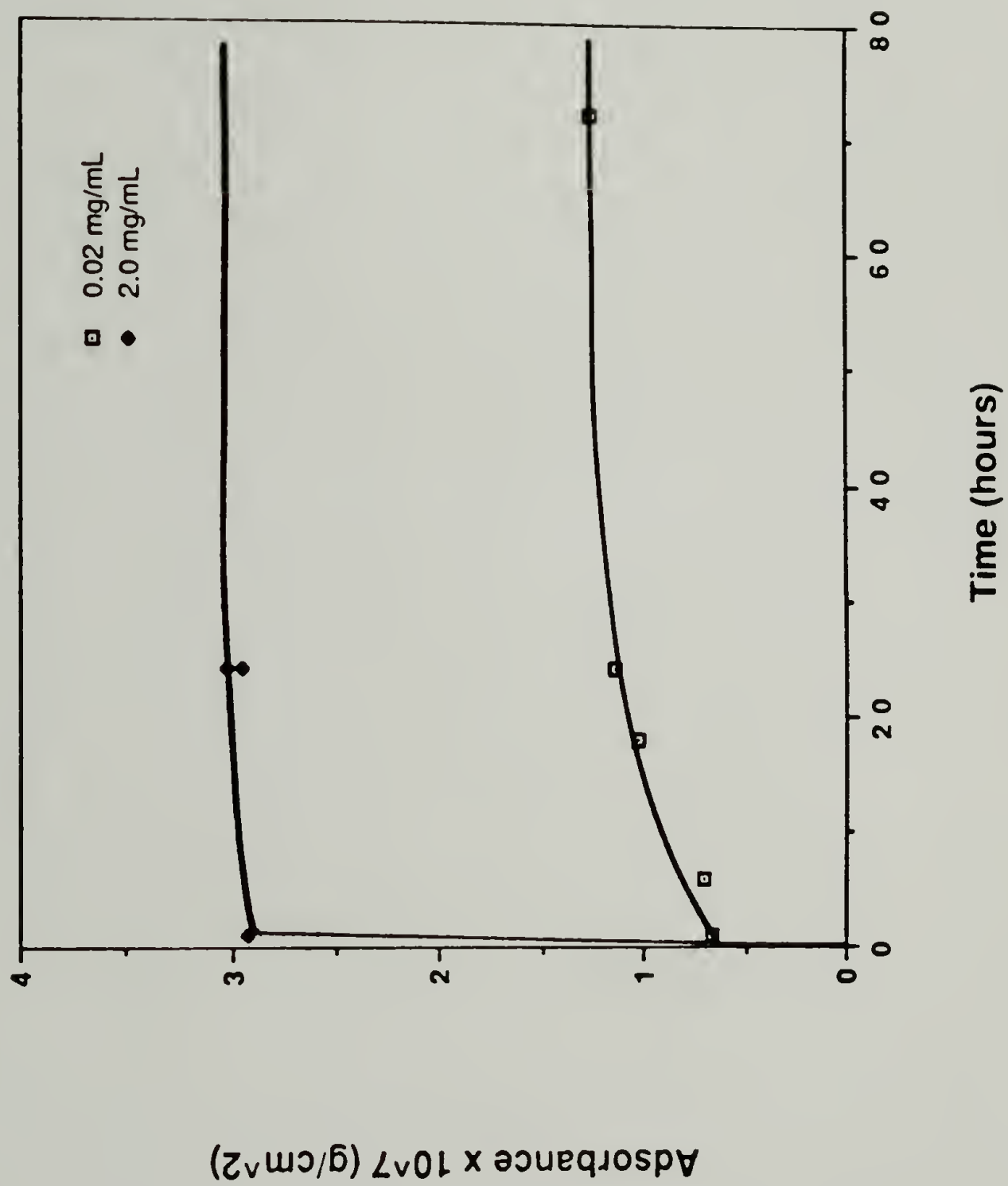


Figure 3.22 Kinetics of polymer adsorption from dilute solution

gold from a good solvent when the molecular weight of the polymer was less than or equal to 200,000. XR IR spectra of adsorbed thin films exhibit characteristic polystyrene absorbances due to C-H stretching in the 3100-2800 cm^{-1} region.¹¹ Figure 3.23 compares the XR IR spectrum (A) obtained from a gold substrate that had been exposed to a solution of thiol-terminated polystyrene, to spectrum (B) obtained from a gold substrate that had been exposed to a solution of polystyrene that did not contain a thiol group. We see in spectrum A that PSSH sample 7-67A ($M_n = 910$) adsorbed to the gold surface whereas a polystyrene sample of the same molecular weight did not absorb (spectrum B). Figures 3.24 - 3.28 show the infrared spectra for thin films of PSSH samples, molecular weights up to 200,000, adsorbed to gold substrates.

Liquid scintillation counting showed how the amount of polymer adsorbed varied with molecular weight. A plot of adsorbance versus molecular weight is shown in Figure 3.29 for tritiated PSSH polymers adsorbed to gold substrates from THF solutions (2.0 mg/ml) after 24 hours. The adsorbance (g/cm^2) was determined from the CPM values obtained from LSC. The data for this plot are listed in Table A.2 in the Appendix. The adsorbance rises sharply in the low molecular weight regime, then reaches a constant value. According to the theory of Scheutjens and Fleer²¹, the amount of polymer adsorbed from a good solvent levels off above a degree of polymerization of 10^2 . These conclusions are in good agreement with theoretical predictions of Silberberg²², and also with the experimental results of Kawaguchi and Takahashi.²⁰

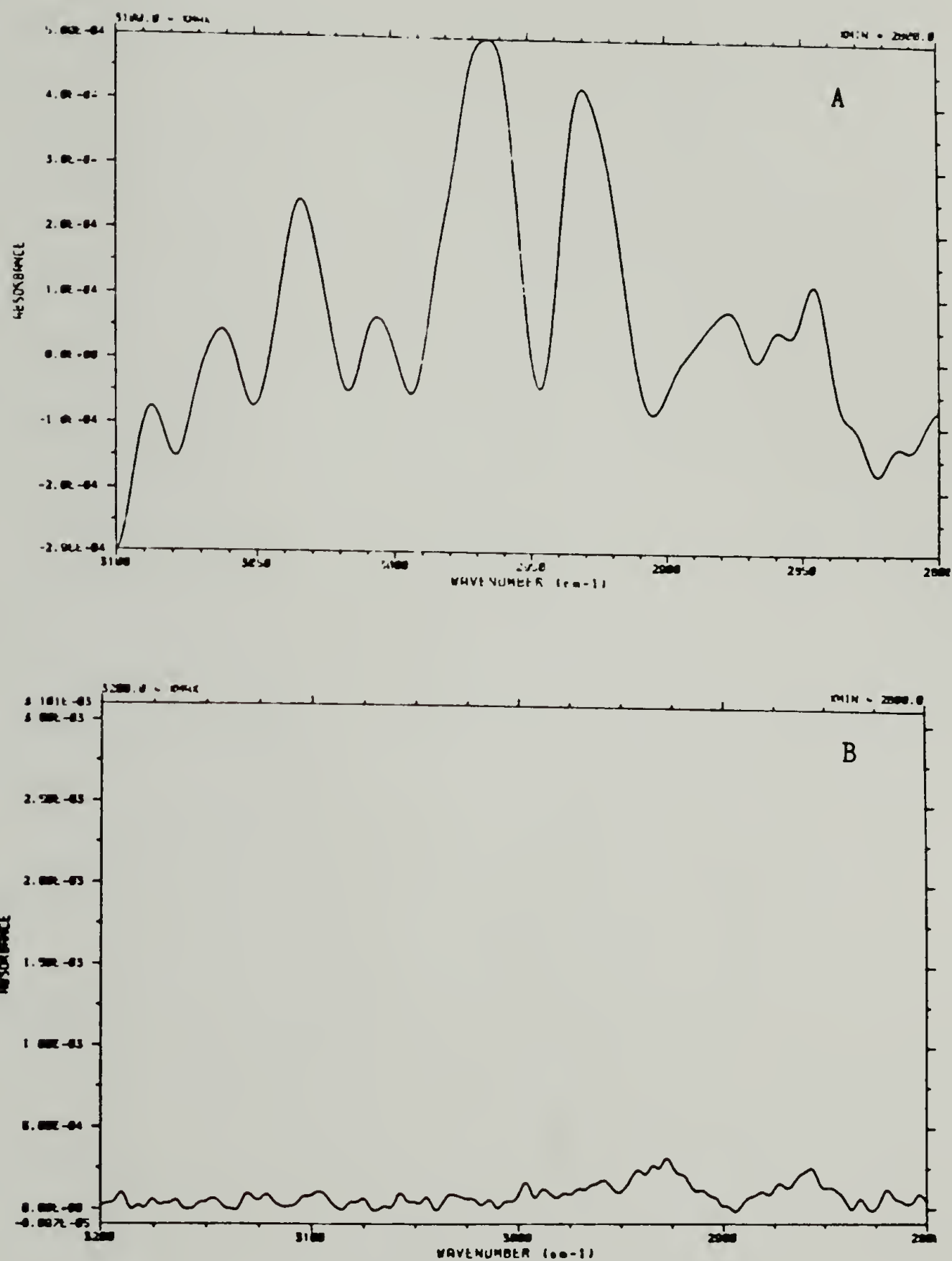


Figure 3.23 Comparison of the XR IR spectrum of a gold surface exposed to a PSSH polymer solution (A) to that of a PS polymer solution (B)

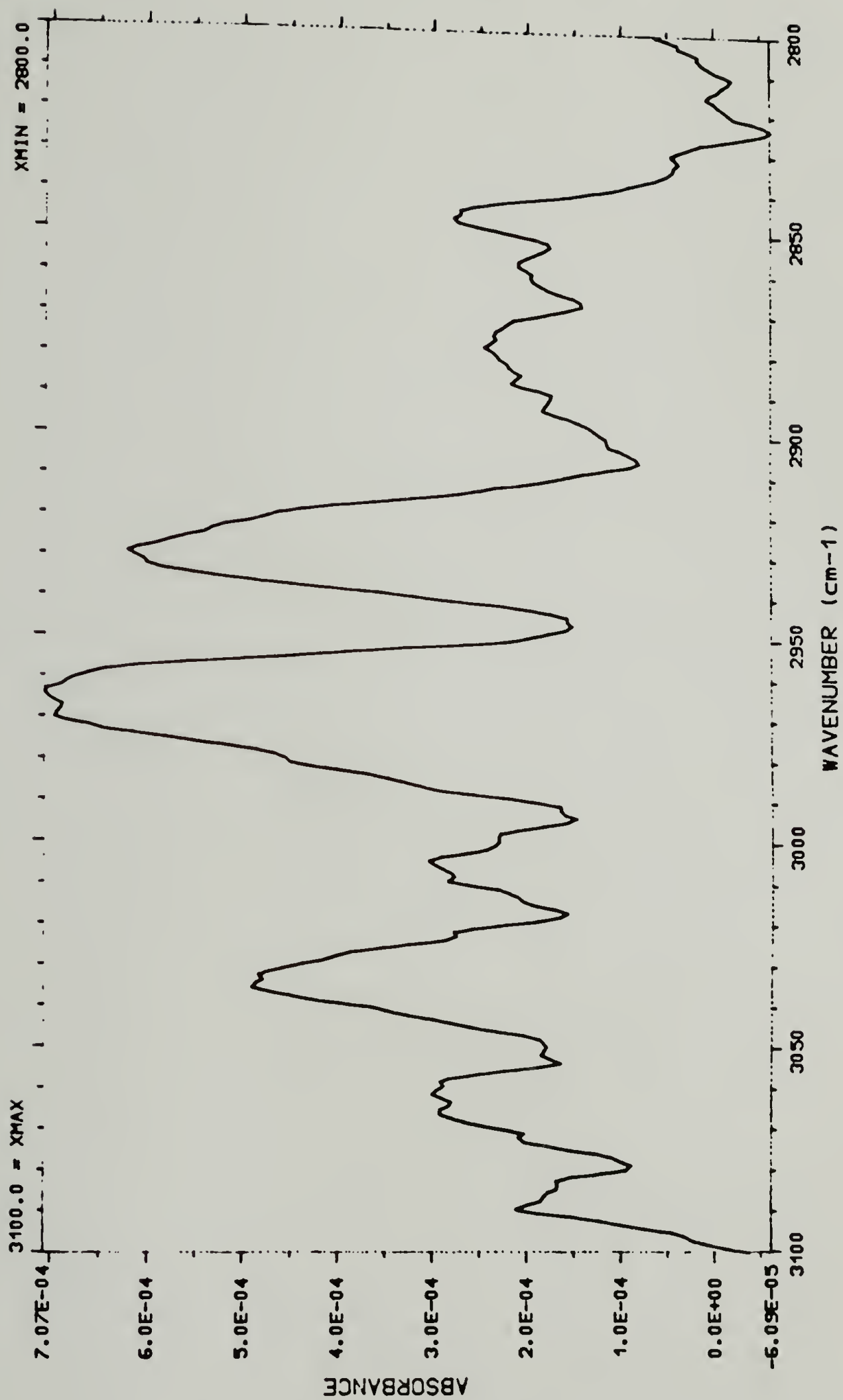


Figure 3.24 XR IR spectrum of PSSH 7-123A adsorbed to gold

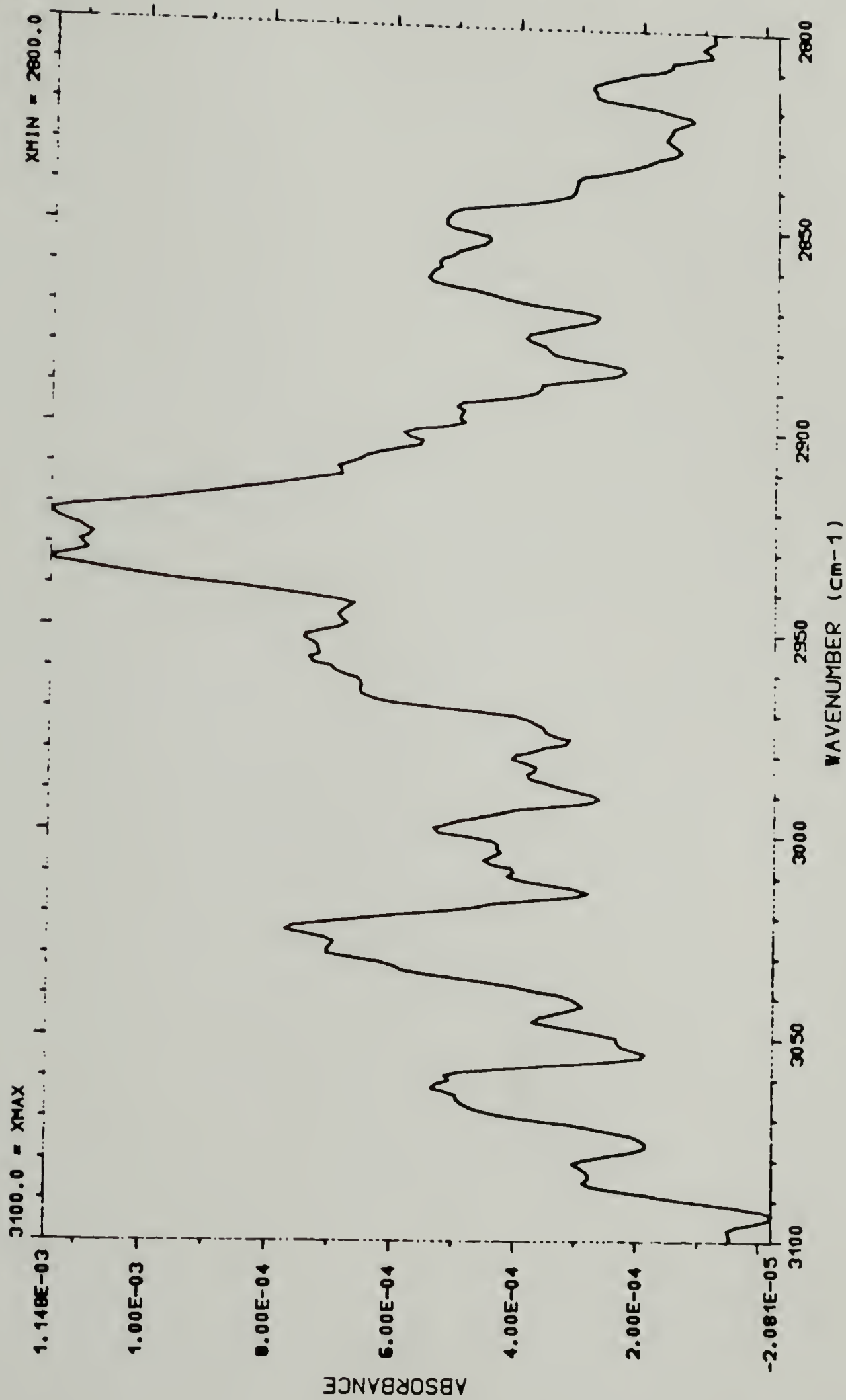


Figure 3.25 XR IR spectrum of PSSH 7-123B adsorbed to gold

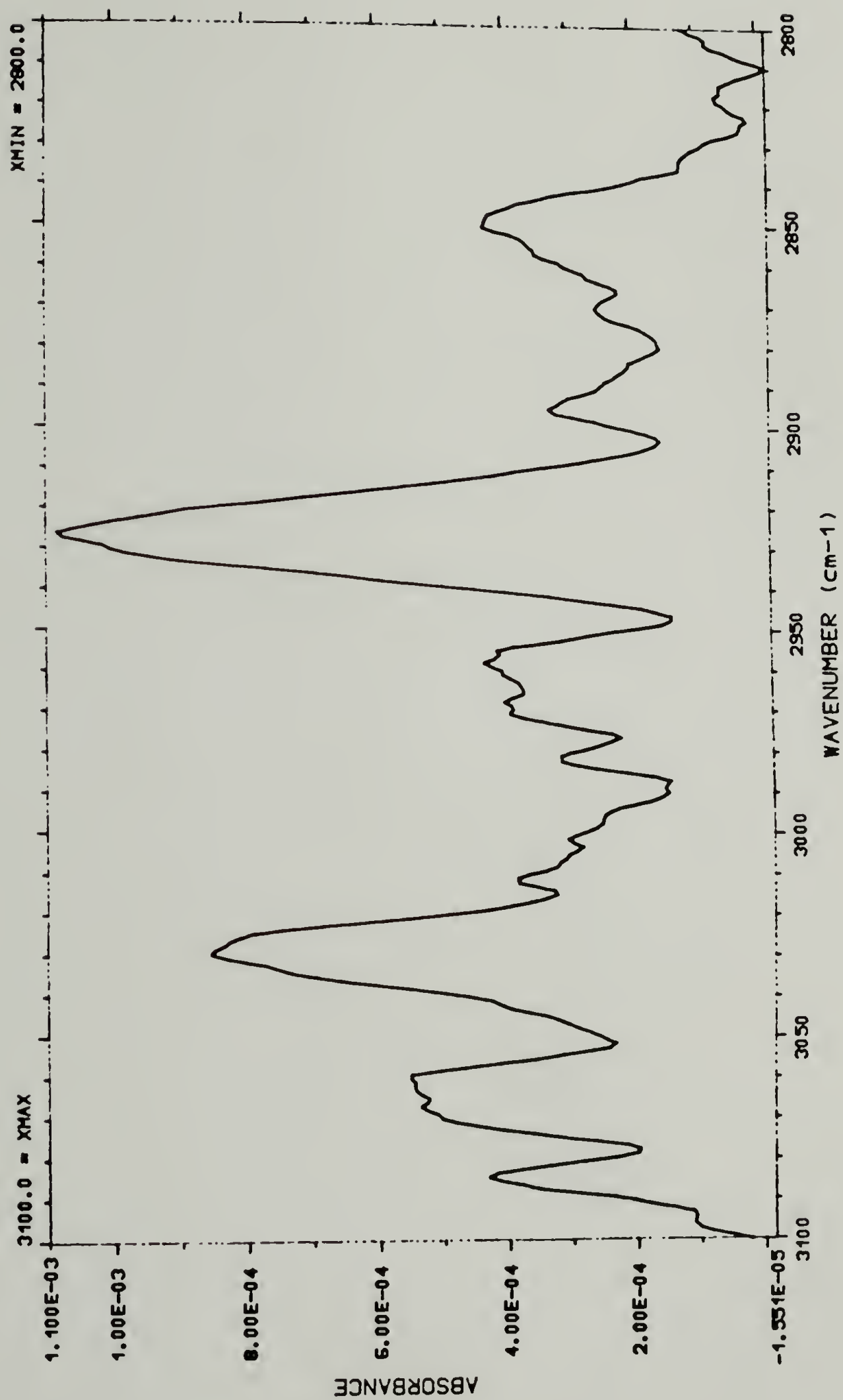


Figure 3.26 XR IR spectrum of PSSH 7-83B adsorbed to gold

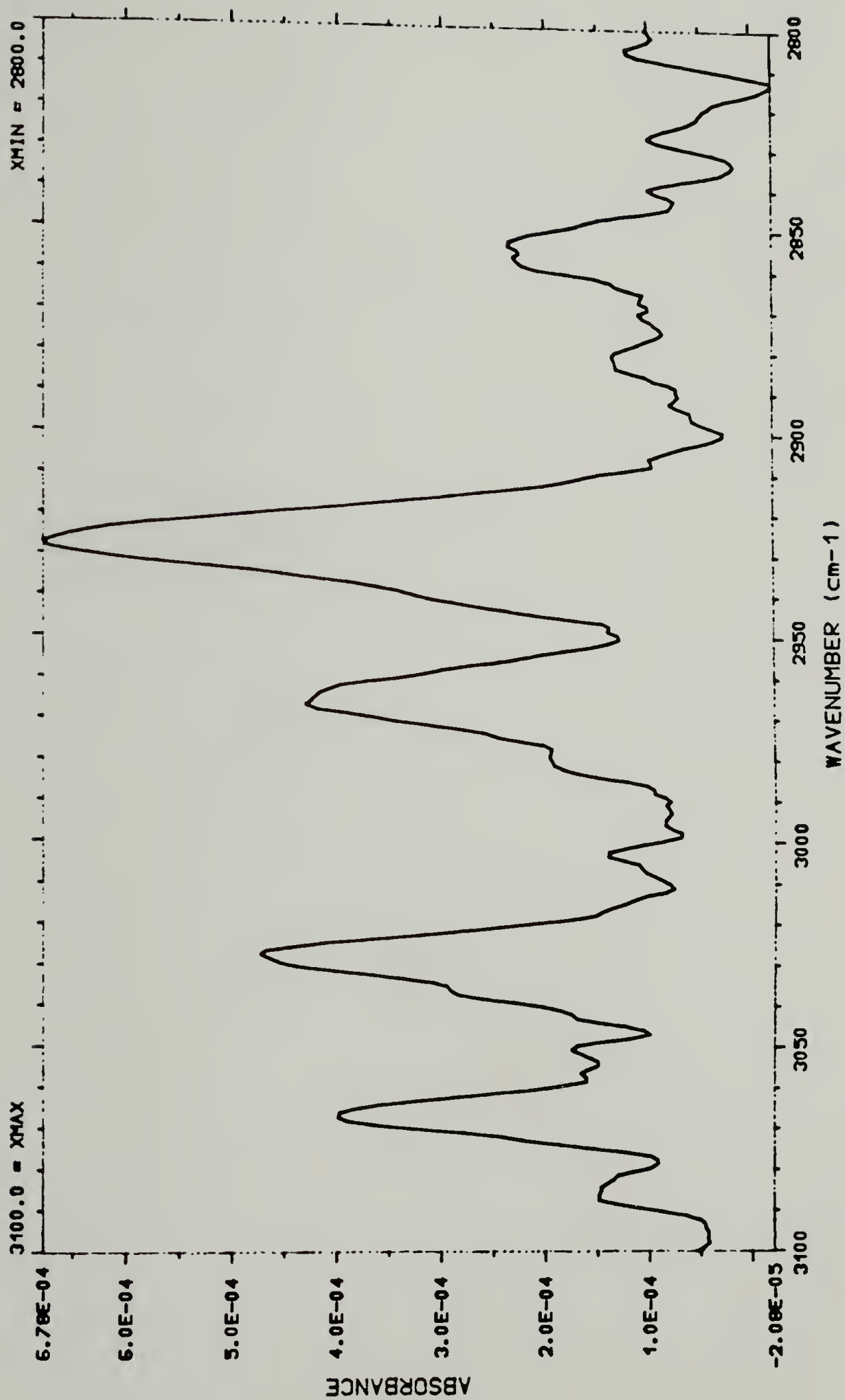


Figure 3.27 XR IR spectrum of PSSH 7-89A adsorbed to gold

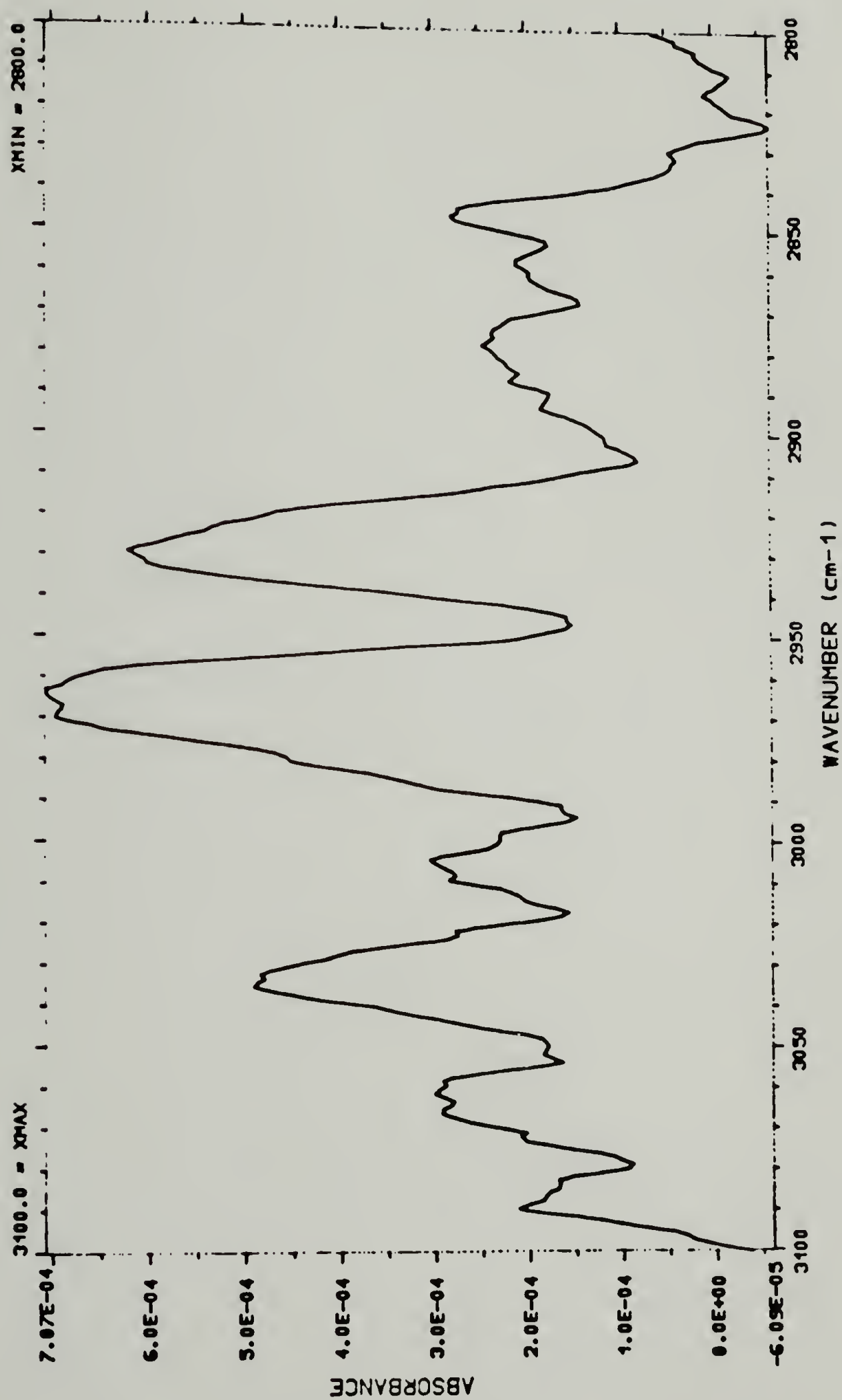
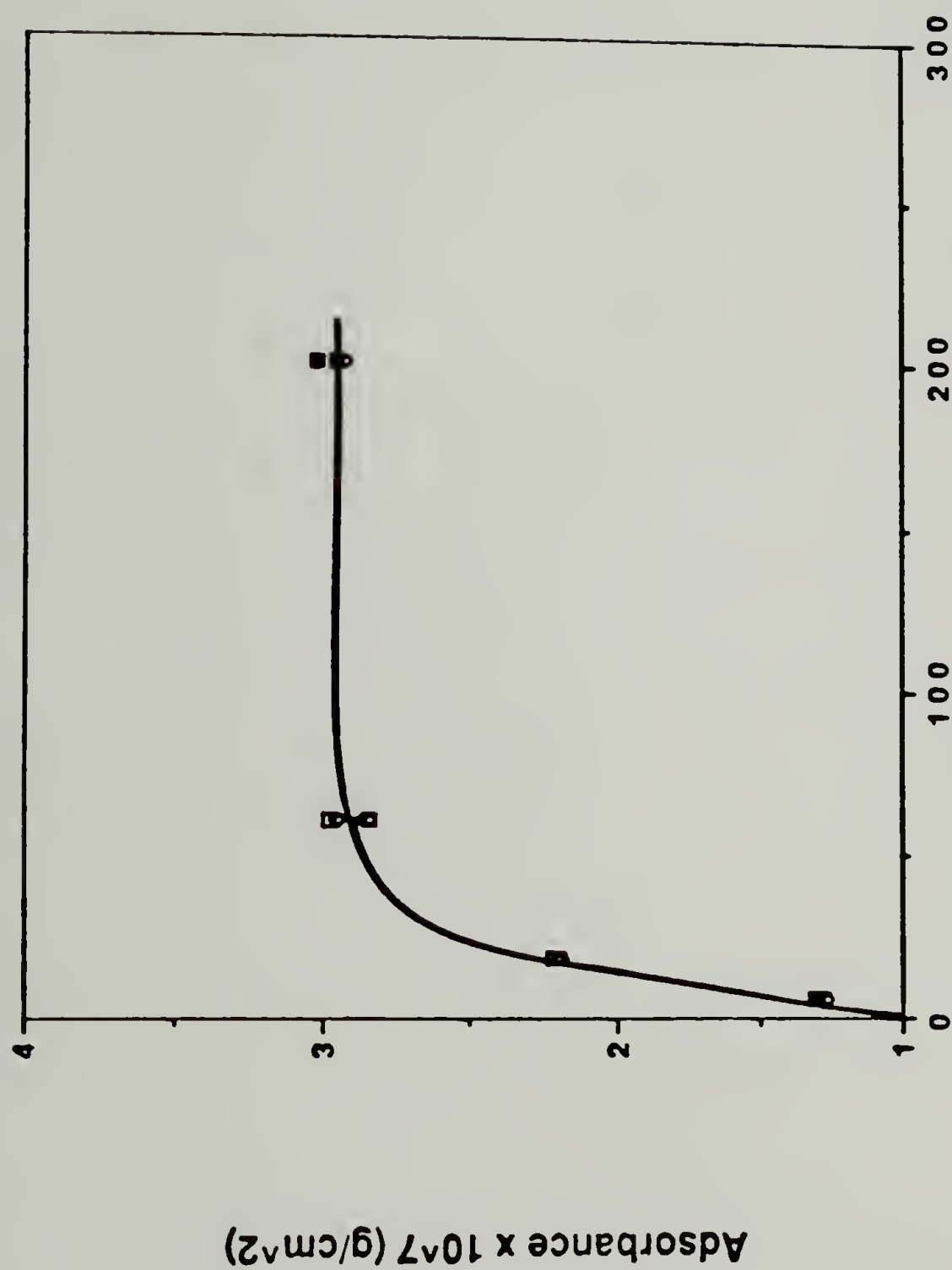


Figure 3.28 XR IR spectrum of PSSH 7-89B adsorbed to gold



Molecular Weight $\times 10^{-3}$

Figure 3.29 Effect of molecular weight on the adsorbance of PSSH polymers onto gold, determined by LSC

The relative thickness of the polymer layer that adsorbed to the surface was determined from the C/Au ratio obtained by XPS analysis. This is a measure of the thickness of the dried polymer layer in the absence of solvent. Thickness (C/Au) is plotted as a function of molecular weight in Figure 3.30; the data for this plot can be found in Table A.3 of the Appendix. For low molecular weight polymers there is a large increase in thickness which begins to level off at $M_n > 10,000$. The carbon observed on the gold samples 7-67A to 7-89B ($M_n = 1,025$ to 203,175) was attributed to polystyrene because the shake up peak was seen 6.7eV to the left of the C_{1s} peak (Figure 3.31).

Angle resolved XPS was used to determine the vertical distribution of carbon and sulfur from the atomic composition of the polymer monolayer. Spectra taken at a grazing angle (15°) provided atomic composition data for C and S from approximately the outer 15 Å; while at 75° information was obtained from approximately the outer 40 Å. A comparison of the S/C ratios taken at 15° and 75° for the adsorbed polymer monolayers is shown in Table 3.15. The S/C value for 75° is higher for each polymer than the 15° value, implying that there is more sulfur deeper in the monolayer, closer to the gold substrate, than in the outer few angstroms. A control XPS analysis was run on thick films of these polymers cast from solution onto glass cover slips. From the atomic composition data obtained at 15° and 75° there was no significant difference between the S/C ratio.

High molecular weight PSSH ($M_n = 512,558$) did not adsorb to the gold substrate from THF after 72h. This was evident by the absence of

polystyrene vibrations in the XR IR spectrum (Figure 3.32) and by a C/Au ratio of ~0.50 obtained from XPS, which is the relative thickness of a thin layer of ambient contamination seen on untreated, freshly evaporated gold substrates. Also, there was no shake up peak observed in the C_{1s} region. These results concur with Killmann's

Table 3.15 Comparison of S/C Ratios from XPS
Taken at 15° and 75°

| <u>Sample</u> | <u>Mn</u> | <u>S/C</u> | |
|---------------|-----------|------------|------------|
| | | <u>15°</u> | <u>75°</u> |
| 7-67A | 910 | .0806 | .1197 |
| 7-123A | 5,057 | .0539 | .0779 |
| 7-123B | 9,623 | .0278 | .0386 |
| 7-83B | 57,029 | .0137 | .0315 |
| 7-89A | 134,729 | .0129 | .0252 |
| 7-89B | 203,175 | .0075 | .0235 |
| 7-85A | 512,558 | -- | -- |

observations by ellipsometry that polystyrene does not adsorb to gold from good solvents.^{23,24} In our adsorption system there is a trade off between the interaction of the polystyrene and THF, which tends to keep the polymer in solution, and the interaction of the thiol with the gold surface, which promotes polymer adsorption. It appears from these results that at a sufficiently high enough molecular weight the polymer-solvent interactions dominate and polymer prefers to stay in solution, whereas, lower molecular weight samples do not have as many polymer-solvent interactions so the thiol-gold interaction dominates; the

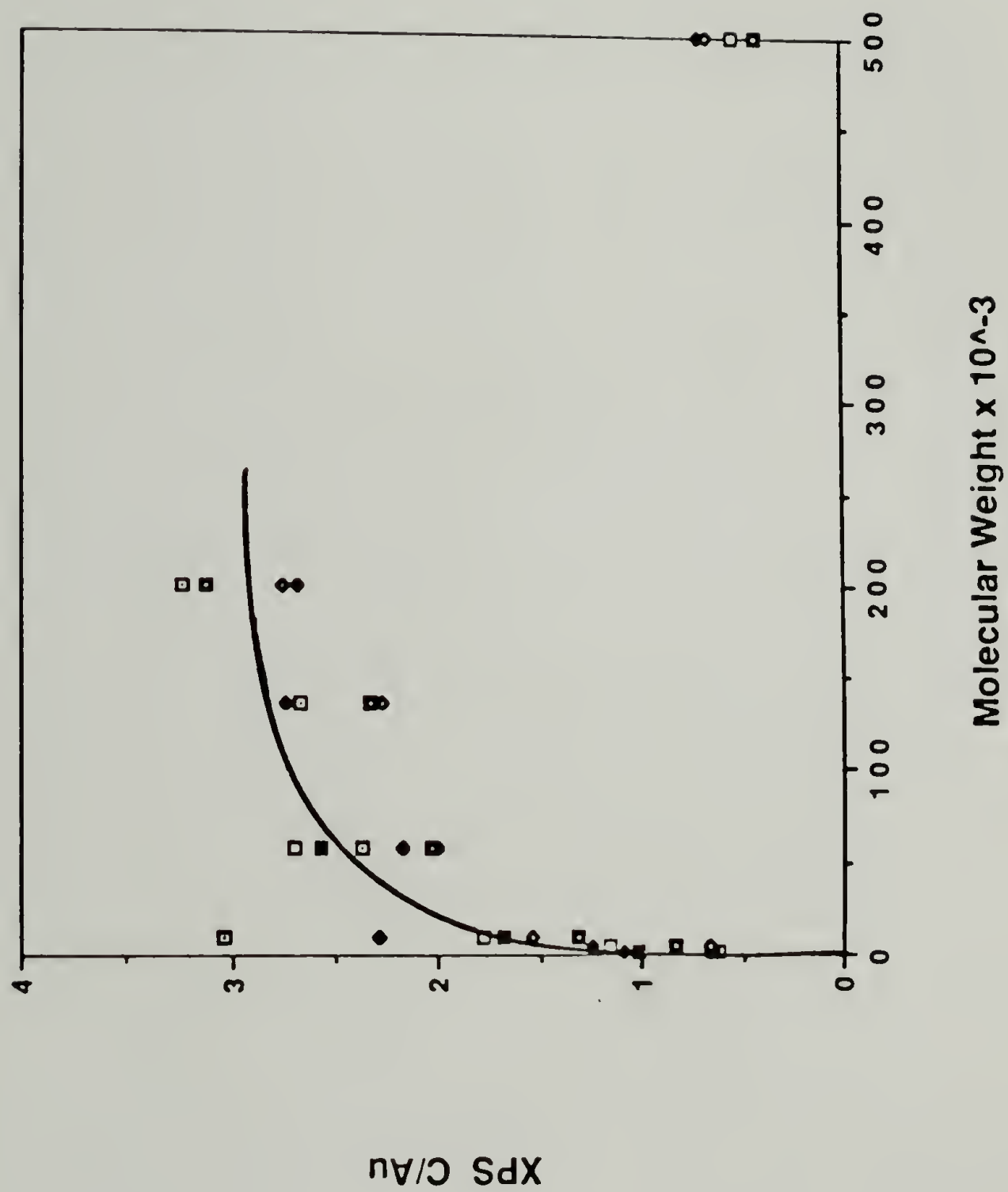


Figure 3.30 Effect of molecular weight on the adsorbance of PSSH polymers onto gold, determined by XPS

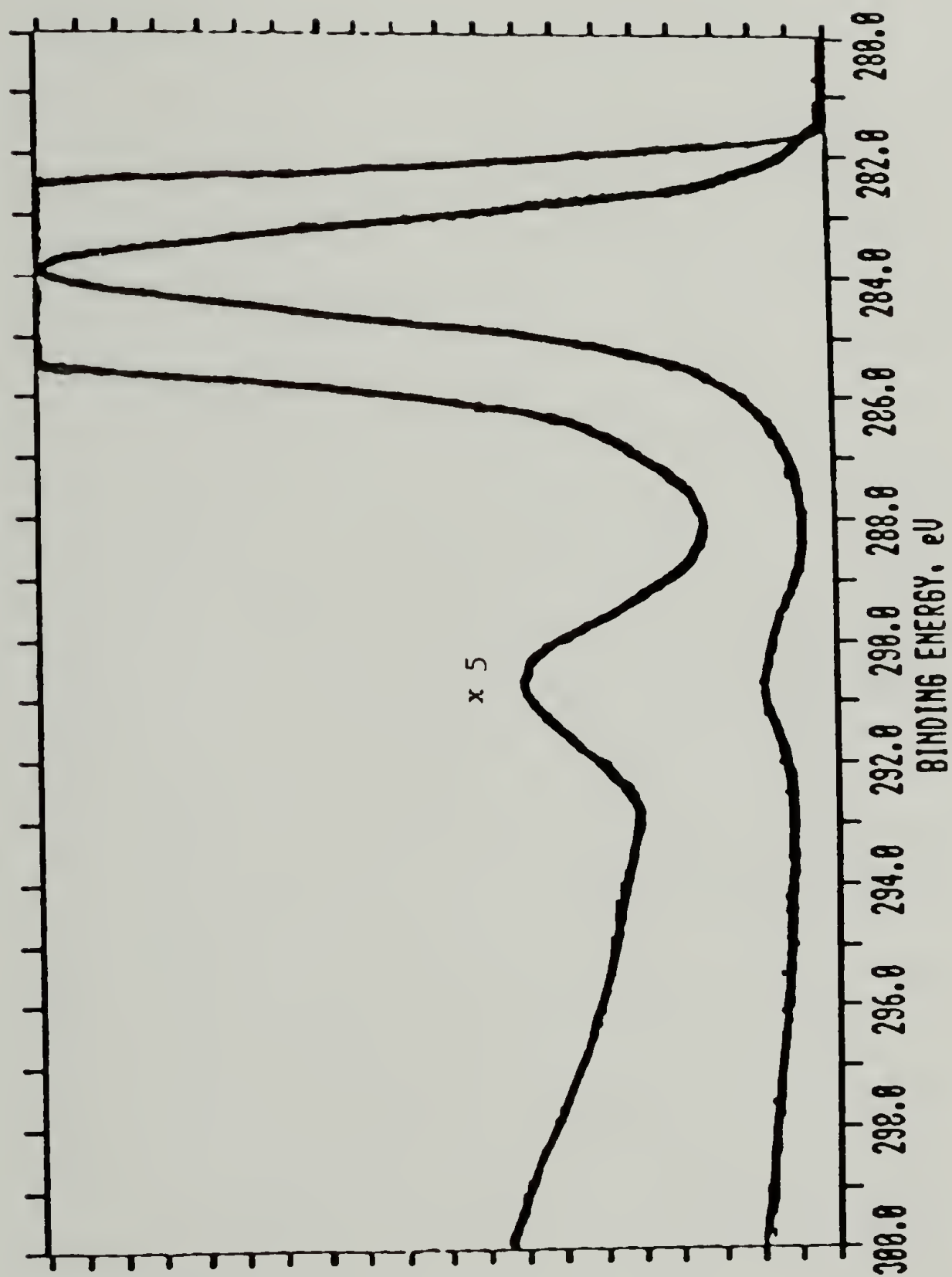


Figure 3.31 XPS spectrum of adsorbed PSSH polymer showing
shake up peak in C_{1s} region

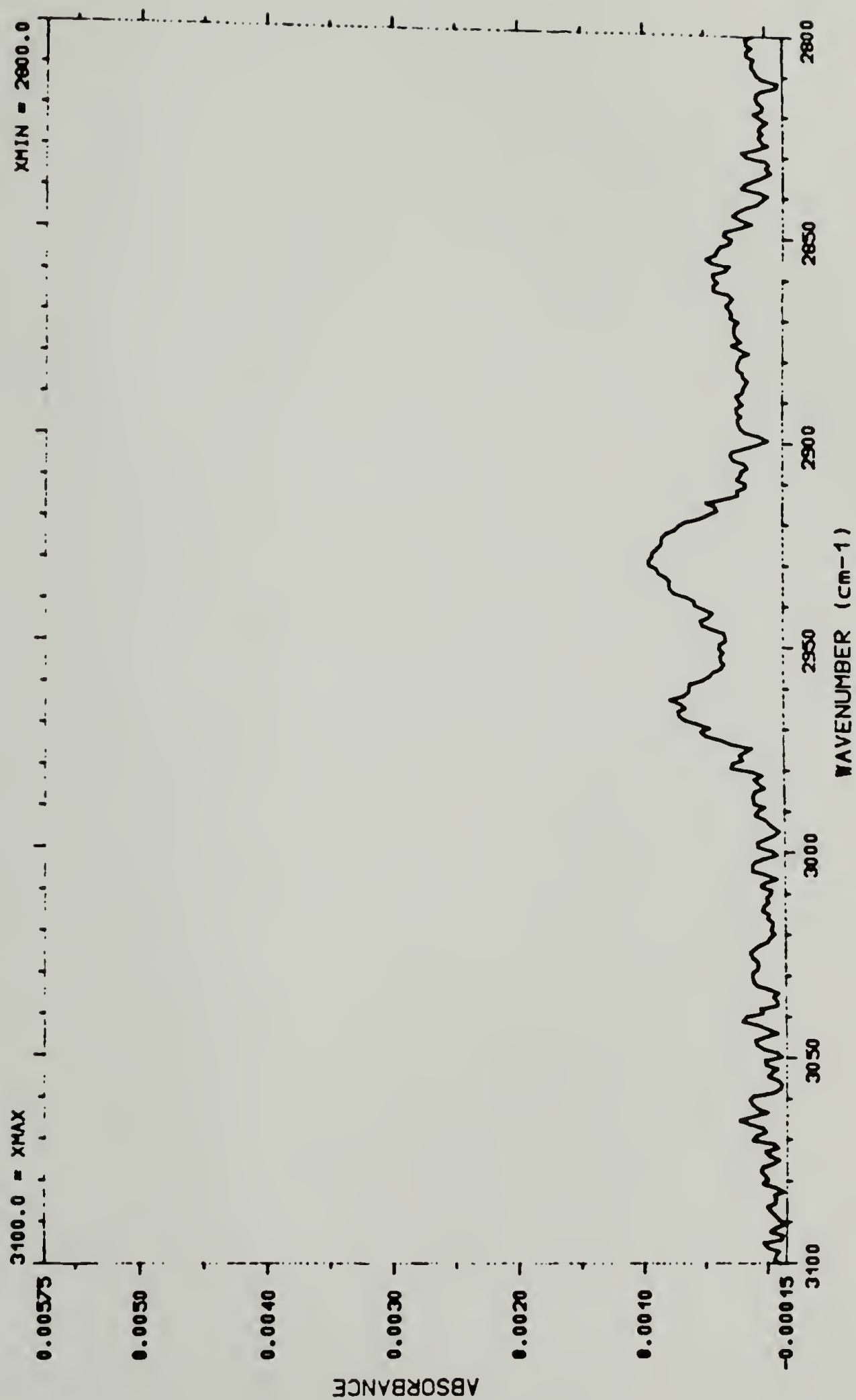


Figure 3.32 XR IR spectrum of a gold substrate exposed to a solution of PSSH 7-85A

molecule behaves more like a long-chain thiol and spontaneously adsorbs to the surface.²⁵

Concentration Dependence. The adsorption isotherm for PSSH ($M_n = 194,993$) in THF (2.0 mg/ml) is shown in Figure 3.33, the data are listed in Table A.4 in the Appendix. The adsorbance values initially rise sharply with increasing concentration then level off, which is typically the behavior of polymers adsorbed from dilute solution.²⁶ The initial slope of the adsorption isotherm curve reflects the distribution tendency of the solute between surface and solution, and is defined as the affinity. The initial steep slope (high-affinity) of the adsorption isotherm indicates that as the concentration increases more polymer is readily adsorbed to the surface until a saturation point is reached. At that point, the surface is at equilibrium for the adsorption of polymer. Scheutjens and Fleer²¹ predict from their theory that the adsorption isotherm for a polymer adsorbed from a good solvent would be of the high-affinity type.

Effect of Solvent. In our study of the effect of solvent on adsorbance we considered a series of mixtures of good and poor solvents (THF/cyclohexane) as well as the extreme cases of the pure solvents. The adsorbance of PSSH ($M_n = 194,993$, 2.0 mg/ml, 24 hours, 45°C) onto gold was determined by LSC for a series of THF/cyclohexane mixtures. Adsorbance is plotted against volume fraction of cyclohexane (ϕ_c) of the solvent mixture in Figure 3.34, the data are listed in Table A.5 in the Appendix. The adsorbance gradually increases with the increasing content of cyclohexane (a poor solvent for polystyrene) relative to THF

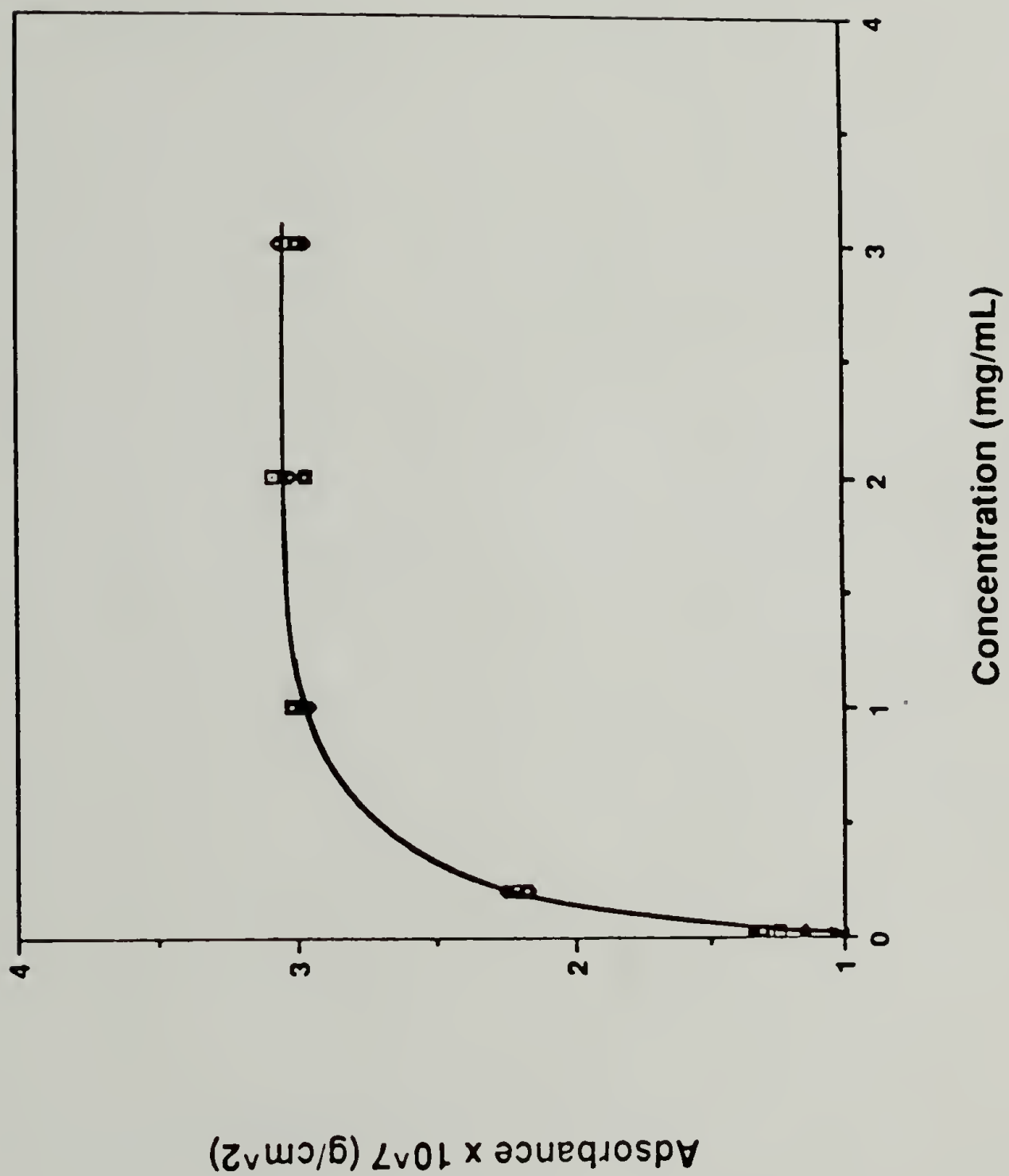


Figure 3.33 Adsorption isotherm for PSSH 7-145H determined by LSC

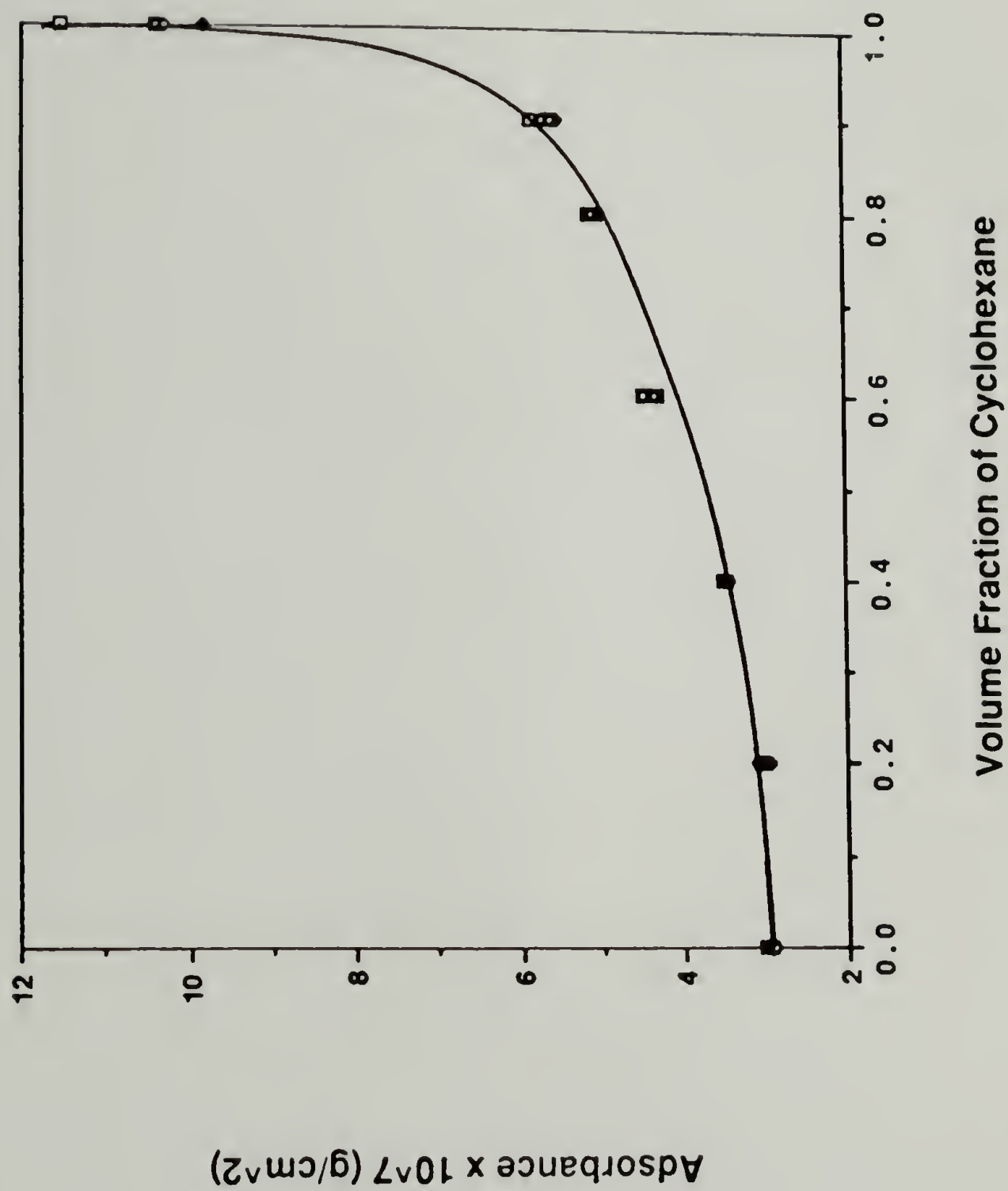


Figure 3.34 Effect of solvent mixtures on the adsorbance of PSSH polymers onto gold, determined by LSC

(a good solvent for polystyrene). At $\phi_c = 1$ there is a large increase in the amount of polymer adsorbed. This same trend was observed by XPS analysis. We did not see a linear relationship between adsorbance (A) and volume fraction of cyclohexane (ϕ_c). What we observed was a gradual increase in A with increasing (ϕ_c), then a large jump in A when $\phi_c = 1$. This can be explained by the phenomenon of preferential adsorption - when a polymer is dissolved in a binary solvent mixture usually one of the solvents preferentially solvates the polymer. Munk^{27,28} studied the adsorption properties of polystyrene in solution over the entire range of composition of benzene/cyclohexane solvent mixture. He discussed the phenomenon of preferential adsorption in terms of phenomenological interaction parameters in a three component system. In our case for polystyrene adsorbed to a wall, the polymer is preferentially solvated by THF so it is more expanded than the same polymer in pure cyclohexane. The larger polymer takes up more space on the surface preventing other polymers from adsorbing. On a molecular level in solvent mixtures the polymer molecule sees a higher concentration of the preferentially adsorbed solvent than the macroscopic concentration of the solvent mixture. Therefore, in our system the amount of polymer adsorbed to the surface did not change drastically as cyclohexane was added to the system. Only when there was no THF in the mixture ($\phi_c=1$) was the polymer completely solvated by cyclohexane and we observed a large increase in adsorbance typical of a polymer adsorbed from a poor solvent.

Effect of Poly(propylene sulfide) Block Size on the Adsorption of Polystyrene/Polypropylene sulfide) Block copolymers. A series of PS/PPS block copolymers was synthesized ($M_n \approx 60,000$) in which the percentage of the poly(propylene sulfide) block was varied from 1% to 90% (Table 3.13). Figure 3.35 shows the results of the adsorption of these block copolymers onto gold from THF (2.0 mg/mL, 24 hours), the data are listed in Table A.6 in the Appendix. The adsorbance decreases as the block size of the PPS increases. One can envisage this situation as the PPS block being the sticky part of the copolymer that adsorbs tightly to the gold and the PS block extends from the surface in a relatively stretched configuration. This same type of adsorption configuration was suggested by Hadziioannou and Tirrell²⁹ in their investigation of the forces between surfaces of block copolymers of poly(vinyl-2-pyridine)/polystyrene adsorbed on mica. This type of adsorption can be compared to de Gennes' theory of grafted polymers for the case of a semidilute solution where the density of graft points is relatively high and the chain extending from the wall is strongly stretched and unmixed with the chains from the solution. For our system the longer PPS block covered up more of the gold surface and reduced the total number of chains that could adsorb to the surface, consequently lowering the total adsorbance, and the thickness of the adsorbed layer.

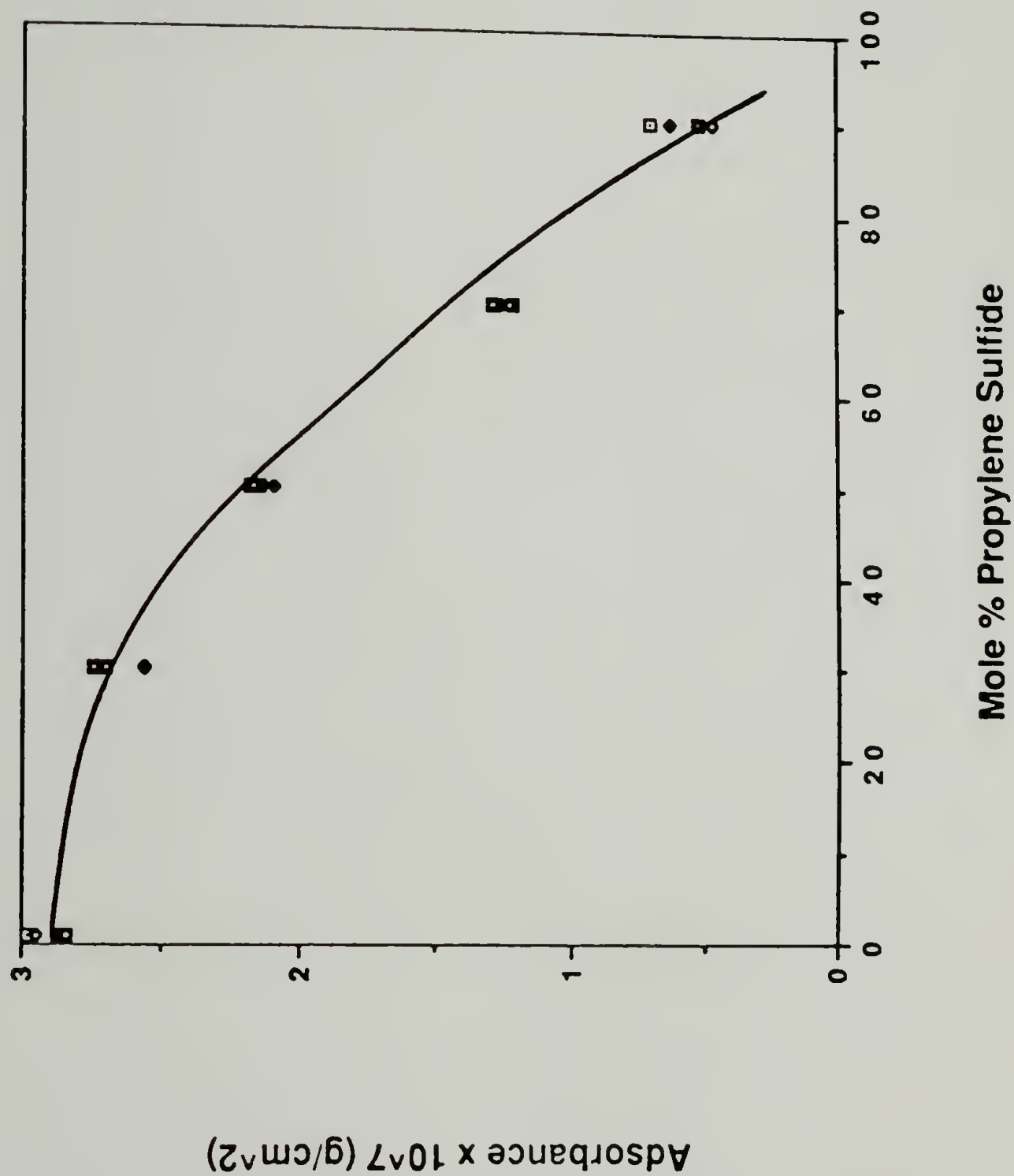


Figure 3.35 Effect of poly(propylene sulfide) block size on the adsorption of PS/PPS copolymer, determined by LSC

Summary

Polystyrene containing a terminal thiol group ($M_n = 1,000-200,000$) adsorbed to gold under conditions that polystyrene did not. The thiol group interacted with the gold surface and the polymer adsorbed rapidly and irreversibly; polymer monolayers were washed with fresh solvent without desorption. At higher molecular weight ($M_n = 500,000$) adsorption did not occur. Molecular weight, concentration and solvent property effects suggest that the adsorption occurred in a fashion similar to polystyrene adsorption from solution. PS/PPS samples adsorbed to gold and the thickness of the adsorbed polymer layer could be controlled by the length of the propylene sulfide block.

References

1. Stouffer, J.M.; McCarthy, T.J. Polym. Prepr. (Am. Chem. Soc., Div. Polym Chem.) **1985**, 26, 80.
2. Garwood, G.A., Jr.; Hubbard, A.T. Surf. Sci. **1982**, 118, 223.
3. Johnson, A.L.; Muttterties, E.L.; Stohr, J. J. Am. Chem. Soc. **1983**, 105, 7183.
4. Wexler, R.M.; Muetterties, E.L. J. Am. Chem. Soc. **1984**, 106, 4810.
5. Arkles, B. Chemtech **1977**, 7, 766.
6. Thompson, S.J.; Webb G. "Heterogenous Catalysis" Oliver and Boyd London.
7. Carbello, L.; Serrano, C.; Wolf, E.E.; Canberry, J.J. J. Catal. **1978**, 52, 507.
8. Pines, H.; Sartoris, N.E. J. Org. Chem. **1969**, 34, 2113 and 9370.
9. Beumel, O.F.; Smith, W.N.; Rybalka, B. Synthesis **1974**, 43.
10. O'Reilly, J.M.; Mosher, R.A. Carbon **1983**, 21, 47.
11. Painter, P.C; Koenig, J.L. J. Polym. Sci., Polym. Phys. Ed. **1977**, 15, 1885.
12. Stouffer, J.M.; McCarthy, T.J. Polym. Prepr. (Am. Chem. Soc., Div. Polym. Chem.) **1986**, 27, 242.
13. Boileau, S.; Sigwalt, P. Compt. Rend. **1961**, 252, 882.
14. Boileau, S.; Coste J.; Raynal, J.M. Compt. Rend. **1962**, 254, 2774.
15. Boileau, S.; Champelier, G.; Sigwalt, P. Makromol. Chem. **1963**, 69, 180.
16. Morton, M.; Kammereck, R.F. J. Am. Chem. Soc. **1970**, 92, 3217.
17. Wallace, T.J.; Schriesheim, A.; Bartok, W. J. Org. Chem. **1963**, 28, 1311.
18. Nevin, R.S.; Pearce, E.M. J. Polym. Sci., Polym. Lett. Ed. **1965**, 3, 487.

19. Hassner, A.; Hoblitt, R.P.; Heathcock, C.; Kropp, J.E.; Lorber, M. J. Am. Chem. Soc. **1970**, 92, 1326.
20. Kawaguchi, M.; Hayakawa, K.; Takahasi, A. Macromolecules **1983**, 16, 631.
21. Scheutjens, J.M.H.M.; Fleer, G.J. J. Phys. Chem. **1979**, 83, 1619.
22. Silberberg, A. J. Phys. Chem. **1968**, 48, 2835.
23. Gebhard, H.; Killmann, E. Ange. Makromol. Chem. **1976**, 53, 171.
24. Killmann, E.; Eisenlauer, J.; Korn M. J. Polym. Sci., Polym. Symp. **1977**, 61, 413.
25. Porter, M.D.; Bright, T.B.; Allara, D.L.; Chidsey, C.E.D. J. Am. Chem. Soc. **1987**, 109, 3559.
26. Eirich, F.R. J. Colloid. Interface Sci **1977**, 58, 423.
27. Mark, P.; Chu, S.G. Macromolecules **1978**, 11, 879.
28. Mark, P.; Aminabhavi, T.M. Macromolecules **1979**, 12, 607.
29. Hadziioannou, G.; Patel, S.; Granick, S.; Tirrell, M. J. Am. Chem. Soc. **1986**, 108, 2869.

Chapter IV

CONCLUSIONS AND SUGGESTIONS

The first part of this research involved the synthesis and characterization of a molecularly defined metal-polymer interface. High surface area platinum black was used because the surface could be easily cleaned of its oxide layer by chemical reduction, the coordination of ligands could be monitored by observing the effect on the rate of olefin hydrogenation and the amount of 4-picoline adsorbed could be determined by three independent methods. Unfortunately, the polystyrene-grafted platinum material was very difficult to analyze. The final grafted sample could only be characterized by elemental analysis and transmission FTIR spectroscopy. The high absorbance of the platinum greatly reduced the energy throughput. Useful information was only obtained in the C-H stretching region ($2700\text{--}3200\text{ cm}^{-1}$). The molecular weight of the grafted polystyrene could not be determined directly. Unsuccessful attempts were made to displace the grafted polystyrene with ethane thiol. All of the picoline molecules adsorbed to the platinum surface did not initiate polymerization of styrene. Polymer growing away from the platinum surface probably hindered monomer from reaching bound picolyanions. This system showed that styrene could be graft polymerized on platinum, but the resulting material did not lend itself to further investigations.

The second part of this research was the investigation of polymer monolayers prepared by the spontaneous adsorption of sulfur-

functionalized polystyrene on gold surfaces. To investigate the effect of molecular weight it was important to be able to prepare polymers with narrow molecular weight distributions by anionic polymerization. Unlike epoxides, the anionic polymerization of episulfides proceeds without chain transfer or termination so it was possible to synthesize high molecular weight polymers and block copolymers. The extent of functionalization was easily controlled by varying the amount of propylene sulfide incorporated in the polymer. Molecular weight, concentration and solvent property effects suggested that the adsorption of PSSH samples ($M_n = 1,000-200,000$) was similar to the adsorption of polystyrene from a poor solvent. PS/PPS samples adsorbed to gold and the thickness of the adsorbed layer could be controlled by the length of the poly(propylene sulfide) block.

This work has demonstrated the importance of using organic chemistry to make specifically designed functional polymers that can be used to investigate interfacial phenomena. Improved surface analytical techniques are being developed which can provide information about the orientation of molecules within an adsorbed polymer layer. Preliminary work on modulated-polarization external reflectance FTIR has demonstrated an improved sensitivity over the conventional XR IR technique.¹

The relatively simple model system that we have used, a functionalized polymer interacting specifically with a surface, can be expanded to address other questions concerning an adsorbed system such as those suggested by de Gennes in his theoretical predictions of

conformations of polymers attached to an interface.² Further work should be done describing the solution state of a grafted polymer when the molecular weight, graft density, concentration and solvent properties are systemically varied. This type of investigation will lead to a better understanding of interfacial phenomena in both solids and solid-liquid environments.

References

1. Waldman, D.; Hsu, S.L.; Stouffer, J.M. University of Massachusetts, unpublished results.
2. de Gennes, P.G. Macromolecules 1980, 13, 1069.

APPENDIX

Data Tables

Table A.1 Radioactivity (CPM) of Solutions of PSSH Polymers
for Beer's Law Plots

| <u>Mass x 10⁶ (g)</u> | CPM of PSSH Polymers | | | |
|----------------------------------|----------------------|---------------|---------------|---------------|
| | <u>7-143H</u> | <u>7-135H</u> | <u>7-131H</u> | <u>7-145H</u> |
| 24.000 | 784.9 | 516.1 | 270.0 | 287.2 |
| 9.600 | 338.6 | 222.9 | 127.2 | 133.8 |
| 3.840 | 154.5 | 110.6 | 71.3 | 70.1 |
| 1.536 | 72.2 | 59.4 | 41.1 | 47.1 |

Table A.2 Radioactivity (CPM) of Solutions of PS/PPS Polymers
for Beer's Law Plots

| <u>Mass x 10⁶ (g)</u> | CPM of PS/PPS Polymers | | | |
|----------------------------------|------------------------|--------------|--------------|--------------|
| | <u>8-43H</u> | <u>8-47H</u> | <u>8-33H</u> | <u>8-51H</u> |
| 24.000 | 574.4 | 310.3 | 435.5 | 192.8 |
| 9.600 | 232.3 | 138.0 | 183.8 | 95.9 |
| 3.840 | 117.0 | 79.8 | 100.7 | 61.7 |
| 1.536 | 76.0 | 47.0 | 55.4 | 37.5 |

Table A.3 Radioassay Data for the Adsorption of Polymers onto Gold.
Effect of Molecular Weight (2 mg/mL, THF, 24 h)

| Molecular Weight | Sample | CPM | Corrections | | A x 10 ⁷ | |
|---------------------|---------|-------------|-------------|----------|---------------------|-------------------|
| | | | Efficiency | Geometry | g | g/cm ² |
| 6,000 | 143H | 51.9 | 64.88 | 129.75 | 3.16 | 1.31 |
| | | 52.1 | 65.13 | 130.25 | 3.17 | 1.31 |
| | | 51.0 | 63.75 | 127.50 | 3.09 | 1.28 |
| | | <u>50.6</u> | 63.25 | 126.50 | 3.06 | <u>1.26</u> |
| | (1h) | | | | | |
| | Average | 51.4 | | | | 1.29 |
| | | | | | | |
| 18,000 | 135H | 55.6 | 69.50 | 139.00 | 5.39 | 2.22 |
| | | 54.8 | 68.50 | 137.00 | 5.29 | 2.19 |
| | | 55.0 | 68.75 | 137.50 | 5.31 | 2.20 |
| | | <u>55.1</u> | 68.88 | 137.75 | 5.33 | <u>2.20</u> |
| | (1h) | | | | | |
| | Average | 55.1 | | | | 2.20 |
| | | | | | | |
| 60,000 | 131H | 40.8 | 51.00 | 102.00 | 7.21 | 2.98 |
| | | 39.7 | 49.63 | 99.25 | 6.94 | 2.87 |
| | | 39.4 | 49.25 | 98.50 | 6.86 | 2.84 |
| | | <u>40.5</u> | 50.63 | 101.25 | 7.13 | <u>2.95</u> |
| | (1h) | | | | | |
| | Average | 40.1 | | | | 2.91 |
| | | | | | | |
| 200,000 | 145H | 43.4 | 54.25 | 108.50 | 7.32 | 3.02 |
| | | 43.5 | 54.38 | 108.75 | 7.34 | 3.03 |
| | | 42.7 | 53.38 | 106.75 | 7.15 | 2.96 |
| | | <u>42.4</u> | 53.00 | 106.00 | 7.08 | <u>2.93</u> |
| | (1h) | | | | | |
| | Average | 43.0 | | | | 2.99 |
| | | | | | | |

Table A.4 C/Au Ratios from XPS Data. Effect of Molecular Weight on Adsorbance (2mg/mL, THF, 24 h)

| <u>Sample</u> | <u>Mn</u> | <u>C/Au Ratios</u> | | | |
|---------------|-----------|--------------------|--------|--------|--------|
| 7-67A | 1,000 | .6204 | .6667 | 1.0881 | 1.0240 |
| 7-123A | 5,000 | 1.1584 | 1.2501 | .8273 | .6628 |
| 7-123B | 10,000 | 3.0326 | 2.2939 | 1.3096 | 1.5368 |
| 7-83B | 57,000 | 2.0344 | 2.1754 | 2.5663 | 2.7039 |
| 7-89A | 135,000 | 2.6685 | 2.7447 | 2.3392 | 2.2754 |
| 7-89B | 200,000 | 3.2346 | 2.6850 | 3.1211 | 2.7515 |
| 7-85A | 500,000 | .5345 | .7002 | .4241 | .6636 |

Table A.5 Radioassay Data for the Adsorption of Polymers onto Gold.
Effect of Concentration (200,000 MW, THF, 24 h)

| <u>mg/mL</u> | <u>CPM</u> | <u>Corrections</u> | | <u>A x 10⁷</u> | |
|--------------|-------------|--------------------|-----------------|---------------------------|-------------------------|
| | | <u>Efficiency</u> | <u>Geometry</u> | <u>g</u> | <u>g/cm²</u> |
| 3.0 | 43.7 | 54.63 | 109.25 | 7.39 | 3.05 |
| | 42.8 | 53.50 | 107.00 | 7.18 | 2.97 |
| | 43.2 | 54.00 | 108.00 | 7.27 | 3.00 |
| | <u>43.9</u> | 54.88 | 109.75 | 7.43 | <u>3.07</u> |
| | Average | 43.4 | | | 3.02 |
| 2.0 | 44.1 | 55.13 | 110.25 | 7.48 | 3.09 |
| | 43.6 | 54.50 | 109.00 | 7.36 | 3.04 |
| | 42.9 | 53.63 | 107.25 | 7.20 | 2.97 |
| | <u>43.4</u> | 54.25 | 108.50 | 7.32 | <u>3.02</u> |
| | Average | 43.5 | | | 3.03 |
| 1.0 | 43.2 | 54.00 | 108.00 | 7.27 | 3.00 |
| | 42.7 | 53.38 | 106.75 | 7.15 | 2.96 |
| | 43.5 | 54.38 | 108.75 | 7.34 | 3.03 |
| | <u>43.0</u> | 53.75 | 107.50 | 7.22 | <u>2.98</u> |
| | Average | 43.1 | | | 2.99 |
| 0.2 | 35.0 | 43.75 | 87.50 | 5.36 | 2.21 |
| | 34.5 | 43.13 | 86.25 | 5.24 | 2.17 |
| | 34.7 | 43.38 | 86.75 | 5.29 | 2.18 |
| | <u>35.4</u> | 44.25 | 88.50 | 5.45 | <u>2.25</u> |
| | Average | 34.9 | | | 2.20 |
| 0.02 | 24.9 | 31.13 | 62.25 | 3.00 | 1.24 |
| | 25.9 | 32.38 | 64.75 | 3.23 | 1.34 |
| | 25.6 | 32.00 | 64.00 | 3.16 | 1.31 |
| | <u>24.0</u> | 30.00 | 60.00 | 2.79 | <u>1.15</u> |
| | Average | 25.1 | | | 1.26 |

Table A.6 Radioassay Data for the Adsorption of Polymers onto Gold.
 Effect of Solvent Mixtures THF/Cyclohexane
 (2 mg/mL, 24 h, 200,000 MW, 45°C)

| Volume Fraction of Cyclohexane ϕ | CPM | Corrections | | $A \times 10^7$ | |
|---|-------------|-------------------|-----------------|-----------------|-------------------------|
| | | <u>Efficiency</u> | <u>Geometry</u> | <u>g</u> | <u>g/cm²</u> |
| 0.0 | 43.4 | 54.25 | 108.50 | 7.32 | 3.02 |
| | 43.5 | 54.38 | 108.75 | 7.34 | 3.03 |
| | 42.7 | 53.38 | 106.75 | 7.15 | 2.96 |
| | <u>42.4</u> | 53.00 | 106.00 | 7.08 | <u>2.93</u> |
| | Average | 43.0 | | | 2.99 |
| 0.2 | 43.3 | 54.13 | 108.25 | 7.30 | 3.01 |
| | 42.7 | 53.38 | 106.75 | 7.15 | 2.96 |
| | 43.8 | 54.75 | 109.50 | 7.41 | 3.06 |
| | <u>44.2</u> | 55.25 | 110.50 | 7.50 | <u>3.10</u> |
| | Average | 43.5 | | | 3.03 |
| 0.4 | 48.0 | 60.00 | 120.00 | 8.39 | 3.47 |
| | 47.8 | 59.75 | 119.50 | 8.34 | 3.45 |
| | 48.7 | 60.88 | 121.75 | 8.55 | 3.53 |
| | <u>48.3</u> | 60.38 | 120.75 | 8.46 | <u>3.50</u> |
| | Average | 48.2 | | | 3.48 |
| 0.6 | 57.0 | 71.25 | 142.50 | 10.49 | 4.33 |
| | 58.3 | 72.88 | 145.75 | 10.79 | 4.46 |
| | 58.8 | 73.50 | 147.00 | 10.90 | 4.51 |
| | <u>57.5</u> | 71.88 | 143.75 | 10.60 | <u>4.38</u> |
| | Average | 57.9 | | | 4.42 |
| 0.8 | 64.6 | 80.75 | 161.50 | 12.26 | 5.07 |
| | 64.2 | 80.25 | 160.50 | 12.17 | 5.03 |
| | 65.9 | 82.38 | 164.75 | 12.56 | 5.19 |
| | <u>65.3</u> | 81.63 | 163.25 | 12.42 | <u>5.13</u> |
| | Average | 65.0 | | | 5.10 |

Table A.6 (continued)

| Volume Fraction of Cyclohexane ϕ | CPM | Corrections | | $A \times 10^7$ | |
|---|---------------|-------------------|-----------------|-----------------|-------------------------|
| | | <u>Efficiency</u> | <u>Geometry</u> | <u>g</u> | <u>g/cm²</u> |
| 0.9 | 73.0 | 91.25 | 182.50 | 14.22 | 5.88 |
| | 69.8 | 87.25 | 174.50 | 13.47 | 5.57 |
| | 70.4 | 88.00 | 176.00 | 13.61 | 5.63 |
| | <u>71.6</u> | 89.50 | 179.00 | 13.89 | <u>5.74</u> |
| | Average 71.2 | | | | 5.70 |
| 1.0 | 131.8 | 164.75 | 329.50 | 27.94 | 11.54 |
| | 114.1 | 142.63 | 285.25 | 23.81 | 9.84 |
| | 120.1 | 150.13 | 300.25 | 25.21 | 10.42 |
| | <u>119.1</u> | 148.88 | 297.75 | 24.97 | <u>10.32</u> |
| | Average 121.3 | | | | 10.53 |

Table A.7 Radioassay Data for the Adsorption of Polymers onto Gold.
Effect of Poly(Propylene Sulfide) Block Size
(2 mg/mL, THF, 24 h, 60,000 MW)

| PS:PPS | Sample | CPM | Corrections | | A x 10 ⁷ | |
|--------|--------|-------------|-------------|----------|---------------------|-------------------|
| | | | Efficiency | Geometry | g | g/cm ² |
| 99:1 | 131H | 40.8 | 51.00 | 102.00 | 7.21 | 2.98 |
| | | 39.7 | 49.63 | 99.25 | 6.94 | 2.87 |
| | | 39.4 | 49.25 | 98.50 | 6.86 | 2.84 |
| | | <u>40.5</u> | 50.63 | 101.25 | 7.13 | <u>2.95</u> |
| | | Average | 40.1 | | | 2.91 |
| | | | | | | |
| 70:30 | 43H | 71.0 | 88.75 | 177.50 | 6.52 | 2.70 |
| | | 68.3 | 85.38 | 170.75 | 6.22 | 2.57 |
| | | 72.1 | 90.13 | 180.25 | 6.65 | 2.75 |
| | | <u>71.0</u> | 88.75 | 177.5 | 6.52 | <u>2.70</u> |
| | | Average | 70.6 | | | 2.68 |
| | | | | | | |
| 50:50 | 33H | 47.5 | 59.38 | 118.75 | 5.27 | 2.18 |
| | | 46.2 | 57.75 | 115.50 | 5.08 | 2.10 |
| | | 47.0 | 58.75 | 117.50 | 5.20 | 2.15 |
| | | <u>47.3</u> | 59.13 | 118.25 | 5.24 | <u>2.17</u> |
| | | Average | 47.0 | | | 2.15 |
| | | | | | | |
| 30:70 | 47H | 26.0 | 32.50 | 65.00 | 2.96 | 1.22 |
| | | 26.4 | 33.00 | 66.00 | 3.05 | 1.26 |
| | | 26.7 | 33.38 | 66.75 | 3.11 | 1.29 |
| | | <u>26.1</u> | 32.63 | 65.25 | 2.98 | <u>1.23</u> |
| | | Average | 26.3 | | | 1.25 |
| | | | | | | |
| 10:90 | 51H | 17.0 | 21.25 | 42.50 | 1.70 | 0.70 |
| | | 16.5 | 20.63 | 41.25 | 1.51 | 0.63 |
| | | 15.8 | 19.75 | 39.50 | 1.25 | 0.52 |
| | | <u>15.5</u> | 19.38 | 38.75 | 1.14 | <u>0.47</u> |
| | | Average | 16.2 | | | 0.58 |
| | | | | | | |

BIBLIOGRAPHY

- Allara, D. L.; Nuzzo, R.G. Langmuir 1985, 1, 45, 52.
- Arkles, B. Chemtech 1977, 7, 766.
- Beumel, O.F.; Smith, W.N.; Rybalka, B. Synthesis 1974, 43.
- Boileau, S.; Sigwalt, P. Compt. Rend. 1961, 252, 882.
- Boileau, S.; Coste J.; Raynal, J.M. Compt. Rend. 1962 254, 2774.
- Boileau, S.; Champelier, G.; G.; Sigwalt, P. Makromol. Chem. 1963, 69, 180.
- Bowden, F.P.; Tabor, D. The Friction and Lubrication of Solids; Oxford University Press: London, 1968.
- Bregman, J.I. Corrosion Inhibitors; MacMillan: New York, 1963.
- Carbello, L.; Serrano, C.; Wolf, E.E.; Canberry, J.J. J. Catal. 1978, 52, 507.
- Clark, D.T.; Thomas, H.R. J. Polym. Sci., Polym. Chem. Ed. 1977, 15, 2843.
- de Gennes, P.G. J. Phys. 1976, 37, 1445.
- de Gennes, P.G. Scaling Concepts in Polymer Physics Cornell University: Ithaca, NY, 1979; p35.
- de Gennes, P.G. Macromolecules 1980, 13, 1069.
- de Gennes, P.G. Macromolecules 1981, 14, 1637.
- Diem, T.; Czajka, B.; Weber, B.; Regen, S.L.; J. Am. Chem. Soc. 1986, 108, 6094.
- DiMarzio, E.A. J. Chem. Phys. 1965 42, 2101.
- DiMarzio, E.A.; McCrackin, F.L. J. Chem. Phys. 1965, 43, 539.
- Eirich, F.R. J. Colloid. Interface Sci. 1977, 58, 423.
- Frisch, H.L.; Simha, R.; Eirich F.R. J. Chem. Phys. 1953, 21, 365.
- Garwood, G.A., Jr.; Hubbard, A.T. Surf. Sci. 1982, 118, 223.

- Gebhard, H.; Killmann, E. Ange. Makromol. Chem. 1976, 53, 171.
- Greenler, R.G. J. Chem. Phys. 1966, 44, 310.
- Greenler R.G. J. Vac. Sci. Technol. 1975, 12, 1410.
- Hadziioannou, G.; Patel, S.; Granick, S.; Tirrell, M. J. Am. Chem. Soc. 1986, 108, 2869.
- Haller, I. J. Am. Chem. Soc. 1978, 100, 8050.
- Handling Air-Sensitive Compounds; Technical Information Bulletin Number A1-134; Aldrich Chemical Company: Milwaukee, WI, 1983.
- Harrick, N.J. Internal Reflection Spectroscopy; Wiley Interscience: New York, 1967.
- Harrick, N.J. J. Opt. Soc. Am. 1965, 55, 851.
- Hassner, A.; Hoblitt, R.P.; Heathcock, C.; Kropp, J.E.; Lorber, M. J. Am. Chem. Soc. 1970, 92, 1326.
- Heinemann, H. Chemtech. 1971, 1, 286.
- How to Use Ace No-Air Glassware; Bulletin Number 570; Ace Glass Incorporated: Vineland, NJ, 1983.
- Hoeve, C.A.J. J. Chem. Phys. 1965, 43, 3007.
- Hoeve, C.A.J. J. Chem. Phys. 1966, 44, 1505.
- Hoeve, C.A.J. J. Polym. Sci., Polym. Phys. Ed. 1970, 30, 361.
- Hoeve, C.A.J. J. Polym. Sci., Polym. Phys. Ed. 1971, 34, 1.
- Hubbard, A.T. Acc. Chem. Res. 1980, 13, 177.
- Hubbard, A.T.; Soriaga, M.P. J. Am. Chem. Soc. 1982, 104, 2735.
- Israelachvili, J.N.; Tirrell, M.; Klein, J.; Almog, Y. Macromolecules 1984, 17, 204.
- Johnson, A.J.; Muettert, E.L.; Stohr, J. J. Am. Chem. Soc. 1983, 105, 7183.
- Juaristi, E.; Martinez-Richa, A.; Garcia-Rivera, A.; Cruz-Sanchez, J.S. J. Org. Chem., 1983, 48, 2603.
- Kawaguchi, M.; Hayakawa, K.; Takahashi, A. Polym. J. 1980, 12, 265.

- Kawaguchi, M.; Takahashi, A.; Hirota, H.; Kato, T. Macromolecules 1980, 13, 884.
- Kawaguchi, M.; Takahashi, A.; J. Polym. Sci., Polym. Phys. Ed. 1980, 18, 943, 2069.
- Kawaguchi, M.; Takahashi, A.; Macromolecules 1983, 16, 631, 635, 1465.
- Kawaguchi, M.; Takahashi, A.; Macromolecules 1984, 17, 1666, 2063, 2066.
- Klasson, M.; Hedman,.; Berndtsson, A.; Nilsson, R.; Nordling, C.; Melnik, P. Phys. Scripta 1972, 5, 93.
- Klein, J.; Nature, 1980, 288, 248.
- Klein, J.; Adv. Colloid. Interface. Sci. 1982, 16, 101.
- Klein, J.; Pinus, P.; Macromolecules 1982, 15, 1129.
- Klein, J.; Luckham, P.; Nature (London) 1982, 300, 429.
- Klein, J.; J. Chem. Soc., Faraday Trans. 1 1983, 79, 99.
- Klein, J.; Luckham, P.; Macromolecules 1984, 17, 1041.
- Klein, J.; Luckham, P.; Nature (London) 1984, 308, 836.
- Klein, J.; Luckham, P.; J. Chem. Soc., Faraday Trans. 1 1984, 80, 865.
- Klein, J.; Luckham, P. Colloids Surf. 1984, 10, 65.
- Klein, J.; Luckham, P. Macromolecules 1985, 18, 721.
- Killmann, E.; Eisenlauer, J.; Korn M. J. Polym. Sci., Polym. Symp. 1977, 61, 413.
- Morton, M.; Kammereck, R.F. J. Am. Chem. Soc. 1970 92, 3217.
- Munk, P.; Chu, S.G. Macromolecules 1978, 11, 879.
- Munk, P.; Aminabhavi, T.M. Macromolecules, 1979, 12, 607.
- Na, T.S.; Rittner, R.C. Modern Elemental Analysis; Marshall Decker: New York, 1979.
- Napper, D. Polymer Stabilization of Colloidal Dispersions; Academic Press: London, 1983.

- Nevin, R. S.; Pearce, E.M. J. Polym. Sci., Polym. Lett. Ed. 1965, 3, 487.
- Nuzzo, R.G.; Allara, D.L. J. Am. Chem. Soc. 1983, 105, 4481.
- Nuzzo, R.G.; Fusco, F.A.; Allara, D.L. J. Am. Chem. Soc. 1987, 109, 2358.
- Nuzzo, R.G.; Zegarski, B.R.; Dubois, L.H. J. Am. Chem. Soc. 1987, 109, 733.
- O'Reilly, J.M.; Mosher, R.A. Carbon 1983, 21, 47.
- Painter, P.C.; Koenig, J.L. J. Polym. Sci., Polym. Phys. Ed. 1977, 15, 1885.
- Palmberg, P.W.; Rhodin, T.N. J. Appl. Phys. 1968, 39, 2425.
- Perrin, D.D.; Armarego, W.L.F.; Perrin, Dawin R. Purification of Laboratory Chemicals, 3rd. ed.; Pergamon Press: New York, 1980.
- Pines, H.; Satoris, N.E. J. Org. Chem. 1969, 34, 2113 and 9370.
- Porter, M.D.; Bright, T.B.; Allara, D.L.; Chidsey, C.E.D. J. Am. Chem. Soc. 1987, 109, 3559.
- Powell, C.J. Surface Science 1974, 44, 29.
- Prest, W.M., Jr.; Mosher, R.A. In Reprographic Technology; ACS Symposium Series 200; American Chemical Society; Washington, DC, 1982 pp 225-247.
- Richard, M.A.; Deutsch, J.; Whitesides, G.M. J. Am. Chem. Soc. 1978, 100, 6613.
- Shivers, D.F. The Manipulation of Air Sensitive Compounds, McGraw-Hill: New York, 1969.
- Scheutjens, J.M.H.M.; Fleer, G.J. J. Phys. Chem. 1979, 83, 1619.
- Scheutjens, J.M.H.M.; Fleer, G.J. J. Phys. Chem. 1980, 84, 178.
- Siegbahn K.; Nordling, C.; Fahlman, A.; Nordberg, R.; Hamrin, J.; Hedman, J.; Johansson, G.; Bergmark, T.; Karlsson, S. -E.; Lingren, I.; Lindberg, B ESCA-Atomic, Molecular and Solid State Structure Studied by Means of Electron Spectroscopy Almqvist and Wiksells: Uppsula, 1967.
- Silberberg, A. J. Phys. Chem. 1962, 66, 1884.

- Silberberg, A. J. Phys. Chem. 1962, 66, 1872.
- Silberberg, A. J. Chem. Phys. 1968, 48, 2835.
- Steinhardt, R.G.; Hudis, J.; Perlman, M.L. Phys. Rev. B. 1972 5, 1016.
- Stouffer, J.M.; McCarthy, T.J. Polym. Prepr. (Am. Chem. Soc., Div. Polym. Chem.) 1985, 26, 80.
- Stouffer, J.M.; McCarthy, T.J. Polym. Prepr. (Am. Chem. Soc., Div. Polym. Chem.) 1986, 27, 242.
- Takahashi, A.; Kawaguchi, M. Adv. Polym. Sci. 1982, 46, 1.
- Technical Manual: 5000 Series ESCA Systems; Perkin-Elmer Physical Electronics Division; Perkin-Elmer: Eden Prairie, MN, 1980.
- Thompson, S.J.; Webb, G. "Heterogeneous Catalysis"; Oliver and Boyd, London.
- Wagner, C.D.; Riggs, W.M.; Moulder, J.F.; Muilenberg, G.E., Ed. Handbook of X-Ray Photoelectron Spectroscopy; Perkin-Elmer: Eden Prairie, MN, 1979.
- Wallace, T.J.; Schriesheim, A.; Bartok, W. J. Org. Chem. 1963 28, 1311.
- Wexler, R.M.; Muetterties, E.L. J. Am. Chem. Soc. 1984, 106, 4810.

